A MODEL FOR A FOUR-DIMENSIONAL INTEGRATED REGIONAL GEODETIC NETWORK

Zur Erlangung des akademischen Grades eines
DOKTOR-INGENIEURS
von der Fakultät für
Bauingenieur- und Vermessungswesen
der Universität Fridericiana zu Karlsruhe (TH)
genehmigte
DISSERTATION

von

BSc. MSc. Sammy M. Musyoka
aus Machakos (Kenia)

Tag der mündlichen
Prüfung: 11.02.1999

Hauptreferent: Prof. Dr.-Ing. B. Heck

Korreferent: Prof. Dr.-Ing. G. Schmitt

Karlsruhe
(1999)

Abstract

Four-dimensional geodesy deals with integrated processing of geodetic observations in order to analyse the network geometry and its variation with time, when these observations depend on the gravity field of the earth and its temporal variation. This consideration introduces the time dimension into the three-dimensional integrated model.

The shape of the earth and consequently its gravity field upon which geodetic observables depend changes continuously with time due to dynamic processes taking place within the earth and also due to third body attractions, for example the moon and the sun. This consideration leads to the requirement of four-dimensional models in precise geodetic networks. In this study, the model of three-dimensional integrated geodesy is extended to the four-dimensional geodesy by considering the temporal variation of the network points both in space and time.

A general derivation of the observation equation for four-dimensional geodesy was carried out. In this derivation, the time dependent geodetic observations are treated as functions of position of points involved in each observation and the gravity potential functionals evaluated at those points. In the first step the position of a point at any desired epoch (time) is decomposed into a provisional position at the initial epoch, a coordinate correction at this initial epoch and a time varying displacement. In the second step the potential functional is decomposed into a known non-temporal normal potential and a time varying disturbing potential. The disturbing potential is further decomposed into two parts: a part at the initial epoch and another part that varies with time. The gravity potential functionals are in general considered as non-linear and were therefore linearised by applying the Taylor series approximation to functionals. In the last step the results of both the first and the second steps were combined and the resulting equation was linearised leading to formation of the basic general model of four-dimensional geodesy.

The basic general model of four-dimensional geodesy consisted of essentially four different types of parameters - the coordinate corrections, the displacements, the disturbing potential functionals and their time variations. The coordinate corrections were considered to be *discrete deterministic* while the other parameters designated as *signals*, were considered as being continuous in both space and time. Following the general model of four-dimensional geodesy just described specific observation equations for most classical terrestrial geodetic observations as well as some space observations were fully derived.

Noting that geodetic observations are usually only made at discrete points and at discrete time instants, the signals had to be treated in such a way as to enable their propagation both in time and space. This treatment was possible through introduction of spatial covariance functions and time covariance functions. Since a network covering a regional area was considered, regional spatial covariance functions with respect to commonly used terrestrial and space geodetic observables were derived. These covariance functions were based on the model described in [Reilly, 1979] and [Heck, 1984]. Introduction of a time dependent term on the spatial covariance functions resulted in the time covariance functions of their respective observables.

Using some profile of free air anomaly data, empirical covariance functions were computed as a test example.These empirical covariance functions were then used to derive values for the model covariance functions derived for the various observables. A further test example to demonstrate the application of the covariance functions as a means of expressing the signals occuring in four-dimensional geodesy was carried out.

In view of the increasing application of *Global Positioning System (GPS)* in precise geodetic work, it was considered appropriate to conduct a GPS antenna calibration. Through spectral analysis of the normal equation matrix containing the antenna offsets, a method of testing for the significance of the non-estimable vertical component of the antenna offsets is presented in the appendix.

Kurzfassung

Die vierdimensionale Geodäsie beschäftigt sich mit den integrierten geodätischen Beobachtungen unter der Annahme, dass sich die Geometrie des Netzes und das beobachtete Schwerefeld im Laufe der Zeit ändern. Damit erweitert diese Betrachtungsweise bekannte dreidimensionale Modelle mit zusätzlichen zeitabhängigen Parametern.

Die Gestalt des Erdkörpers und damit auch sein Schwerepotential, wovon die geodätischen Observablen abhängig sind, ändert sich auf Grund dynamischer Prozesse innerhalb des Erdinnern und anderer Effekte (z.B. Anziehungskraft vom Mond und der Sonne) kontinuierlich. Diese Kinematik ist Grundlage zur Entwicklung von vierdimensionalen Modellen, die vor allem in Netzen höchster Präzision bei der Analyse von sehr genauen geodätischen Messungen anzuwenden sind. In der vorliegenden Arbeit wird das Modell der dreidimensionalen integrierten Geodäsie auf das Modell der vierdimensionalen Geodäsie durch Betrachtung zeitlicher Änderungen der Netzpunkte erweitert.

Bei der Ableitung einer allgemeinen Beobachtungsgleichung werden zeitabhängige Beobachtungen sowohl als Funktion des Beobachtungsortes, als auch als Funktion der Schwerepotentialfunktion betrachtet. Hierzu werden in einer ersten Stufe die Koordinaten eines Punktes zu einem beliebigen Zeitpunkt t_i zerlegt in Näherungskoordinaten für einen beliebig wählbaren Anfangszeitpunkt t_o, Verbesserungen dieser Näherungskoordinaten und eine zeitabhängige Verschiebung. In der zweiten Stufe der Modellbildung wird die Schwerepotentialfunktion in ein bekanntes zeitunabhängiges Normalpotential und ein zeitabhängiges Störpotential zerlegt. Das zeitlich abhängige Störpotential wiederum wird aufgeteilt in einen Anteil zum Anfangszeitpunkt t_o und einen zeitlichen abhängigen Teil. Da die Beobachtungsgleichungen in Abhängigkeit von der Schwerepotentialfunktion im allgemeinen nichtlinear sind, werden diese durch entsprechende Taylorreihen approximiert. In der dritten und letzten Stufe werden die zuvor dargestellten Ergebnisse zusammengefasst. Die Linearisierung dieser Ergebnisse führt letztlich zum allgemeinen Modell der vierdimensionalen Geodäsie.

Das in der vorliegenden Arbeit vorgestellte allgemeine Modell der vierdimensionale Geodäsie enthält vier verschiedene Gruppen von Parametern. Hierbei handelt es sich um die Koordinatenunbekannten, die Verschiebungen, die Funktionale des Störpotentials und seine zeitliche Änderungen. Die Koordinatenunbekannten werden als diskrete deterministische Grössen betrachtet, die anderen Unbekannten, die als Signale bezeichnet werden, sind kontinuierlich sowohl im Raum als auch in der Zeit.

Auf der Grundlage des Modells der vierdimensionalen Geodäsie werden individuelle Beobachtungsgleichungen für klassische terrestrische geodätische Beobachtungen und einige räumliche Beobachtungen abgeleitet. Dabei ist zu berücksichtigen, dass geodätische Beo-bachtungen nur auf diskreten räumlichen Punkten und zu diskreten Zeitpunkten durchgeführt werden können. Eine kontinuisierung im Raum und Zeit erreicht man im Rahmen eines stochastischen Konzepts, in dem die als Signale bezeichneten Grössen formal als stochastisch betrachtet werden. Dies hat zur Folge, dass hierfür die Ableitung von Kovarianzfunktionen über Kovarianzen-Fortpflanzung erforderlich ist, wobei sowohl räumliche Kovarianzfunktionen und als auch zeitliche Kovarianzfunktionen benötigt werden. Ausgehend von bekannten Modellen räumlicher Kovarianzfunktionen ([Reilly, 1979] und [Heck, 1984]) werden in der Arbeit Modelle für regionale räumliche und zeitliche Kovarianzfunktionen für die am häufigsten auftretenden Beobachtungen abgeleitet.

Für ein Profil von Freiluftanomalien werden beispielhaft die empirischen Kovarianzfunktionen berechnet. Aus diesen empirischen Kovarianzfunktionen sind dann Kovarianzfunk-

tionen für andere Observable ableitbar, die wiederum im Modell der vierdimensionalen Geodäsie einzusetzen sind. Im weiteren Verlauf der Arbeit wird die Nutzung dieser Kovarianzfunktionen in den Beobachtungsgleichungen der vierdimensionalen Geodäsie an Beispielen gezeigt.

In Hinblick auf die verbesserten Einsatzmöglichkeiten des GPS in hochgenauen geodätischen Netzen wurde in einem Testfeld eine GPS-Kampagne zur Kalibrierung von GPS-Empfängern durchgeführt. Nach der Spektralanalyse der Anteile des Antennen-Offsets in der entstehenden Normalgleichungsmatrix wird im Anhang eine Methode vorgestellt, um die nicht schätzbare vertikale Komponente eines GPS-Antennen-Offsets auf Signifikanz zu prüfen.

Contents

Abstract **2**

Kurzfassung **4**

1. Introduction **13**

1.1 Geodetic Positioning 13

1.1.1 Classical Geodetic Networks 14

1.1.2 Three-dimensional Networks 15

1.1.3 Geodynamic Phenomena 16

1.2 The Statement of the Problem 19

1.3 Outline of the Report 20

2. Historical Development of Four-dimensional Geodesy **22**

2.1 General Remarks 22

2.2 The Beginning of Four-dimensional Geodesy 22

2.3 Suitability of Classical Geodetic Networks in Four-Dimensional Positioning 24

3. The Integrated Four-dimensional Model **27**

3.1 The Coordinate Reference Systems 27

3.1.1 Establishment of a Coordinate Reference System 27

3.1.2 The Physical Coordinate System 28

3.1.3 The Model Coordinate System 29

3.1.4 The Epoch Coordinate Transformation 29

3.2 Similarity Transformations 30

3.3 The Integrated Model in a Three-dimensional Space 31

3.4 The Integrated Four-dimensional Model 32

4. Observation Equations for Integrated Four-dimensional Geodesy **36**

4.1 The General Scheme for Purely Gravity Dependent Observables 36

4.2 One Point Observations 38

4.2.1 Astronomical Latitude 38

4.2.2 Astronomical Longitude 40

4.2.3 Gravity Intensity . . . 42
4.3 Two Point Observations . . . 43
4.3.1 Gravity Intensity Difference . . . 43
4.3.2 Spatial Distances . . . 44
4.3.3 Zenith Angles . . . 45
4.3.4 Astronomical Azimuth . . . 47
4.3.5 Horizontal Directions . . . 50
4.3.6 Gravity Potential Differences . . . 51
4.4 Three Point Observations . . . 52
4.4.1 Horizontal Angles . . . 52
4.5 Space Observations . . . 53
4.5.1 GPS Observations . . . 53
4.5.2 Very Long Baseline Interferometry - VLBI . . . 57

5. The Integrated Four-dimensional Network Adjustment Models 58
5.1 Basic considerations . . . 58
5.2 The Four-dimensional Adjustment Models . . . 59
5.2.1 The Deterministic Approach . . . 60
5.2.2 The Functional Signal Approach . . . 64
5.2.3 The Stochastic Signal Approach . . . 64
5.3 The Covariance Functions . . . 67
5.3.1 Covariance Functions of Four-dimensional Geodesy . . . 67
5.3.2 The Covariance Functions . . . 68
5.3.3 Covariance Function for Absolute Potential on the Deformable Surface 73
5.3.4 Covariance Function of the Potential Difference . . . 74
5.3.5 Covariance Function for Gravity Intensity . . . 74
5.3.6 Covariance Functions of Other Gravity Field Dependent Observations 75
5.4 The Time Covariance Function . . . 77

6. The Test Examples 82
6.1 The Karlsruhe Network . . . 82
6.1.1 General Information about the Network . . . 82
6.1.2 The Computation of the Test Network . . . 83
6.2 The Kenyan Gravity Network . . . 85

7. Summary and Conclusions 88

References 90

Appendix A 97

A GPS Antenna Calibration **97**

A.1 The Mathematical Approach . . . 97

A.1.1 The Coordinate Systems. . . . 97

A.1.2 The Method of Adjustment . . . 99

A.1.3 The Classical Approach . . . 99

A.1.4 The Pseudoinverse Approach . . . 100

A.1.5 The Partial Norm Minimization Approach . . . 100

A.1.6 The Special Partial Norm Minimization . . . 101

A.2 Parameter Testing . . . 101

A.3 The Test Network and Results . . . 102

A.3.1 The Ground Truth . . . 102

A.3.2 The GPS Network . . . 102

A.3.3 Computation of the Antenna Offsets . . . 103

A.3.4 Adjustment of Offsets and only one Set of Rotation Transformation Parameters as Unknowns . . . 103

A.3.5 Adjustment when Rotational Transformation Elements are excluded 108

A.3.6 Adjustment of Offsets and Transformation Parameters for each Session . . . 108

Acknowledgement . . . 111

Curriculum Vitae . . . 112

List of Figures

1.1 The GPS station velocities from 1993 to 1998. (from [Gendt et al., 1998]) 18

1.2 Diagramatic illustration of space and time - discrete epoch model 21

2.1 Summary of crustal deformation spectrum 23

5.1 The Hirvonen and the Gaussian covariance functions 69

6.1 The Karlsruhe Test Network. 83

6.2 The empirical covariance function computed from free air gravity anomalies 85

6.3 The distribution of the free air gravity anomaly points 86

6.4 The model covariance function for potential 87

6.5 The model covariance function for the vertical derivative of potential -T_z . 87

A.1 The eigenvalues of **N** plotted against the parameters. 100

A.2 The Layout of the GPS Antenna Calibration Terrestrial Network 103

List of Tables

1.1 Classical and integrated geodesy . . . 16
5.2 Signal modeling in four-dimensional geodesy . . . 60
5.3 Signal pairing . . . 67
6.1 Types of observations . . . 84
6.2 Approximate geocentric coordinates of the test network . . . 84
6.3 Adjusted coordinates . . . 84
6.4 Standard errors of adjusted coordinates . . . 85

A.1 The Terrestrial network coordinates . . . 104
A.2 Types of antenna used and numbering adopted . . . 104
A.3 Antenna positions and directions in sessions 1 and 2 . . . 105
A.4 Antenna positions and directions in sessions 3 and 4 . . . 105
A.5 The null space of **N** for each of the three components of the offset when only one set of rotation parameters is used . . . 106
A.6 Results obtained by fixing one station $e_{az} = 0$ - classical approach . . . 106
A.7 The rotational angles in radians . . . 107
A.8 Results of all four sessions . . . 107
A.9 The rotational angles in radians . . . 107
A.10 Results according to classical approach (sessions 1 & 2) . . . 108
A.11 Results according to the classical approach . . . 109
A.12 The rotational angles in radians for session 1 . . . 109
A.13 The rotational angles in radians for session 2 . . . 109
A.14 Results from partial, special partial and pseudoinverse solution - $e_{z5} = -0.0134$ . . . 109
A.15 The rotational angles in radians for session 1 . . . 110
A.16 The rotational angles in radians for session 2 . . . 110
A.17 Results of all four sessions . . . 110
A.18 The rotational angles in radians for session 1 . . . 110
A.19 The rotational angles in radians for session 2 . . . 110
A.20 The rotational angles in radians for session 3 . . . 110
A.21 The rotational angles in radians for session 3 . . . 111

Commonly used symbols and abbreviations

In general matrices are represented by bold uppercase while row and column matrices are represented by bold lowercase. Physical vectors shall also be represented by bold lowercase. Further the usage of δ shall not be restricted to the *Euler* considerations but merely as a symbol of convenience. The same applies to the usage of Δ which is often used in geodesy to represent an *anomaly*.

Unless otherwise stated in the text, the symbols and the abbreviations used in this dissertation carry the following meaning:

Abbreviations

GFZ	Geoforschungszentrum, Potsdam
GPS	Global Positioning System
IAG	International Association of Geodesy
ITRF	International Terrestrial Reference Frame
IUGG	International Union of Geodesy and Geophysics
SLR	Satellite Laser Ranging
SVLBI	Space Very Long Baseline Interferometry
VLBI	Very Long Baseline Interferometry

Some commonly used symbols

$\mathbf{A}$	The configuration or the design matrix
C_0	Variance
$cov(.,.)$	Covariance function
$\Delta\mathbf{x}(t)$	Vector of coordinate corrections
$\delta\mathbf{x}(t)$	Displacement vector
$grad$	Gradient
$\Phi(t)$	Time dependent astronomical latitude
ζ	Geoid undulation
ξ	Correlation length
$l(t)$	A time dependent single observation
Lap	Laplace operator
λ	Ellipsoidal longitude
$\Lambda(t)$	Time dependent astronomical longitude
P_i	Denotes a network point
r	Distance between two points
$\mathbf{R}$	Rotation matrix
$\mathbf{s}$	The signal vector
t	The time variable
T	The disturbing potential
T_{Xi}	The components of the derivatives of the disturbing potential
U	The normal gravity potential
U_{Xi}	Components of the normal gravity potential gradient
$\mathbf{v}$	Vector of residuals
$\mathbf{\Gamma}$	The gravity vector
W	The gravity potential

$\mathbf{W}$	The weight matrix
W_{Xi}	Components of the gravity potential gradient
σ_0^2	Apriori variance of unit weight
$\hat{\sigma}^2$	Aposteriori variance of unit weight
,	The magnitude of the gravity vector
$\boldsymbol{\gamma}$	The magnitude of the normal gravity vector
$< .,. >$	Inner or scalar product of two vectors

1. Introduction

1.1 Geodetic Positioning

The classical definition of geodesy was given by *F.R. Helmert* in 1880 [Helmert, 1880] as the *science of measurement and mapping of the earth's surface.* Accordingly the end product of geodesy has been a map of fixed positions on the earth's surface. *Bruns* [Bruns, 1878] had already recognised in 1878 that most of the geodetic measurements depend on the earth's gravity field thus creating a relationship between the geometrical space and the physical space under which the measurements are made. With advances in technology and particularly in satellite positioning, Draheim [Draheim, 1971] re-stated the problem of geodesy as *the determination of the figure and external gravity field of the earth and of other heavenly bodies as functions of time; as well as the determination of the mean earth ellipsoid from parameters observed on and exterior to the earth's surface.* Draheim's statement brings in explicitly the *time* aspect in geodesy in recognition of the earth's continously changing shape as well as its gravity field both in time and space. [Vanicek and Krakiwsky, 1978] referred to a similar definition when expounding on the role of a modern surveyor.

Traditionally geodesists have approached the problem of the determination of the shape of the earth from the point of view that the earth's shape and its gravity field were static. Where observations are known to vary with time, a reduction is made so that all computations are referred to one epoch of measurements. Unfortunately only a few of the geodetic measurements can be sufficiently well modelled by use of peripheral models so as to remove the effects of time variations. The tidal effects on the gravity measurements are well modelled and can be removed by peripheral models with high accuracy. The astronomical observations are also corrected by use of peripheral models due to time effects associated with polar motion. The bulk of the other geodetic observables is assumed time invariant and in a majority of cases the dependency of the observations on the gravity field is ignored.

The solution of the problem of geodetic positioning has been developed over the years. The classical approach preceded the purely three-dimensional approach. Shortly afterwards the physical gravity field was incorporated in the network adjustment models and this was the beginning of *integrated geodesy.*

1.1.1 Classical Geodetic Networks

In classical geodetic network establishment, respectively positioning, one set out horizontal and vertical networks separate from one another. In this approach, the three-dimensional space is separated into a two-dimensional horizontal and a one-dimensional vertical space. A reference ellipsoid is chosen as the basis for the horizontal control within the horizontal space and the geoid is adopted as a reference for the vertical control. This separation of the geodetic networks was made due to the human visualisation of heights and plan whereby both aspects are automatically perceived to be of different nature. Another reason was the fact that heights were more accurately determined than the horizontal coordinates and there was also the unsolved problem of a combined modelling to produce three-dimensional positions.

The levelling accuracy is computed from $\pm k_{mm} \cdot \sqrt{s_{km}}$ where s is the distance in kilometres and k is a constant (usually $0.2mm$) for geodetic work. The horizontal accuracy in position is affected by many factors among others, atmospheric refraction, theodolite errors and errors in distance measurement. The effects of vertical refraction are high particularly in areas of extreme altitude differences and vast extent. Since heights in three-dimensional positions had to be obtained from vertical angles, their accuracy was limited by the irregular effects of refraction. On the other hand effects of lateral refraction are usually small so that the planimetric information obtained from the observations is still of appreciable accuracy. Spirit leveling combined with gravity measurements along the leveling line served as the main means of vertical control while triangulation and later trilateration or a combination of both provided the main means of horizontal control. Gravity networks were also established as one-dimensional networks. A reference for the gravity network e.g the IGSN71 network which incorporates various stations covering the whole world ([Morelli et al., 1974], [Uotila, 1978]), is required. The means of observations are the relative gravimeter measurements and absolute gravity measurements using either the pendulum or the rise and fall method. Accuracies of a few microgals ($10^{-8}ms^{-2}$) are obtainable nowadays [Becker, 1984].

The classical approach in geodetic positioning is selective as regards the type of observations to be used. Classical models are limited to (a) particular type(s) of data thus ignoring vast and relevant geodetic data including physical data that have been acquired over the years.

The measuring instruments and the observables react differently to the inherent atmospheric and gravity conditions thus requiring other models to filter these effects. The measurement conditions and the influences of the atmosphere and gravity field are not static. Repeated measurements at different time instants may differ due to the changing nature of these effects, thus requiring separate models to predict the shape of the network with respect to time. The dependency of the observations on the gravity field is accounted for by pheripheral models by way of reductions of the observations. While this procedure is simple in application, the advantage of the common dependence of the observations on the gravity field is ignored and the conception of three-dimensional space is lost.

1.1.2 Three-dimensional Networks

Three-dimensional models eliminate the need to reduce the observations to a reference surface. The original idea of three-dimensional geodesy goes back to H. Bruns in 1878 [Bruns, 1878]. However his ideas could not be practically realised at that time because it was not possible to obtain the necessary measurements with an appreciable accuracy. It was not until in the early 1950's when Marussi [Marussi, 1949], [Marussi, 1950], [Marussi, 1951] revived the idea that was picked up by *Hotine* [Hotine, 1957] and later [Wolf, 1963a], [Wolf, 1963b] developed observation equations for three-dimensional geodesy in the geometric field. The parameters of Wolf's model are the three-dimensional coordinates and two parameters per point defining the direction of the plumbline, namely: the astronomical- latitude and longitude. *Marussi* had considered the problem of three-dimensional geodesy in a way that included not only the geometric aspects but also the physical gravity field influencing the observations. This consideration was termed *intrinsic geodesy* and was developed to what was later to become *integrated* or *operational geodesy*.

The main hindrance to establishment of three-dimensional networks has been the observation of vertical angles whose influence by the atmospheric refraction is high. However three-dimensional models can accomodate satellite observations in an optimal way and the observations can be processed in a unified manner without need for reducing the original observations. Satellite methods e. g. the Global Positioning System (GPS) provide a faster and efficient way of establishing such networks.

In three-dimensional integrated geodesy the remaining disturbing potential is modelled as a harmonic function either as a deterministic or a stochastic quantity e.g [Klein, 1997]. The final model thus contains deterministic geometric quantities with either deterministic parameters of the potential function or the parameters of a stochastic function. In the stochastic case an estimation is made with respect to the deterministic parameters and a prediction with respect to the stochastic ones. When the gravity field parameters are considered as stochastic, the solution of the parameters follows the least squares collocation approach proposed by [Krarup, 1971] and further developed in [Moritz, 1973]. Stochastic prior information can also be incorporated in three-dimensional integrated geodesy [Schaffrin, 1985], [Aduol, 1989].

Basically integrated geodesy differs from classical geodesy in that the influence of the disturbing potential on the observations is not ignored in integrated networks. Although both cases take as input discrete geodetic observations, their unknowns are of different nature. The classical case has discrete unknowns while the integrated case has both discrete and continous unknowns, (see Table (1.1)). The continuous unknown is the disturbing gravity potential while the discrete parameters are the geometrical parameters of positioning (the coordinates) and other auxiliary unknowns.

Although the three-dimensional integrated geodesy takes into account the dependency of the observations on the physical gravity field, it ignores the temporal variations of the observations resulting from the changes of the gravity field and also the change of shape of the network with time.

Data Analysis	Observations	Parameters
Classical geodesy	Discrete	Discrete
Integrated Geodesy	Discrete	Discrete + Continuous

Table 1.1: Classical and integrated geodesy

1.1.3 Geodynamic Phenomena

About the same time integrated geodesy was being developed the theory of plate tectonics was widely being investigated and gaining credibilty. When it became clear that the continents, or the plates which they belong to, are in continuous motion, geodetic accuracy was becoming higher and the need to monitor the geodetic network stations was emerging. The idea of plate tectonics pushed geodesy into otherwise purely geodynamic problems.

Why is the geodesist interested in geodynamics? The role of geodesy in geodynamics is explained in [Lambeck, 1989a] where he has described geodesy as *high frequency geology* or *low frequency seismology.* [Vanicek and Krakiwsky, 1978] refer to geodesy as *contemporary geodynamics* with reference to the emerging role of geodesy in geodynamic studies. For example, the reference system, usually a three-dimensional geocentric cartesian coordinate system has its origin at the mass centre of the earth. The $Z^{\bullet}$ axis is directed along the earth's axis of rotation. Precession and nutation of the pole change the direction of this axis in inertial space thus influencing geodetic observations. The polar motion changes the orientation of this axis thereby altering the orientation of the reference system. The changes in the angular velocity of the earth affect the length of the day (LOD) with ultimate effects on the reference system. Further, tidal forces cause periodic variations in the gravity field thus influencing the geodetic observations that are dependent on the gravity field. There are also associated deformations from the tidal forces that affect the geodetic observations.

Following the Bullen classification ([Bullen, 1975]), the earth's interior is made of distinct layers, namely the upper mantle, the lower mantle, the outer core and the inner core. The earth's crust is contained in the upper mantle which itself is further classified into an outer region, the lithosphere and an inner region, the asthenosphere. The lithosphere is rather rigid while the underlying regions can undergo plastic and elastic deformation. More causal factors of deformations are discussed below.

Terrestrial mass displacements cause time changes in the gravity field as well as the physical surface of the earth. The mass displacements may be caused by erosion and sedimentation, volcanic activity and earthquakes, changes in the water table, glacial effects (see [Menard, 1975]) , evaporation etc. For example the postglacial rebounds of the last 10,000 years or so are being observed by geodetic means with uplift rates of about 10mm per year in Fennoscandia. The resulting melt water becomes another crustal load which may help explain the rise in sea level (see also [Lambeck, 1989b]). Man-made activities, for example large constructions - dams, excavations, mining activities, large buildings, large mass deposits etc. also affect the mass distributions of the earth which in turn alter the gravity field upon which geodetic observations depend.

From the theory of plate tectonics it is known that expanding material from the asthenosphere results in the relative movement of the lithospheric plates (see [Le Pichon et al., 1973]). As the plates slide over the asthenosphere they bend at *bumps* that they meet on the asthenosphere thereby causing displacements of surface points. There are six major plates. These are the Pacific plate, the North and South American plates, the Eurasian plate, the African plate, the Indian plate, and the Antarctic plate. There are also a larger number of smaller plates as shown in Figure (1.1). Whenever two plates collide the heavier one sinks into the upper mantle and there is subduction. Deep trenches are formed and mountains are uplifted near the plate boundaries. It is postulated that the density of the core changes with time. Such changes will have effects on the dynamics of the earth which may cause the plates to move.

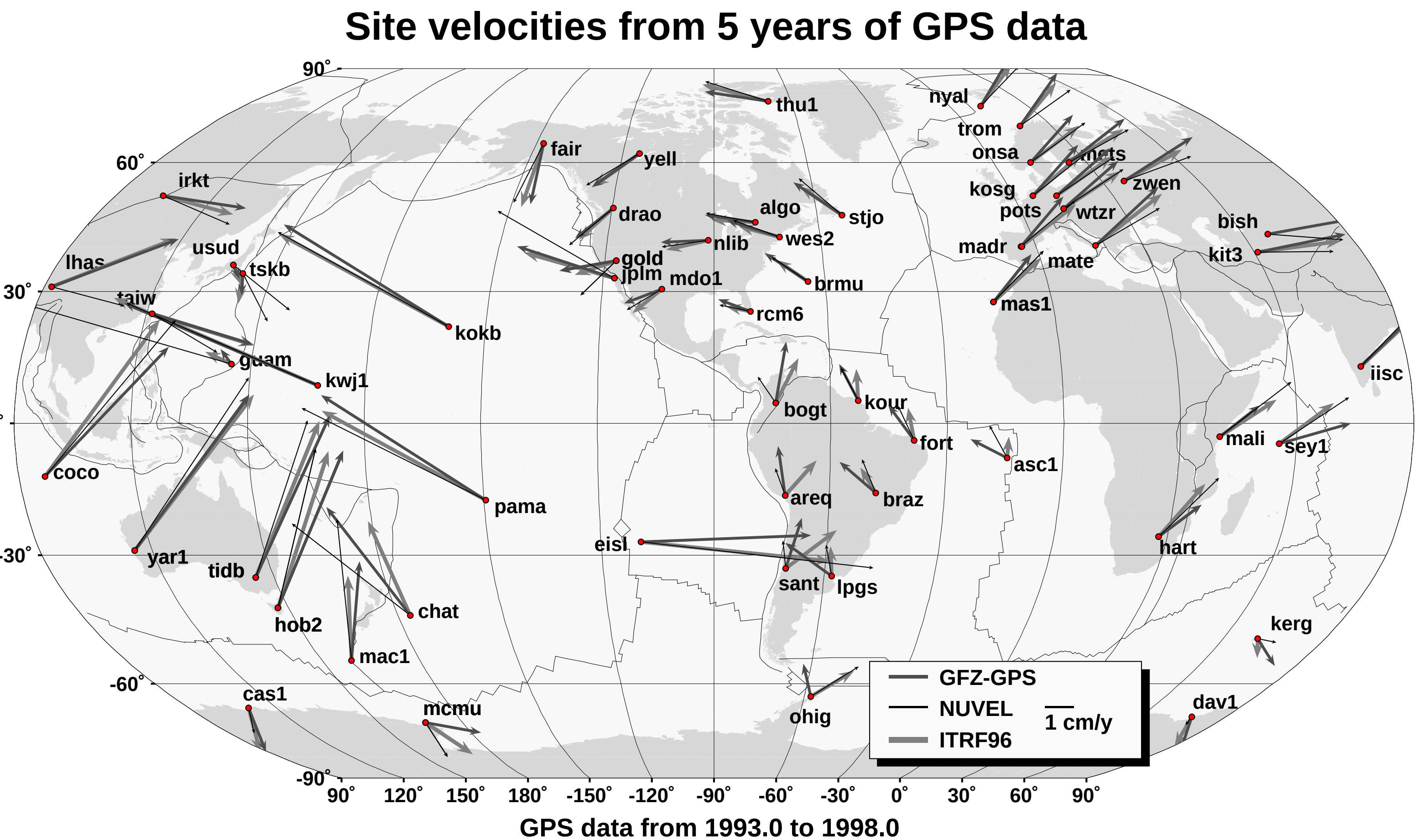

Figure 1.1: The GPS station velocities from 1993 to 1998. (from [Gendt et al., 1998])

While seismology has been able to provide information on recent crustal motions, geological past motions have been obtained from paleomagnetic data. Due to the broad nature of the earth dynamics and the emerging space and computer technology, various disciplines need to be involved in trying to answer the question 'when the movements may occur'. In geodetic science this problem has been dealt with mainly under recent vertical motions and particularly for local regions [Heck, 1984], [Zippelt, 1988]. With the coming of space technology, particularly GPS, Satellite- and Lunar Laser Ranging and VLBI, it has become possible to monitor geodynamically large regions including global areas.

Figure (1.1) shows the velocity vectors of some IGS stations located on various plates in comparison with those of NUVEL-1 and ITRF [Gendt et al., 1998]. The results from GPS observations over the five years agree fairly well with geological information indicating a maximum drift of the lithospheric plates of upto nearly 10cm per year (see also e.g [Lambeck, 1988]). This conformity emphasises the potential of the use of GPS in geodynamics in crustal deformation monitoring. Tectonic plate motions obtained from geological evidence have also been confirmed to agree with evidence from satellite laser ranging to *LAGEOS* [Smith et al., 1989].

Gravity changes on the order of $10^{-8}ms^{-2}$ per year are also experienced [Torge, 1980]. The integrated four-dimensional approach does not ignore the dependency of the observations on the gravity field and the integrated nature of the observation model is expected to yield the best possible results about the velocity vectors of surface points.

1.2 The Statement of the Problem

The shape of the earth and its gravity field upon which geodetic observables depend changes continuously with time due to dynamic processes taking place within the earth and also due to the attraction effects of the earth by third body effects - the moon, sun and the planets. The major tectonic plates of the earth have been shown to be in motion by use of geological methods and lately by use of GPS techniques ([Gendt et al., 1995]). For global and continental or regional networks these motions are normally taken care of by pheripheral models. The geodetic observables are reduced to a particular reference time and the network is computed for this particular time reference. The re-observation of the network is usually made after some time, say two or three years, and the shape of the network within this period can be then interpolated.

There are two discrete aspects as far as the observation of any geodetic network is concerned. These are:

- geodetic measurements are made at discrete points that make up the network, and
- geodetic measurements are made at discrete time epochs.

However, the elements of the gravity field and the time aspect upon which the geodetic measurements depend are continuous. If the ordinary methods of network computation are followed, then only positioning elements at the discrete network points and at discrete time epochs are obtained. What about the positioning elements at the other non-observation points of the network? Based on this reasoning the problem of study can be summarised as follows: equipped with discrete observations at discrete time epochs how can the positioning elements, not only at the discrete network points, but also those of other points as well as between measurement epochs, be estimated while taking into account the dependency of the measurements on the continuous nature of gravity field and time?

In this study a model for computation of a four-dimensional integrated network taking into consideration all available common geodetic observables within a unified adjustment model is proposed. The proposed model is an extension of the three-dimensional integrated case into a four-dimensional situation considering that the network measurements are made only at a few points while the network displacements occur at an infinite number of points (i. e. over the continuum). From measurements we can determine displacements at network points only. *What are the displacements in other points outside those of the network points*? Put in another way, *how can the estimation of displacements in space be continued or propagated*?

The geodetic observations are made at a given time epoch, say within a week, short enough for there to be no changes in the observables. If a campaign is performed at some other epoch, then we would wish to know how the displacements changed with time. The question asked is *how can the estimation of displacements within the time interval of observation campaigns be continued*? Figure (1.2) is a two-dimensional discrete- epoch model representation with one axis showing time and the others are *spatial axes*. The spatial axis are related to the elements of a three-dimensional integrated geodesy while the time axis consists of campaign epochs. The aim is to determine the geometrical elements of positioning as well as the physical aspects concerning the gravity field when their temporal variations are considered as continuous.

As part of the main problem of study and taking into account the promising future of the GPS in crustal deformation studies, it was found necessary to carry out a study leading to improved GPS evaluation and in particular the calibration of the GPS antenna.

1.3 Outline of the Report

An overview about the past developments and possibilities of four-dimensional geodesy is provided in Chapter Two. Following the model of three-dimensional integrated geodesy, a model of four-dimensional geodesy is derived in Chapter Three. Observation equations for common geodetic observables, both terrestrial and spatial are derived in Chapter Four according to the model of four-dimensional geodesy derived in Chapter Three. In Chapter Five possibilities of handling the parameters appearing in the four-dimensional model mentioned above are discussed. In particular, covariance functions for signals appearing in this model are derived. Some test results are presented in Chapter Six to demonstrate the application of the proposed model of four-dimensional networks. Conclusions are presented in Chapter Seven and a GPS anntena calibration test and results are reported in Appendix A.

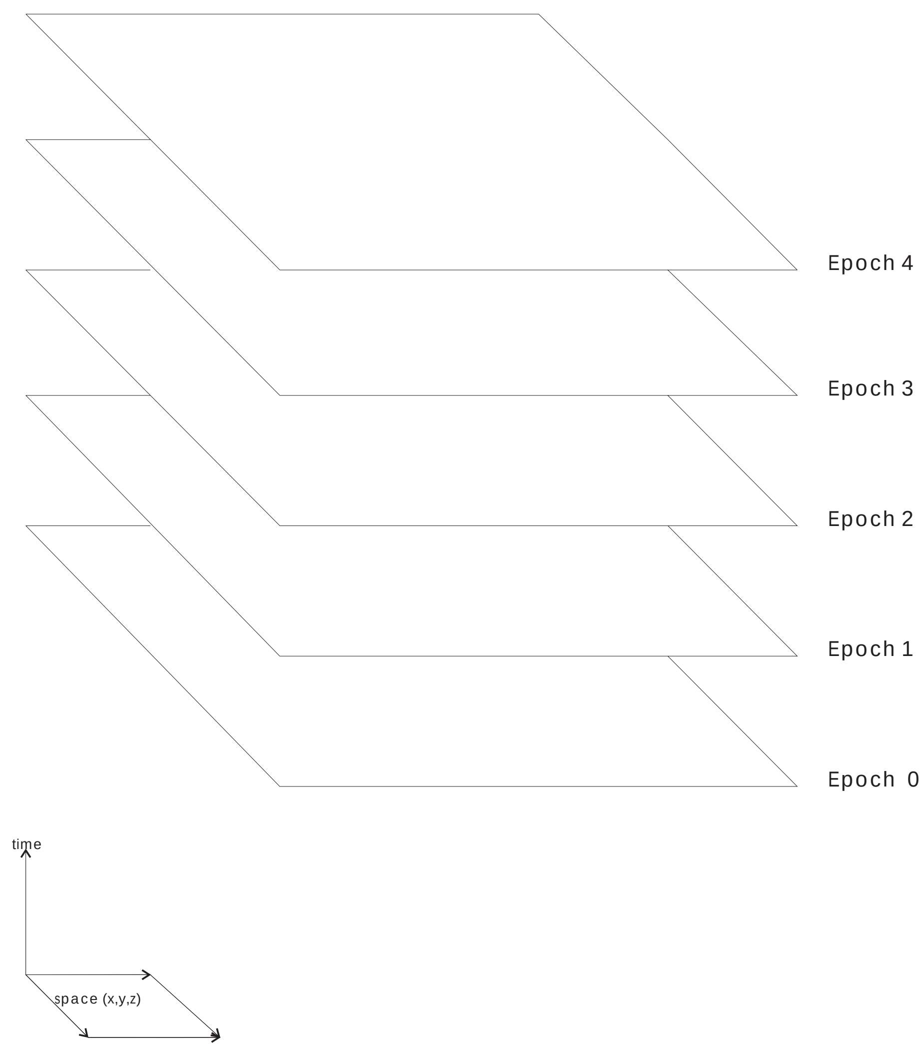

Figure 1.2: Diagramatic illustration of space and time - discrete epoch model

2. Historical Development of Four-dimensional Geodesy

2.1 General Remarks

The earth appears as a rigid structure that does not undergo deformation when viewed with respect to the life span of a human being. A few exceptions occur when such events like powerful earthquakes occur and tear apart parts of the earth's crust suddenly. However, when the earth dynamics is studied over a long period of time, say thousands or millions of years, the picture is different. Paleomagnetic evidence indicates that the earth must have undergone strong deformations over the years. Again seismological instruments register continuous but small motions. Two scenerios are thus evident: low frequency dynamic phenomena (from paleomagnetic evidence) and a high frequency one (from seismology). A middle frequency dynamic phenomenon is required to link and complete the above deformation spectrum (see also [Lambeck, 1989a]).

Improved instrumentation in geodetic science has led to observations whose low noise level can reveal deformation effects that occur within geodetic operation periods while the determination of that part of the deformation spectrum that occurs very slowly still remains the task of geology. Geodetic operation periods vary between a few minutes or hours to even a century. Geodesy then fits well to serve as the missing link between the low frequency paleomagnetic evidence and the high frequency seismological evidence in the deformation spectrum. A summary of this link is given in Figure (2.1). At the ends of either side (paleomagnetic or seismological) the geodetic link serves as a check.

From repeated geodetic data, displacements are obtained and are transformed into strain and relative velocities which can be directly compared with paleomagnetic evidence.

2.2 The Beginning of Four-dimensional Geodesy

In section 1.1 the development of classical geodetic networks through the purely geometrical three-dimensional networks and finally the three-dimensional integrated geodesy was discussed in detail. A common feature that seems to have triggered each development is the increased demand for higher accuracy in geodetic positioning and also improvement in geodetic instrumentation. Nowadays the invention of space surveying techniques, par-

Paleomagnetic data	geodetic data	seismological data

low frequency — high frequency

Figure 2.1: Summary of crustal deformation spectrum

ticularly the GPS and the VLBI, have continued to exert the pressure for more precise geodetic positioning models to compete with the high precision measurement they are offering as it was mentioned in the last section. This means that the high reputation three-dimensional integrated geodesy of the last two decades is not the culmination for the quest of highly precise modelling of geodetic networks. This development will be briefly reviewed in the following discussion.

An improvement of the three-dimensional integrated geodesy brings into consideration the time dependency of the geodetic observables and also the time dependency on the gravity potential functionals upon which most geodetic observations depend. The introduction of this time dependency on the three-dimensional integrated geodesy leads to four-dimensional geodesy. A brief review of three- dimensional geodesy leading to the coming of four-dimensional geodesy follows.

The three-dimensional integrated geodesy implies integrated data processing in which all available and relevant data are used for the determination of the coordinates and gravity potential in one unified model. The traditional reductions of observations which lead to horizontal and vertical networks or even reductions based on normal gravity field resulting in purely geometric three-dimensional networks are avoided. In integrated geodesy the remaining part of the disturbing potential is taken into account.

The present concept of integrated geodesy was introduced by [Krarup, 1971], [Eeg and Krarup, 1975] and various works on integrated three-dimensional geodesy are found in [Moritz, 1973], [Grafarend, 1978a], [Grafarend, 1978b], [Grafarend, 1981], [Hein and Landau, 1989] [Hein, 1986], [Hein et al., 1987]. Further relevant work is also reported in [Aduol, 1989], [Jinsheng et al., 1992], [Dermanis, 1991a], [Dong et al., 1998] among others. Also in [Schaffrin, 1986] estimation and prediction techniques for determination of crustal deformations when prior information, e. g. in the form of geophysical data is available are discussed.

Four-dimensional geodesy on the other hand deals with processing of integrated geodetic observations in order to analyse the network geometry and its variation with time, when these observations depend on the gravity field of the earth and its temporal variation. Thus the time dimension is introduced into the three-dimensional integrated model. Previous work on four-dimensional geodesy is reported in [Grafarend, 1979], [Grafarend, 1982], [Collier et al., 1988], [Dermanis and Rossikopoulos, 1988] and [Dermanis, 1991b] just to mention a few.

Integrated geodesy is also referred to as operational geodesy. It is operational in that it uses the available observations to extract all possible geodetic information as opposed to the model approach whereby a model is first designed and then limits itself only to some particular data. The situation in geodesy today is that a lot of different types of data is available. Therefore, in order to realise the goal of the determination of the shape of the earth and its (external) gravity field e.g. [Torge, 1980] presently, the problem should be best approached from the operational way.

As geodesy became involved in geophysical research, at least in studies involving crustal deformations, contradictions within the discipline emerged. For example geodetic positions once determined are treated and published as if they are time invariant information. Furthermore the classical approach of positioning was used which separated the three-dimensional approach within which displacements occur.

In order to harmonise the operations of geodetic positioning, the *IAG* appointed a *Special Study Group 4.96* in 1983 at the *IUGG* Assembly in Hamburg to study models in four-dimensional positioning. The rationale for appointing this group is summarised in the following quotation [Vanicek et al., 1987]: "*There is a clear dichotomy in the present approaches to geodetic positioning, both horizontal and vertical. On the one hand, positioning (terrestrial and extra-terrestrial) is used to detect and quantify the movements (deformations) of the earth's surface. .... On the other hand, positions (of control network points) are published and treated in most other applications as invariant in time except perhaps in regions of very significant co-seismic movements, ...*" The study group looked into matters concerning the causes of deformations with a view to mapping out strategies for four-dimensional positioning.

The forces leading to earth deformations are in general not known. However it is believed that secular, periodic and episodic deformations occur. If the whole spectrum of forces or the deformation is known, then this may explain some of the mysteries of the earth, for example, the rise in sea level and also help in weather and earthquake prediction etc.

2.3 Suitability of Classical Geodetic Networks in Four-Dimensional Positioning

Classical national networks consist of a horizontal and a vertical network. Both types of networks were established in some hierachical order. The first order networks consisted of widely spaced points or marks and were of higher accuracy than lower order networks. The lower order networks were a densification of the higher order networks.

The horizontal first order networks were formed by means of triangulation and network points had to be established at higher grounds where intervisibility was assured. The scale of the network was provided for by measuring a baseline. Lower order networks were established by means of both triangulation and a system of traverses. Due to the requirement of intervisibility more often than not extra auxiliary survey points had to be established to enable the control reach desired areas.

In the computation of the horizontal control, the three-dimensional space is projected onto a two-dimensional surface of a reference ellipsoid. This is done because of lack or poor quality observations of vertical angles and astronomical- latitudes and longitudes. The vertical angles measured during triangulation are used in determination of the height of the triangulation points at very low accuracies. In other areas observations like deflection of the vertical, heights and geoidal heights that are necessary for the projection of the three-dimensional space onto the two-dimensional reference surface are lacking. The result is a poor projection leading to distortions. In addition not all all measurements could be processed by use of least squares method due to lack of computing power. Sub-networks were each separately adjusted by non-rigorous methods which led to more errors.

In order to control the accuracy of geodetic networks, IAG at its *XIII* Assembly in 1963 set out a resolution requiring that the fundamental networks be established such that the standard error of relative positions between two points in an absolutely oriented system should not exceed $S/100,000$ or 10 ppm (S is the distance between the two points). Such accuracies are too low for applications concerning crustal motion studies considering that such accuracies allow a metre discrepancy in every hundred kilometres. It can be generally concluded that earlier data on horizontal positioning is thus not useful for earth deformation studies even for detection of non cyclic deformations.

The datum for the heights in national control networks is the mean sea level (MSL) which is assumed to coincide with the geoid. The MSL is determined by tide gauge measurements which have an accuracy of about 1 to 2 metres. Generally the MSL does not coincide with an equipotential surface and its departure from the geoid gives rise to sea surface topography (SST), see e. g. [Vanicek and Krakiwsky, 1982].

The spirit level and a levelling staff are used to determine the level of points further inland. Generally regional levelling networks have existed in some countries for about 100 years with gradual densification and probably with a clear repetition in about 50 years. Owing to the SST common points at the boundaries of national networks established using different tide gauges are expected to differ by an amount up to several metres. Older levelling networks have accuracies of about 1.5 to 4mm/$\sqrt{km}$ compared to present accuracies of 0.5 to 0.8mm/$\sqrt{km}$. Thus older levelling networks may be used in regional crustal motion investigations to some extent.

The modern trends in positioning point towards increased use of electronic devices and in particular space technology. The electronic distance measuring (EDM) instruments came into use in 1950's and have improved distance measurement accuracies since. Horizontal control has been provided by combined angular and distance measurements. The precision of EDM has reached about 0.5 to 5 ppm with EDM having capabilities of measuring distances to several tens of kilometres. Networks derived by means of EDM can be thus useful in investigating local and regional crustal motions.

The first of the satellite positioning techniques was the *Transit* system whose accuracies never exceeded about 30 cm for relative positioning. The problem was poor orbit determination, low quality oscillators and poor vehicle configuration. Observation periods were also too long. The result was that the quality of data from the *Transit* system was too low for crustal motion studies.

Next came the GPS that reached the full operational capability (FOC) in 1995. The system has a relative accuracy level of a couple of millimetres and is capable of measuring points hundreds of kilometers apart while still maintaining the high accuracy levels. The observation periods may range from a few minutes to a few hours. With improvement in modelling of further GPS error sources, GPS or similar satellite navigation systems are set to be the standard means of measurement in future positioning. The GPS provides three-dimensional coordinates of points or baselines referenced to a world geocentric coordinate system. The system has already been used in crustal deformation investigations on global extent (see Figure 1.1) and can be as well applied to both local and regional networks even in combination with triangulation data e. g. [Asteriadis and Schwan, 1998].

Other space techniques are the satellite laser ranging (SLR) and the VLBI methods. The SLR has relative accuracy of about 1 cm and is capable of positioning points several hundred kilometres apart. Most SLR equipment is built on permanent bases and this makes SLR only suitable as additional data source for global studies concerning crustal motions. The VLBI delivers the most accurate baselines over long distances (relative accuracies of 0.01 ppm have been reported). The system has no terrestrial limitation on distance separation between points and is readily useful in investigating global crustal motions. A further improvement in the VLBI system is the space VLBI (SVLBI) whereby the baseline distance is tremendously increased by mounting a VLBI antenna on to a satellite flying at high altitudes (say 30,000 km). The extended baseline between a ground antenna and a space antenna results to an equivalent single antenna with a diameter greater than the earth which in turn gives higher accuracies in baseline determinations (see e. g. [Adam, 1990], [Kulkarni, 1992]). SVLBI is expected to become an essential tool in crustal motions and one expects its application to be extended even to crustal motion studies of other space bodies, e. g. the moon.

3. The Integrated Four-dimensional Model

3.1 The Coordinate Reference Systems

3.1.1 Establishment of a Coordinate Reference System

Coordinate reference systems serve as the basis for description of positions in space. A geodetic coordinate system can be realised through a set of points regarded as fixed. However, while the earth is in continuous motion and deformable, for example through tides, plate motions, postglacial rebound, seismicity etc. (see also Chapter Two), there are no such fixed points in existence. Two principal types of reference systems are identified (see also [Moritz, 1979], [Mueller, 1982], [Mueller, 1988], [Heck, 1991]): the celestial reference system often used in geodetic astronomy and whose axes show no rotations. The other system is the terrestrial reference system which is defined with the origin at the geocenter. The terrestrial reference system is a quasi-inertial system because the origin shows some irregular motions.

The introduction of the aspect of time dependency in coordinate reference systems requires that the coordinate reference systems should not just serve as basis for position of points in the geometrical sense but should also carry an extra piece of information - *time*. Thus six positioning elements $(X, Y, Z, \dot{X}, \dot{Y}, \dot{Z})$ (the $(\dot{})$ represents station velocities) for description of position and velocity are required.

On a regional scale material points (network) on the earth's surface that are accessible to geodetic observations have to be put in place to act as the reference system. The network points can be observed using space techniques e.g. GPS satellite methods and at the initial epoch only the three geometrical coordinates (X, Y, Z) per station are estimated. A later epoch of observations of the same network can be adjusted under certain conditions, for example that there is no net rotation of the network (e.g. [Drewes, 1995], [Moritz, 1979]), so as to establish a deformation model. Each region can be divided into deformation zones depending on local motions and a *no net rotation model* used for adjustment. This way a kinematic reference system is established. The International Terrestrial Reference Frame (ITRF) reference system is established on similar basis as discussed above and regional networks (e.g. South American Geocentric Reference System [SIRGAS, 1997], [Kaniuth et al., 1996]) can be tied to it. It is here noted that a kinematic coordinate reference frame can be used to provide the provisional displacement field required by some of the approaches for four-dimensional geodesy discussed in Chapter Five.

The usual positioning of geodetic points is based on a choice of coordinate systems in a three-dimensional Euclidean space. Next are presented some of the coordinate systems in common use.

3.1.2 The Physical Coordinate System

The geocentric Cartesian coordinate system

The origin of this system is at the center of mass of the earth. The $Z^\bullet$ axis coincides with the average axis of the earth's rotation. The $X^\bullet$ axis is at right angles with $Z^\bullet$ axis and lies in the equatorial plane and is parallel to the Greenwich meridian. The $Y^\bullet$ axis is orthogonal to the $X^\bullet$ axis and completes the right-handed system. The positional vector of a point P is expressed in this system by the column vector $\mathbf{x}$

$$\mathbf{x} = \begin{bmatrix} X^\bullet \\ Y^\bullet \\ Z^\bullet \end{bmatrix}.$$

The curvilinear natural coordinate system

At point P the coordinates (Φ_P, Λ_P) defining the direction of the plumbline and the potential (W_P) are used as *natural coordinates* of the point P. The coordinates (Φ_P, Λ_P) are determined from observations of fixed stars. The differences of W_P with respect to some datum e.g. the geoid are obtained by means of spirit levelling combined with gravity measurements along the levelling line.

The local Cartesian coordinate system

This is a topocentric coordinate system with the origin at the observation point P. The Z^* axis points in the direction of the local zenith. The X^* axis is perpendicular to the Z^* axis but lying on the tangential plane to the equipotential surface at P and pointing in the direction of astronomical north. The Y^* axis is orthogonal to the X^* while lying on the same plane and points in the direction of east. The system is a left-handed one.

The position vector of a point P is expressed by the column vector $\mathbf{x}^*$

$$\mathbf{x}^* = \begin{bmatrix} X^* \\ Y^* \\ Z^* \end{bmatrix}.$$

3.1.3 The Model Coordinate System

This system is based on some conventionally chosen reference frame, mostly related to a reference ellipsoid. As above, an ellipsoidal- global cartesian, curvilinear and local coordinate systems are derived.

The ellipsoidal Cartesian coordinate system

The $z^\bullet$ axis coincides with the semi-minor axis of the ellipsoid and is positive in the in the direction of the north pole. The $x^\bullet y^\bullet$- plane is orthogonal to the $z^\bullet$- axis, thus coinciding with the model equatorial plane. The direction of $x^\bullet$ is that of Greenwich while $y^\bullet$ is perpendicular to $x^\bullet$ and completes the right-handed system.

The position vector of a point P is expressed in this system by the column vector $\mathbf{x}^\bullet$

$$\mathbf{x}^\bullet = \begin{bmatrix} x^\bullet \\ y^\bullet \\ z^\bullet \end{bmatrix}.$$

The ellipsoidal curvilinear coordinate system

The ellipsoidal latitude φ is the angle between the ellipsoidal normal at P and the ellipsoidal equator. The ellipsoidal longitude λ is the angle between the meridian containing the $x^\bullet$- axis and the meridian passing through P. The ellipsoidal height h is the distance between the ellipsoidal surface and the point P as measured along the ellipsoidal normal.

3.1.4 The Epoch Coordinate Transformation

Different observations may be related to different coordinate systems. In order to make the computations in one coordinate system, coordinate transformations have to be done. Rotation matrices $\mathbf{R}$ are used in all coordinate transformations involving two orthonormal frames, e. g. $\mathbf{x}$ and $\mathbf{x}'$. The two frames are related as $\mathbf{x}' = \mathbf{R}\mathbf{x}$ where $\mathbf{x} = [X, Y, Z]^T$ and $\mathbf{x}' = [X', Y', Z']^T$ with $\mathbf{R}$ being either a *Euler matrix*, $\mathbf{R}_E(\epsilon_1, \epsilon_2, \epsilon_3) = \mathbf{R}_3(\epsilon_1)\mathbf{R}_2(\frac{\pi}{2} - \epsilon_2)\mathbf{R}_3(\epsilon_3)$ or the *Cardanian* matrix, $\mathbf{R}_C(\epsilon_1, \epsilon_2, \epsilon_3) = \mathbf{R}_3(\epsilon_3)\mathbf{R}_2(\epsilon_2)\mathbf{R}_1(\epsilon_1)$. The components of the matrix $\mathbf{R}$ are

$$\mathbf{R}_1(\epsilon_1) = \begin{bmatrix} 1 & 0 & 0 \\ 0 & \cos\epsilon_1 & \sin\epsilon_1 \\ 0 & -\sin\epsilon_1 & \cos\epsilon_1 \end{bmatrix}$$

$$\mathbf{R}_2(\epsilon_2) = \begin{bmatrix} \cos\epsilon_2 & 0 & -\sin\epsilon_2 \\ 0 & 1 & 0 \\ \sin\epsilon_1 & 0 & \cos\epsilon_2 \end{bmatrix}$$

$$\mathbf{R}_3(\epsilon_3) = \begin{bmatrix} \cos\epsilon_3 & \sin\epsilon_3 & 0 \\ -\sin\epsilon_3 & \cos\epsilon_3 & 0 \\ 0 & 0 & 1 \end{bmatrix}$$

where $\epsilon_1, \epsilon_2, \epsilon_3$ are rotation angles about respective coordinate axes. Transformations of the frames discussed above are visualised by means of a commutative diagram (see [Grafarend and Richter, 1978]).

3.2 Similarity Transformations

In four-dimensional geodesy observations are repeated at different time epochs (refer to Figure (1.2)) which results to a discrete time situation. When these observations are described with respect to some coordinate frame, there exists a datum problem at each epoch and all epoch solutions need to be interrelated to each other in some way. The choice of datum at each epoch can give rise to apparent deformations if datum dependent parameters such as coordinates are used. In order to avoid this situation the practice is to solve the datum problem at the initial epoch t_o and then use this datum definition to solve for all other epochs. This way ensures that the choice of datum for all epochs is close together as much as possible.

The epoch solutions can be interrelated together either by a similarity transformation when no distances or distances from different groups are involved e.g. EDM and GPS derived baselines or by orthogonal transformations when distances have been observed.

Let $\mathbf{x}_o(t_o)$ be the datum definition at the initial epoch and $\mathbf{x}_i$ be a datum definition at the $i-th$ epoch. The solution $\mathbf{x}_o(t_o)$ can be transformed onto the solution at the $i-th$ epoch by the similarity transformation

$$\mathbf{x}_i = \lambda \mathbf{R}(\theta)\mathbf{x}_o(t_o) + \mathbf{t}. \tag{3.1}$$

The parameters are three rotation angles (θ), three displacement parameters $(\mathbf{t})$, a scale factor λ and the time element t upon which the coordinate vector $\mathbf{x}_o$ depends.

The orthogonal transformation is expressed as

$$\mathbf{x}_i = \mathbf{R}(\theta)\mathbf{x}_o(t_o) + \mathbf{t}. \tag{3.2}$$

where the scale factor λ has now been omitted.

In cases where the geodetic observations are registered on a *continuous* basis, for example the *Permanent Geodetic Survey Array (PGSA)* in South California [Bevis et al., 1997] and the *National GPS Array in Japan* [Tsuji et al., 1995], the transformation parameters are replaced by time dependend functions [Dermanis, 1995]. Thus the similarity transformation becomes

$$\mathbf{x}_i(t) = \lambda(t)\mathbf{R}(\theta(t))\mathbf{x}_o(t) + \mathbf{t}(t) \tag{3.3}$$

and the orthogonal transformation becomes

$$\mathbf{x}_i(t) = \mathbf{R}(\theta(t))\mathbf{x}_o(t) + \mathbf{t}(t). \tag{3.4}$$

3.3 The Integrated Model in a Three-dimensional Space

The three-dimensional integrated model is here briefly outlined since it provides the basic form from which the four-dimensional integrated model is developed.

Consider the observation l that depends on the position $\mathbf{x}$ and the gravity potential functional $LW(\mathbf{x})$. The operator L is in general a non-linear operator acting on W. The observation l may thus depend in various forms on the potential W, for example the gravity potential W in case of potential differences or the derivatives of W in case of absolute gravity. The gravity potential W is usually decomposed into two components: the gravitational potential V and the centrifugal potential Φ.

Symbolically the dependency of the observation on the position vector and the potential functional can be represented as follows:

$$l = F(\mathbf{x}, LW(\mathbf{x})) \tag{3.5}$$

with

$$\mathbf{x} = \begin{bmatrix} X \\ Y \\ Z \end{bmatrix},$$

$$W = V + \Phi$$

and

$$\Phi = \frac{1}{2}\omega^2 r^2 \cos^2 \overline{\varphi}, \quad \text{where } r = (X^2 + Y^2 + Z^2)^{1/2}$$

and $\overline{\varphi}$ is the geocentric latitude. The position vector $\mathbf{x}$ is defined with respect to a fixed origin O (e.g the geocenter).

It is now aimed at determining the positions of material points on the surface (or in external space) of the earth and the gravity potential function on and outside the earth's surface. The gravity potential functional $LW(\mathbf{x})$ and the function F are nonlinear functions of position $\mathbf{x}$. These functions are linearised using Taylor series approximations with linear terms only.

A model form of W denoted by U is identified. U is the normal or reference potential e.g. Somigliana-Pizzetti field or a low degree spherical harmonic expansion. The normal potential is a known function of position, given by an analytical expression. W can be decomposed into this known model part U and an unknown part T - the disturbing potential [Heiskanen and Moritz, 1967]. The true position vector $\mathbf{x}$ is similarly decomposed into a known, approximate position $\mathbf{x}^o$ and a residual, unknown part $\Delta\mathbf{x}$. Thus

$$\begin{aligned} \mathbf{x} &= \mathbf{x}^o + \Delta\mathbf{x} \\ W &= U + T \end{aligned} \tag{3.6}$$

where $\mathbf{x}^o$ consists of approximate values of $\mathbf{x}$ and $\Delta\mathbf{x}$ are unknown parameters to be added to the approximate values of $\mathbf{x}^o$. Like the gravitative part of the normal potential function U, the disturbing potential function T is also harmonic outside the attracting masses. Thus the Laplacian of T

$$Lap \quad T = 0.$$

Then the linearization of equation (3.5) can be related to the *Taylor point* $(\mathbf{x}^o, U)$.

For the three-dimensional integrated geodesy, the general linearized observation equation is of the form e.g [Hein, 1986]

$$\Delta\mathbf{l} = \mathbf{A}\Delta\mathbf{x} + LT + \mathbf{v} \tag{3.7}$$

$\Delta\mathbf{l}$ is the column vector of reduced observation in the sense *observed minus computed.* The linear operator L acts on the disturbing potential T and $\mathbf{v}$ is an inconsistency random column vector of observational errors.

Various methods for the solution of (3.7) have been proposed and applied by various authors e.g. [Moritz, 1978], [Grafarend, 1978b] depending on how the operator L is applied (see also section 3.1).

3.4 The Integrated Four-dimensional Model

In order to derive the basic model of four-dimensional integrated geodesy, the concept of three-dimensional integrated geodesy is applied but now considering the time dependency of the observations as well as the coordinates and the disturbing potential. Following equation (3.5) in the previous section the observation l is expressed as a function of time as

$$l(t) = F(\mathbf{x}(t), LW(\mathbf{x}(t), t)). \tag{3.8}$$

The argument t is used to indicate an arbitrary epoch while t_o refers to the reference epoch, usually taken as the initial epoch of the measurements.

The expression (3.8) represents the general functional form of four-dimensional geodesy. Simpler expressions are derived from this general model depending on whether the observations are influenced by the gravity potential or not; for example distance measurements are not dependent on the gravity field and therefore the gravity function W is discarded as follows:

$$l(t) = F(\mathbf{x}(t)) \tag{3.9}$$

In the derivation of the general model of four-dimensional geodesy the general functional form (3.8) is considered. The principles according to [Dermanis and Rossikopoulos, 1988] are also taken into account.

Considering the position vector of a material point $\mathbf{x}(t_o)$ at epoch t_o, $\mathbf{x}(t_o)$ can be expressed as a sum of the approximate coordinates $\mathbf{x}^o(t_o)$ at the initial epoch and a small increment $\Delta\mathbf{x}(t_o)$

$$\begin{aligned}
\mathbf{x}(t_o) &= \mathbf{x}^o(t_o) + \Delta\mathbf{x}(t_o) \text{ at the initial epoch } t_o \\
\mathbf{x}(t) &= \mathbf{x}(t_o) + \delta\mathbf{x}(t) \text{ at epoch } t \\
&= \mathbf{x}^o(t_o) + \Delta\mathbf{x}(t_o) + \delta\mathbf{x}(t) \\
&= \mathbf{x}^o(t_o) + \Delta\mathbf{x}(t)
\end{aligned} \tag{3.10}$$

where $\mathbf{x}^o(t_o)$ refers to the approximate position vector at the reference epoch t_o $(t > t_o)$, $\Delta\mathbf{x}(t) = \Delta\mathbf{x}(t_o) + \delta\mathbf{x}(t)$ is the difference between the approximate coordinates at the fixed epoch t_o and the true coordinates of a material point at an arbitrary epoch t. This quantity consists of the discrepancy between the approximate coordinates at epoch t_o $(\Delta\mathbf{x}(t_o))$ and coordinate changes between epochs t_o and t due to temporal position changes giving rise to a displacement $\delta\mathbf{x}(t)$.

The potential W is also decomposed into a model part U and a disturbing part T as follows:

$$W(\mathbf{x}(t), t) = U(\mathbf{x}(t)) + T(\mathbf{x}(t), t) \tag{3.11}$$

The approximate coordinates are considered time independent i.e. $\mathbf{x}^o(t) = \mathbf{x}^o(t_o)$ and therefore constant for all epochs, and the model potential U remains fixed in time. However, due to the movement of the points, U also changes according to $U(\mathbf{x}^o(t_o)) \to U(\mathbf{x}(t))$. The potential U remains time independent as far as fixed points in space are considered.

The model potential U usually contains all available (the best) prior information about the potential function. Further, the model part U can be decomposed into a *simple* part (e.g the Somigliana- Pizzetti field) and a computable second part describing the shorter wavelength features.

The disturbing potential function is further decomposed into two components: the part at the initial epoch $T(\mathbf{x}(t), t_o) = W(\mathbf{x}(t), t_o) - U(\mathbf{x}(t), t_o)$ and the part corresponding to the temporal change of the potential function at a fixed point in space denoted by

$\delta T(\mathbf{x}(t),t)$. It is assumed that the temporal positional changes induce negligible changes in the potential function so that $T(\mathbf{x}(t_o),t_o) \approx T(\mathbf{x}(t),t_o)$, which is consistent with the postulated degree of approximation. From here onwards the notation $T(\mathbf{x}(t_o),t_o)$ will be used to imply either of the two representations. Thus

$$\begin{aligned} T(\mathbf{x}(t),t) &= T(\mathbf{x}(t),t_o) + \delta T(\mathbf{x}(t),t) \\ &\approx \quad T(\mathbf{x}(t_o),t_o) + \delta T(\mathbf{x}(t),t). \end{aligned} \tag{3.12}$$

Introducing the decomposed position vector (3.10) into the disturbing potential function (3.12), the disturbing potential function can be written as

$$\begin{aligned} T(\mathbf{x}(t),t) = T[\mathbf{x}^o(t_o) + \Delta\mathbf{x}(t_o) + \delta\mathbf{x}(t), t_o] \\ +\delta T[\mathbf{x}^o(t_o) + \Delta\mathbf{x}(t_o) + \delta\mathbf{x}(t), t] \end{aligned} \tag{3.13}$$

Linearization of equation (3.13) gives

$$\begin{aligned} T(\mathbf{x}(t),t) &= \\ &= T(\mathbf{x}^o(t_o),t_o) + grad_x T(\mathbf{x}^o(t_o),t_o) \cdot [\Delta\mathbf{x}(t_o) + \delta\mathbf{x}(t)] \\ &+ \underbrace{\delta T(\mathbf{x}^o(t_o),t)}_{\textit{potential change } W(t_o) \rightarrow W(t)} \\ &+ \underbrace{grad_x \delta T(\mathbf{x}^o(t_o),t_o) \cdot (\Delta\mathbf{x}(t_o) + \delta\mathbf{x}(t))}_{\textit{influence on potential due to displacement - negligible.}} \end{aligned} \tag{3.14}$$

The second braced part in (3.14) is a second order quantity of δT and can be neglected as being small.

Considering (3.11) and substituting (3.10), $W(\mathbf{x}(t),t)$ can be expressed as

$$\begin{aligned} W(\mathbf{x}(t),t) = & \quad U(\mathbf{x}(t)) + T(\mathbf{x}(t),t) \\ = & \quad U[\mathbf{x}^o(t_o) + \Delta\mathbf{x}(t_o) + \delta\mathbf{x}(t)] + T(\mathbf{x}(t),t). \end{aligned} \tag{3.15}$$

Linearization gives

$$\begin{aligned} W(\mathbf{x}(t),t) &= \\ &= U(\mathbf{x}^o(t_o)) + \boldsymbol{\gamma}(\mathbf{x}^o(t_o),t_o)^T \cdot (\Delta\mathbf{x}(t_o) + \delta\mathbf{x}(t)) \\ &+ T(\mathbf{x}^o(t_o),t_o) + \delta T(\mathbf{x}^o(t_o),t) \\ &+ \underbrace{grad_x T(\mathbf{x}^o(t_o),t_o) \cdot (\Delta\mathbf{x}(t_o) + \delta\mathbf{x}(t))}_{\textit{negligible}} \\ &+ \underbrace{grad_x \delta T(\mathbf{x}^o(t_o),t_o)) \cdot (\Delta\mathbf{x}(t_o) + \delta\mathbf{x}(t))}_{\textit{influence on potential due to displacement - negligible.}} \end{aligned} \tag{3.16}$$

Using equations (3.10) and (3.16) the observation functional $l(t)$ in equation (3.8) can be written in the form

$$
\begin{aligned}
l(t) &= F(\mathbf{x}(t), LW(\mathbf{x}(t), t)) \\
&= F\{\mathbf{x}^o(t_o) + \Delta\mathbf{x}(t_o) + \delta\mathbf{x}(t), LW(\mathbf{x}^o(t_o) + \Delta\mathbf{x}(t_o) + \delta\mathbf{x}(t), t)\}.
\end{aligned}
\tag{3.17}
$$

Linearization of (3.17) yields

$$
\begin{aligned}
l(t)- & \quad F\{\mathbf{x}^o(t_o), LU(\mathbf{x}^o(t_o))\} \\
= & \quad grad_x F[\mathbf{x}^o(t_o), LU(\mathbf{x}^o(t_o))] \cdot (\Delta\mathbf{x}(t_o) + \delta\mathbf{x}(t)) \\
+ & \quad \tfrac{\partial F}{\partial LU}(\mathbf{x}^o(t_o), LU(\mathbf{x}^o(t_o))) \cdot \{grad_x LU(\mathbf{x}^o(t_o)) \cdot (\Delta\mathbf{x}(t_o) + \delta\mathbf{x}(t)) \\
+ & \quad L(T(\mathbf{x}^o(t_o), t_o) + \delta T(\mathbf{x}^o(t_o), t))\}.
\end{aligned}
\tag{3.18}
$$

Rearranging equation (3.18) gives

$$
\begin{aligned}
l(t) - F\{\mathbf{x}^o(t_o), LU(\mathbf{x}^o(t_o))\} &= \\
\{grad_x F[\mathbf{x}^o(t_o), LU(\mathbf{x}^o(t_o))] + \frac{\partial F}{\partial LU}(\mathbf{x}^o(t_o), LU(\mathbf{x}^o(t_o))) \cdot grad_x LU(\mathbf{x}^o(t_o))\} & \\
\cdot(\Delta\mathbf{x}(t_o) + \delta\mathbf{x}(t)) + \frac{\partial F}{\partial LU}(\mathbf{x}^o(t_o), LU(\mathbf{x}^o(t_o))) & \\
\{L(T(\mathbf{x}^o(t_o), t_o) + \delta T(\mathbf{x}^o(t_o), t))\}. &
\end{aligned}
\tag{3.19}
$$

Adding the observational noise v_i, equation (3.19) can be written using simpler notation as

$$
y_i = \mathbf{A}_i \cdot (\Delta\mathbf{x}(t_o) + \delta\mathbf{x}(t)) + B_i T(\mathbf{x}^o(t_o), t_o) + B_i \delta T(\mathbf{x}^o(t_o), t) + v_i \tag{3.20}
$$

where i is the running number of observations, $\mathbf{A}_i$ is i-th row in the design matrix and B_i is a linear operator. Equation (3.19) or (3.20) becomes the general model of four-dimensional geodesy in the framework of operational geodesy. The next step is to derive the observation equations for each of the various geodetic observables according to (3.20).

4. Observation Equations for Integrated Four-dimensional Geodesy

4.1 The General Scheme for Purely Gravity Dependent Observables

The common purely gravity dependent observables are

- astronomical latitude Φ,
- astronomical longitude Λ,
- absolute gravity $\mathbf{\Gamma}$,
- gravity differences,
- potential differences.

These observables depend entirely on the functional LW either directly on W or through its derivatives and only relate to the position vector implicitly through LW.

The gravity vector $\mathbf{\Gamma}$ is related to the astronomical- latitude and longitude by e.g. [Heiskanen and Moritz, 1967] p. 57

$$-\mathbf{\Gamma} = \begin{bmatrix} , \cos\Phi\cos\Lambda \\ , \cos\Phi\sin\Lambda \\ , \sin\Phi \end{bmatrix} \tag{4.1}$$

and the gravity vector $\mathbf{\Gamma}$ is also the gradient of the gravity potential. Thus

$$-\mathbf{\Gamma} = gradW = \begin{bmatrix} W_X \\ W_Y \\ W_Z \end{bmatrix} \tag{4.2}$$

where

$$W_X = \frac{\partial W}{\partial X}, \qquad W_Y = \frac{\partial W}{\partial Y}, \qquad W_Z = \frac{\partial W}{\partial Z}. \tag{4.3}$$

X, Y, Z refer to a geocentric Cartesian coordinate system (see section (3.1.2)). Corresponding to the potential W is the reference potential U whose derivatives are denoted by U_X, U_Y, U_Z. The absolute gravity is denoted by $\boldsymbol{\gamma}$ where

$$-\boldsymbol{\gamma} = gradU = \begin{bmatrix} U_X \\ U_Y \\ U_Z \end{bmatrix}$$

and

$$U_X = \frac{\partial U}{\partial X}, \qquad U_Y = \frac{\partial U}{\partial Y}, \qquad U_Z = \frac{\partial U}{\partial Z}, \tag{4.4}$$

Transformation to curvilinear coordinates

$$\begin{bmatrix} U_X \\ U_Y \\ U_Z \end{bmatrix} = - \begin{bmatrix} \gamma \cos\phi_\gamma \cos\lambda_\gamma \\ \gamma \cos\phi_\gamma \sin\lambda_\gamma \\ \gamma \sin\phi_\gamma \end{bmatrix}. \tag{4.5}$$

The geocentric coordinates can be obtained from curvilinear coordinates by the following relationship

$$\begin{bmatrix} X \\ Y \\ Z \end{bmatrix} = \begin{bmatrix} (N+h)\cos\phi\cos\lambda \\ (N+h)\cos\phi\sin\lambda \\ (N(1-f)^2+h)\sin\phi \end{bmatrix}. \tag{4.6}$$

The coordinates $(\phi_\gamma, \lambda_\gamma)$ indicate the direction of the normal vertical and in general $\lambda_\gamma \equiv \lambda$ for a rotationally symmetric normal field while $\phi_\gamma \neq \phi$.

After linearization the gradient of the disturbing potential is represented in the following form:

$$\begin{aligned} \begin{bmatrix} T_X \\ T_Y \\ T_Z \end{bmatrix} &= \begin{bmatrix} W_X \\ W_Y \\ W_Z \end{bmatrix} - \begin{bmatrix} U_X \\ U_Y \\ U_Z \end{bmatrix} \\ &= \begin{bmatrix} -\sin\phi\cos\lambda & -\sin\lambda & \cos\phi\cos\lambda \\ -\sin\phi\sin\lambda & \cos\lambda & \cos\phi\sin\lambda \\ \cos\phi & 0 & \sin\phi \end{bmatrix} \cdot \begin{bmatrix} , -\gamma \\ \Phi - \phi_\gamma \\ \Lambda - \lambda_\gamma \end{bmatrix} \end{aligned} \tag{4.7}$$

The general observation equation of this group of observations is derived from the four-dimensional observation equation (3.19) as

$$\begin{aligned} & l(t) - F\{\mathbf{x}^o(t_o), \boldsymbol{\gamma}(\mathbf{x}^o(t_o))\} = \\ = & [grad_{\boldsymbol{\gamma}} F(\mathbf{x}^o(t_o), \boldsymbol{\gamma}(\mathbf{x}^o(t_o)))]^T \cdot grad_{\mathbf{x}} \boldsymbol{\gamma}(\mathbf{x}^o(t_o)) \cdot (\Delta \mathbf{x}(t_o) + \delta \mathbf{x}(t)) \\ + & [grad_{\boldsymbol{\gamma}} F(\mathbf{x}^o(t_o), \boldsymbol{\gamma}(\mathbf{x}^o(t_o)))]^T \cdot grad_{\mathbf{x}} (T(\mathbf{x}^o(t_o), t_o) + \delta T(\mathbf{x}^o(t_o), t)). \end{aligned} \tag{4.8}$$

The derivative of F with respect to the position vector $\mathbf{x}$ as seen in the general linearised equation (3.19) vanishes since this group of observations does not depend explicitly on the position vector $\mathbf{x}$, thus $grad_{\mathbf{x}} F \equiv 0$.

4.2 One Point Observations

4.2.1 Astronomical Latitude

Let $\Phi(t)$ denote the astronomical latitude observed at the standpoint P_1 at epoch t. The expression for astronomical latitude in terms of the potential W is

$$\begin{aligned} \Phi(t) &= \arctan \frac{-W_Z(\mathbf{x}(t))}{\sqrt{[W_X(\mathbf{x}(t))^2 + W_Y(\mathbf{x}(t))^2]}} \\ &= F(\mathbf{x}(t), LW(\mathbf{x}(t), t)) \end{aligned} \tag{4.9}$$

or in symbolical vectorial form e.g [Heck, 1987]

$$\Phi(t) = \arcsin\left(< \mathbf{n}, \mathbf{f}_3 >\right) \tag{4.10}$$

where $<,>$ denotes the inner or dot product of vectors and W_X, W_Y, W_Z denote the first derivatives of W with respect to the coordinate directions indicated by the indices. $\mathbf{n}$ is the unit vector in the direction of local zenith while $\mathbf{f}_i \quad (i = 1(1)3)$ are base vectors of a global quasi-geocentric orthonormal system with $\mathbf{f}_3$ coinciding with the earth's axis of rotation.

From (4.8) and considering a time independent normal gravity field the following is established:

$$F\{\mathbf{x}, \boldsymbol{\gamma}(\mathbf{x})\} := \arctan \frac{-\gamma_Z(\mathbf{x})}{\sqrt{((\gamma_X(\mathbf{x}))^2 + (\gamma_Y(\mathbf{x}))^2)}} = \phi(\mathbf{x}) \tag{4.11}$$

$$[grad_{\boldsymbol{\gamma}} F\{\mathbf{x}, \boldsymbol{\gamma}(\mathbf{x})\}]^T = \frac{1}{\gamma^2} \cdot \begin{bmatrix} \frac{\gamma_X \gamma_Z}{\sqrt{((\gamma_X(\mathbf{x}))^2 + (\gamma_Y(\mathbf{x}))^2)}} \\ \frac{\gamma_Y \gamma_Z}{\sqrt{((\gamma_X(\mathbf{x}))^2 + (\gamma_Y(\mathbf{x}))^2)}} \\ -\sqrt{((\gamma_X(\mathbf{x}))^2 + (\gamma_Y(\mathbf{x}))^2)} \end{bmatrix} \tag{4.12}$$

$$grad_{\mathbf{X}}\boldsymbol{\gamma}(\mathbf{x}^o(t_o)) = \begin{bmatrix} U_{XX} & U_{XY} & U_{XZ} \\ U_{YX} & U_{YY} & U_{YZ} \\ U_{ZX} & U_{ZY} & U_{ZZ} \end{bmatrix} \tag{4.13}$$

$$grad_{\mathbf{X}}T(\mathbf{x}^o(t_o)) = \begin{bmatrix} T_X \\ T_Y \\ T_Z \end{bmatrix} \tag{4.14}$$

$$grad_{\mathbf{X}}\delta T(\mathbf{x}^o(t_o)) = \begin{bmatrix} \delta T_X \\ \delta T_Y \\ \delta T_Z \end{bmatrix} \tag{4.15}$$

Putting equations (4.11) through (4.15) into equation (4.8) gives the linearised equation for astronomical latitude in the form:

$$\Phi(t) - \phi(t_o) = \Delta\Phi_x + \delta\Phi_{\delta x} + \Phi_{TX} + \delta\Phi_{\delta TX} + v_\Phi \tag{4.16}$$

The signals appearing in equation (4.16) can be treated in various ways (see Chapter Five). Equation (4.16) is expanded to obtain the expression for the observation equation for astronomical latitude.

Using index *1* to indicate the stand point P_1 and further using letters to represent the associated coefficients, the observation equation for latitude is thus:

$$\begin{aligned} \Phi(t) - \phi(t_o) &= a_{1\Phi}\Delta X + b_{1\Phi}\Delta Y + c_{1\Phi}\Delta Z \\ &+ a_{1\Phi}\delta X + b_{1\Phi}\delta Y + c_{1\Phi}\delta Z \\ &+ d_{1\Phi}T_X + e_{1\Phi}T_Y + f_{1\Phi}T_Z \\ &+ d_{1\Phi}\delta T_X(t) + e_{1\Phi}\delta T_Y(t) + f_{1\Phi}\delta T_Z(t) + v_\Phi. \end{aligned} \tag{4.17}$$

The coefficients are

$$\begin{aligned} a_{1\Phi} &= \frac{U_Z}{\gamma^2 \cdot \sqrt{(U_X^2 + U_Y^2)}} \cdot [U_X \cdot U_{XX} + U_Y \cdot U_{YX}] - \frac{\sqrt{U_X^2 + U_Y^2} \cdot U_{ZX}}{\gamma^2} \\ b_{1\Phi} &= \frac{U_Z}{\gamma^2 \cdot \sqrt{(U_X^2 + U_Y^2)}} \cdot [U_X \cdot U_{XY} + U_Y \cdot U_{YY}] - \frac{\sqrt{U_X^2 + U_Y^2} \cdot U_{ZY}}{\gamma^2} \\ c_{1\Phi} &= \frac{U_Z}{\gamma^2 \cdot \sqrt{(U_X^2 + U_Y^2)}} \cdot [U_X \cdot U_{XZ} + U_Y \cdot U_{YZ}] - \frac{\sqrt{U_X^2 + U_Y^2} \cdot U_{ZZ}}{\gamma^2} \end{aligned}$$

$$
\begin{aligned}
d_{1\Phi} &= \frac{U_Z U_X}{\gamma^2 \cdot \sqrt{(U_X^2 + U_Y^2)}} \\
e_{1\Phi} &= \frac{U_Z U_Y}{\gamma^2 \cdot \sqrt{(U_X^2 + U_Y^2)}} \\
f_{1\Phi} &= -\frac{\sqrt{(U_X^2 + U_Y^2)}}{\gamma^2}
\end{aligned}
\tag{4.18}
$$

and

$$
\phi(t_o) = \arctan \frac{-U_Z(\mathbf{x}^o(t_o))}{\sqrt{[U_X(\mathbf{x}^o(t_o))^2 + U_Y(\mathbf{x}^o(t_o))^2]}} \tag{4.19}
$$

$$
\Delta t = t - t_o \tag{4.20}
$$

4.2.2 Astronomical Longitude

Like astronomical latitude, this observable is only implicitly related to the position vector $\mathbf{x}$. Both astronomical- latitude and longitude give the direction of the plumbline while the corresponding model values ϕ and λ give the orientation of the normal vertical.

Introducing a time argument in the usual equation for astronomical longitude (e.g [Heiskanen and Moritz, 1967]), the equation for astronomical longitude becomes:

$$
\begin{aligned}
\Lambda(t) &= \arctan \frac{W_Y(\mathbf{x}(t))}{W_X(\mathbf{x}(t))} \\
&= F(\mathbf{x}(t), LW(\mathbf{x}(t), t))
\end{aligned}
\tag{4.21}
$$

or in symbolic vectorial form [Heck, 1987]

$$
\Lambda = \arcsin (< \mathbf{n} \times \mathbf{f}_3, \mathbf{f}_1 >) \tag{4.22}
$$

where the symbol $\times$ indicates the cross product of vectors.

Considering a time independent normal gravity field, the general equation (4.8) has the following terms for the astronomical longitude:

$$
F\{\mathbf{x}, \boldsymbol{\gamma}(\mathbf{x})\} := \arctan \frac{\gamma_Y(\mathbf{x})}{\gamma_X(\mathbf{x})} = \lambda(\mathbf{x}) \tag{4.23}
$$

$$
[grad_{\boldsymbol{\gamma}} F\{\mathbf{x}, \boldsymbol{\gamma}(\mathbf{x})\}]^T = \frac{1}{(\gamma_X^2 + \gamma_Y^2)} \cdot \begin{bmatrix} -\gamma_Y \\ \gamma_X \\ 0 \end{bmatrix} \tag{4.24}
$$

$$grad_{\mathbf{X}}\boldsymbol{\gamma}(\mathbf{x}^o(t_o)) = \begin{bmatrix} U_{XX} & U_{XY} & U_{XZ} \\ U_{YX} & U_{YY} & U_{YZ} \\ U_{ZX} & U_{ZY} & U_{ZZ} \end{bmatrix} \tag{4.25}$$

$$grad_{\mathbf{X}}T(\mathbf{x}^o(t_o)) = \begin{bmatrix} T_X \\ T_Y \\ T_Z \end{bmatrix} \tag{4.26}$$

$$grad_{\mathbf{X}}\delta T(\mathbf{x}^o(t_o)) = \begin{bmatrix} \delta T_X \\ \delta T_Y \\ \delta T_Z \end{bmatrix} \tag{4.27}$$

Putting equations (4.23) through (4.27) into equation (4.8) gives the linearised equation for astronomical longitude in the form:

$$\Lambda(t) - \lambda(t_o) = \Delta\Lambda_x + \delta\Lambda_{\delta x} + \Lambda_{TX} + \delta\Lambda_{\delta TX} + v_\Lambda \tag{4.28}$$

$$\begin{aligned} \Lambda(t) - \lambda(t_o) &= a_{1\Lambda}\Delta X + b_{1\Lambda}\Delta Y + c_{1\Lambda}\Delta Z \\ &+ a_{1\Lambda}\delta X + b_{1\Lambda}\delta Y + c_{1\Lambda}\delta Z \\ &+ d_{1\Lambda}T_X + e_{1\Lambda}T_Y + f_{1\Lambda}T_Z \\ &+ d_{1\Lambda}\delta T_X(t) + e_{1\Lambda}\delta T_Y(t) + f_{1\Lambda}\delta T_Z(t) + v_\Lambda. \end{aligned} \tag{4.29}$$

The coefficients are expressed by the following functionals

$$\begin{aligned} a_{1\Lambda} &= \frac{1}{(U_X^2 + U_Y^2)} \cdot [-U_Y \cdot U_{XX} + U_X \cdot U_{YX}] \\ b_{1\Lambda} &= \frac{1}{(U_X^2 + U_Y^2)} \cdot [-U_Y \cdot U_{XY} + U_X \cdot U_{YY}] \\ c_{1\Lambda} &= \frac{1}{(U_X^2 + U_Y^2)} \cdot [-U_Y \cdot U_{XZ} + U_X \cdot U_{YZ}] \\ d_{1\Lambda} &= \frac{-U_Y}{(U_X^2 + U_Y^2)} \\ e_{1\Lambda} &= \frac{U_X}{(U_X^2 + U_Y^2)} \\ f_{1\Lambda} &= 0 \\ &\text{and} \\ \lambda(t_o) &= \arctan\frac{U_Y(\mathbf{x}^o(t_o))}{U_X(\mathbf{x}^o(t_o))}. \end{aligned} \tag{4.30}$$

4.2.3 Gravity Intensity

Let , (t) denote the gravity intensity at some network point P_1 and epoch t. The gravity intensity is expressed as the absolute value of the gradient of the gravity potential function as

$$
\begin{aligned}
,_1(t) &= \left[W_X^2(\mathbf{x}(t),t) + W_Y^2(\mathbf{x}(t),t) + W_Z^2(\mathbf{x}(t),t)\right]^{1/2} \\
&= F(LW(\mathbf{x}(t),t)) \qquad (4.31)
\end{aligned}
$$

having introduced a time argument. The model intensity of gravity is computed from the approximate coordinates at epoch t_o and is denoted by $\gamma(\mathbf{x}^o(t_o))$ and expressed as

$$\boldsymbol{\gamma}(t_o) = \left[U_X^2(\mathbf{x}^o(t_o),t_o) + U_Y^2(\mathbf{x}^o(t_o),t_o) + U_Z^2(\mathbf{x}^o(t_o),t_o)\right]^{1/2} \qquad (4.32)$$

Following equation (4.8), it is established that

$$F\{\mathbf{x}, \boldsymbol{\gamma}(\mathbf{x})\} := \sqrt{\gamma_X^2 + \gamma_Y^2 + \gamma_Z^2} \qquad (4.33)$$

$$[grad_{\boldsymbol{\gamma}} F\{\mathbf{x}, \boldsymbol{\gamma}(\mathbf{x})\}]^T = \frac{1}{\gamma} \cdot \begin{bmatrix} U_X \\ U_X \\ U_X \end{bmatrix} \qquad (4.34)$$

$$grad_{\mathbf{X}} \boldsymbol{\gamma}(\mathbf{x}^o(t_o)) = \begin{bmatrix} U_{XX} & U_{XY} & U_{XZ} \\ U_{YX} & U_{YY} & U_{YZ} \\ U_{ZX} & U_{ZY} & U_{ZZ} \end{bmatrix} \qquad (4.35)$$

$$grad_{\mathbf{X}} T(\mathbf{x}^o(t_o)) = \begin{bmatrix} T_X \\ T_Y \\ T_Z \end{bmatrix} \qquad (4.36)$$

$$grad_{\mathbf{X}} \delta T(\mathbf{x}^o(t_o)) = \begin{bmatrix} \delta T_X \\ \delta T_Y \\ \delta T_Z \end{bmatrix} \qquad (4.37)$$

Substituting equations (4.33) through (4.37) in equation (4.8) gives the linearised equation for gravity intensity as:

$$,(t) - \gamma^o(t_o) = \Delta ,_x + \delta ,_{\delta x} + \delta ,_{TX} + \delta ,_{\delta TX} + v_, \qquad (4.38)$$

which in a more explicit form and considering a discrete deterministic gravity field as before can be written as

$$
\begin{aligned}
\Gamma_1(t) - \gamma^o(t_o) &= \\
&= a_{1\Gamma}\Delta X + b_{1\Gamma}\Delta Y + c_{1\Gamma Z}\Delta Z \\
&+ a_{1\Gamma}\delta X + b_{1\Gamma}\delta Y + c_{1\Gamma}\delta Z \\
&+ d_{1\Gamma}T_X + e_{1\Gamma}T_Y + f_{1\Gamma}T_Z \\
&+ d_{1\Gamma}\delta T_X + e_{1\Gamma}\delta T_Y + f_{1\Gamma}\delta T_Z + v_\Gamma
\end{aligned}
\tag{4.39}
$$

with coefficients expressed by the following functionals:

$$
\begin{aligned}
a_{1\Gamma} &= \frac{1}{\gamma(\mathbf{x}^o(t_o))} \cdot (U_X \cdot U_{XX} + U_Y \cdot U_{YX} + U_Z \cdot U_{ZX}) \\
b_{1\Gamma} &= \frac{1}{\gamma(\mathbf{x}^o(t_o))} \cdot (U_X \cdot U_{XY} + U_Y \cdot U_{YY} + U_Z \cdot U_{ZY}) \\
c_{1\Gamma} &= \frac{1}{\gamma(\mathbf{x}^o(t_o))} \cdot (U_X \cdot U_{XZ} + U_Y \cdot U_{YZ} + U_Z \cdot U_{ZZ}) \\
d_{1\Gamma} &= \frac{U_X}{\gamma}(\mathbf{x}^o(t_o)) \\
e_{1\Gamma} &= \frac{U_Y}{\gamma}(\mathbf{x}^o(t_o)) \\
f_{1\Gamma} &= \frac{U_Z}{\gamma}(\mathbf{x}^o(t_o)).
\end{aligned}
\tag{4.40}
$$

4.3 Two Point Observations

4.3.1 Gravity Intensity Difference

The derivation of this observation equation follows that of the gravity intensity. Using subscripts to denote the gravity at different network points, at points P_1 and P_2, the gravity intensity at each of the two points is expressed as

$$
\begin{aligned}
\Gamma_1(t) &= \left[W_{X1}^2(\mathbf{x}(t),t) + W_{Y1}^2(\mathbf{x}(t),t) + W_{Z1}^2(\mathbf{x}(t),t)\right]^{1/2} \\
\Gamma_2(t) &= \left[W_{X2}^2(\mathbf{x}(t),t) + W_{Y2}^2(\mathbf{x}(t),t) + W_{Z2}^2(\mathbf{x}(t),t)\right]^{1/2}
\end{aligned}
\tag{4.41}
$$

so that the gravity difference is expressed by

$$
\begin{aligned}
\Gamma_2(t) - \Gamma_1(t) &= \\
&= \left[W_{X2}^2(\mathbf{x}(t),t) + W_{Y2}^2(\mathbf{x}(t),t) + W_{Z2}^2(\mathbf{x}(t),t)\right]^{1/2} \\
&- \left[W_{X1}^2(\mathbf{x}(t),t) + W_{Y1}^2(\mathbf{x}(t),t) + W_{Z1}^2(\mathbf{x}(t),t)\right]^{1/2}.
\end{aligned}
\tag{4.42}
$$

Following the same procedure as with the case of gravity intensity, the gravity intensity difference observation equation can be deduced to be

$$
\begin{aligned}
,_2(t) - ,_1(t) \quad - \quad & \gamma_2(t_o) + \gamma_1(t_o) = \\
- \quad & a_{1\Gamma}\Delta X_1 - b_{1\Gamma}\Delta Y_1 - c_{1\Gamma Z}\Delta Z_1 \\
+ \quad & a_{2\Gamma}\Delta X_2 + b_{2\Gamma}\Delta Y_2 + c_{2\Gamma Z}\Delta Z_2 \\
- \quad & a_{1\Gamma}\delta X_1 - b_{1\Gamma}\delta Y_1 - c_{1\Gamma}\delta Z_1 \\
+ \quad & a_{2\Gamma}\delta X_2 + b_{2\Gamma}\delta Y_2 + c_{2\Gamma}\delta Z_2 \\
- \quad & d_{1\Gamma}T_{X1} - e_{1\Gamma}T_{Y1} - f_{1\Gamma}T_{Z1} \\
+ \quad & d_{2\Gamma}T_{X2} + e_{2\Gamma}T_{Y2} + f_{2\Gamma}T_{Z2} \\
- \quad & d_{1\Gamma}\delta T_{X1} - e_{1\Gamma}\delta T_{Y1} - f_{1\Gamma}\delta T_{Z1} \\
+ \quad & d_{2\Gamma}\delta T_{X2} + e_{2\Gamma}\delta T_{Y2} + f_{2\Gamma}\delta T_{Z2} + v_{\Delta\Gamma} \qquad (4.43)
\end{aligned}
$$

with the coefficients given as in equations (4.39) and 4.40).

4.3.2 Spatial Distances

Let $S_{12}(t)$ denote the spatial distance between two geodetic network points P_1 and P_2 at some epoch t. The usual expression for the spatial distance is

$$
\begin{aligned}
S_{12}(t) &= \sqrt{(X_2(t) - X_1(t))^2 + (Y_2(t) - Y_1(t))^2 + (Z_2(t) - Z_1(t))^2} \\
&= F(\mathbf{x}(t)) \qquad (4.44)
\end{aligned}
$$

Since there is no influence of gravity potential on the distance $S_{12}(t)$ the gravity potential functional LW in the equation for four-dimensional geodesy (3.19) vanishes. Thus the linearised equation for spatial distance observation in four-dimensional geodesy becomes

$$S_{12}(t) - s^o_{12}(t_o) = grad_{\mathbf{x}} F(\mathbf{x}^o(t_o)) \cdot [(\Delta\mathbf{x}(t_o) + \delta\mathbf{x}(t))_2 - (\Delta\mathbf{x}(t_o) + \delta\mathbf{x}(t))_1] \qquad (4.45)$$

where $s^o_{12}(t_o)$ is the model distance as computed at the initial or reference epoch and given by

$$s^o_{12}(t_o) = \sqrt{(X^o_2(t_o) - X^o_1(t_o))^2 + (Y^o_2(t_o) - Y^o_1(t_o))^2 + (Z^o_2(t_o) - Z^o_1(t_o))^2}. \qquad (4.46)$$

The observation equation for distances can be then written as

$$S(t) - s^o(t_o) = \Delta S_x + \delta S_{\delta x} + v_s \qquad (4.47)$$

or in expanded form as

$$
\begin{aligned}
S(t) - s^o(t_o) &= \\
&= a_{2s}\Delta X_2 + b_{2s}\Delta Y_2 + c_{2s}\Delta Z_2 \\
&- a_{1s}\Delta X_1 - b_{1s}\Delta Y_1 - c_{1s}\Delta Z_2 \\
&+ a_{2s}\delta X_2 + b_{2s}\delta Y_2 + c_{2s}\delta Z_2 \\
&- a_{1s}\delta X_1 - b_{1s}\delta Y_1 - c_{1s}\delta Z_1 + v_s
\end{aligned}
\tag{4.48}
$$

with coefficients given by

$$
\begin{aligned}
a_{1s} = a_{2s} &= \frac{\Delta X^o(t_o)}{s_{12}^o(t_o)} \\
b_{1s} = b_{2s} &= \frac{\Delta Y^o(t_o)}{s_{12}^o(t_o)} \\
c_{1s} = c_{2s} &= \frac{\Delta Z^o(t_o)}{s_{12}^o(t_o)}
\end{aligned}
\tag{4.49}
$$

and

$$
\begin{aligned}
\Delta X^o(t_o) &= X_2^o(t_o) - X_1^o(t_o) \\
\Delta Y^o(t_o) &= Y_2^o(t_o) - Y_1^o(t_o) \\
\Delta Z^o(t_o) &= Z_2^o(t_o) - Z_1^o(t_o).
\end{aligned}
\tag{4.50}
$$

4.3.3 Zenith Angles

Let P_1 be the standpoint and P_2 be the target point to which the zenith angle Z_{12} is referred. Z_{12} is represented in vectorial form [Heck, 1987] p. 92 with modification as

$$
Z_{12}(t) = \arccos \frac{< \Delta\mathbf{x}_{12}(t), -\mathbf{\Gamma}(\mathbf{x}_1(t), t) >}{\mid \mathbf{\Gamma}(\mathbf{x}_1(t), t) \mid \cdot \mid \Delta\mathbf{x}_{12}(t) \mid}
\tag{4.51}
$$

Expanding equation (4.51) at the epoch t results in

$$
Z_{12}(t) = \arccos \frac{(-\Delta X W_X - \Delta Y W_Y - \Delta Z W_Z)}{\sqrt{W_X{}^2 + W_Y{}^2 + W_Z{}^2} \cdot \sqrt{(\Delta X^2 + \Delta Y^2 + \Delta Z^2)}}.
\tag{4.52}
$$

The zenith angle can be also represented using polar coordinates by considering equations (4.1) through (4.4) as

$$
\begin{aligned}
Z_{12}(t) &= \arccos \frac{\Delta X \cos\Phi \cos\Lambda + \Delta Y \cos\Phi \sin\Lambda + \Delta Z \sin\Phi}{\sqrt{\Delta X^2 + \Delta Y^2 + \Delta Z^2}} \\
&= F(\mathbf{x}(t), LW(\mathbf{x}(t), t))
\end{aligned}
\tag{4.53}
$$

where Φ, Λ refer to the observation point P_1 at the epoch t. Both expressions (4.52) and (4.53) are equivalent.

Linearization of equation (4.52) or (4.53) is done in two steps: first the functional LU is differentiated with respect to $\mathbf{x}$ during the Taylor series approximation to give

$$\begin{aligned}
W_i(\mathbf{x}(t), t) &= \frac{\partial U}{\partial x_i}(\mathbf{x}^o(t_o)) + \frac{\partial^2 U}{\partial x_i \partial x_j}(\mathbf{x}^o(t_o)) \cdot [\Delta x_j(t_o) + \delta x_j(t)] \\
&+ \frac{\partial T}{\partial x_i}(\mathbf{x}^o(t_o)) + \frac{\partial \delta T}{\partial x_i}(\mathbf{x}^o(t_o), t)
\end{aligned} \tag{4.54}$$

and secondly the general function F is differentiated with respect to the position vector $\mathbf{x}$. The zenith angle depends on the vector $\mathbf{x}$ both directly and implicitly. The linearized observation equation for zenith angle (4.52) can be thus written as

$$\begin{aligned}
Z_{12}(t) - \zeta_{12}^o(t_o) &= \\
&= \frac{\partial Z(\mathbf{x}^o(t_o)}{\partial U_i} \cdot \{ \frac{\partial^2 U}{\partial x_i \partial x_j}(\mathbf{x}^o(t_o)) \cdot [\Delta x_j(t_o) + \delta x_j(t)]_1 \\
&+ \frac{\partial T}{\partial x_i}(\mathbf{x}^o(t_o)) + \frac{\partial \delta T}{\partial x_i}(\mathbf{x}^o(t_o), t) \} \\
&+ \frac{\partial Z(\mathbf{x}^o(t_o)}{\partial x_i} \cdot [(\Delta x_i(t_o) + \delta x_i(t))_2 - (\Delta x_i(t_o) + \delta x_i(t))_1] \\
&+ v_Z.
\end{aligned} \tag{4.55}$$

(having used the Einstein's summation convention). Writing out the coefficients explicitly

$$\begin{aligned}
Z_{12}(t) - \zeta_{12}^o(t_o) &= a_{2Z} \Delta X_2(t_o) + b_{2Z} \Delta Y_2(t_o) + c_{2Z} \Delta Z_2(t_o) \\
&- (a_{1Z} + a_{2Z}) \Delta X_1(t_o) - (b_{1Z} + b_{2Z}) \Delta Y_1(t_o) \\
&- (c_{1Z} + c_{2Z}) \Delta Z_1(t_o) \\
&+ a_{2Z} \delta X_2 + b_{2Z} \delta Y_2 + c_{2Z} \delta Z_2 \\
&- (a_{1Z} + a_{2Z}) \delta X_1 - (b_{1Z} + b_{2Z}) \delta Y_1 \\
&- (c_{1Z} + c_{2Z}) \delta Z_1 \\
&+ d_{1Z} T_X(t_o) + e_{1Z} T_Y(t_o) + f_{1Z} T_Z(t_o) \\
&+ d_{1Z} \delta T_X(t_o) + e_{1Z} \delta T_Y(t_o) + f_{1Z} \delta T_Z(t_o) \\
&+ v_Z.
\end{aligned} \tag{4.56}$$

The coefficients are expressed by

$$\begin{aligned}
a_{1Z} &= \frac{-1}{\gamma^2 \sqrt{\gamma^2 \cdot (s_{12}^o)^2 - (\Delta X \gamma_X + \Delta Y \gamma_Y + \Delta Z \gamma_Z)^2}} \cdot [\\
& \quad \Delta X^o \cdot (\gamma^2 U_{XX} - \gamma_X \cdot (\gamma_X U_{XX} + \gamma_Y U_{XY} + \gamma_Z U_{XZ})) \\
&+ \Delta Y^o \cdot (\gamma^2 U_{XY} - \gamma_Y \cdot (\gamma_X U_{XX} + \gamma_Y U_{XY} + \gamma_Z U_{XZ})) \\
&+ \Delta Z^o \cdot (\gamma^2 U_{XZ} - \gamma_Z \cdot (\gamma_X U_{XX} + \gamma_Y U_{XY} + \gamma_Z U_{XZ}))]
\end{aligned} \tag{4.57}$$

$$
\begin{aligned}
b_{1Z} &= \frac{-1}{\gamma^2\sqrt{\gamma^2\cdot(s_{12}^o)^2-(\Delta X\gamma_X+\Delta Y\gamma_Y+\Delta Z\gamma_Z)^2}}\cdot[\\
& \quad \Delta X^o\cdot(\gamma^2 U_{YX}-\gamma_X\cdot(\gamma_X U_{XY}+\gamma_Y U_{YY}+\gamma_Z U_{ZY}))\\
&+ \Delta Y^o\cdot(\gamma^2 U_{YY}-\gamma_Y\cdot(\gamma_X U_{XY}+\gamma_Y U_{YY}+\gamma_Z U_{ZY}))\\
&+ \Delta Z^o\cdot(\gamma^2 U_{YZ}-\gamma_Z\cdot(\gamma_X U_{XY}+\gamma_Y U_{YY}+\gamma_Z U_{ZY}))]
\end{aligned} \tag{4.58}
$$

$$
\begin{aligned}
c_{1Z} &= \frac{-1}{\gamma^2\sqrt{\gamma^2\cdot(s_{12}^o)^2-(\Delta X\gamma_X+\Delta Y\gamma_Y+\Delta Z\gamma_Z)^2}}\cdot[\\
& \quad \Delta X^o\cdot(\gamma^2 U_{ZX}-\gamma_X\cdot(\gamma_X U_{XZ}+\gamma_Y U_{YZ}+\gamma_Z U_{ZZ}))\\
&+ \Delta Y^o\cdot(\gamma^2 U_{ZY}-\gamma_Y\cdot(\gamma_X U_{XZ}+\gamma_Y U_{YZ}+\gamma_Z U_{ZZ}))\\
&+ \Delta Z^o\cdot(\gamma^2 U_{ZZ}-\gamma_Z\cdot(\gamma_X U_{XZ}+\gamma_Y U_{YZ}+\gamma_Z U_{ZZ}))].
\end{aligned} \tag{4.59}
$$

The other coefficients are

$$
\begin{aligned}
a_{2Z} &= \frac{(s_{12}^o)^2\cdot\gamma_X-\Delta X^o\cdot(\Delta X\gamma_X+\Delta Y\gamma_Y+\Delta Z\gamma_Z)}{(s_{12}^o)^2\sqrt{\gamma^2\cdot(s_{12}^o)^2-(\Delta X\gamma_X+\Delta Y\gamma_Y+\Delta Z\gamma_Z)^2}}\\
b_{2Z} &= \frac{(s_{12}^o)^2\cdot\gamma_Y-\Delta Y^o\cdot(\Delta X\gamma_X+\Delta Y\gamma_Y+\Delta Z\gamma_Z)}{(s_{12}^o)^2\sqrt{\gamma^2\cdot(s_{12}^o)^2-(\Delta X\gamma_X+\Delta Y\gamma_Y+\Delta Z\gamma_Z)^2}}\\
c_{2Z} &= \frac{(s_{12}^o)^2\cdot\gamma_Z-\Delta Z^o\cdot(\Delta X\gamma_X+\Delta Y\gamma_Y+\Delta Z\gamma_Z)}{(s_{12}^o)^2\sqrt{\gamma^2\cdot(s_{12}^o)^2-(\Delta X\gamma_X+\Delta Y\gamma_Y+\Delta Z\gamma_Z)^2}}
\end{aligned} \tag{4.60}
$$

which correspond to [Heck, 1987]. The other coefficients are

$$
\begin{aligned}
d_{1Z} &= \frac{\gamma^2\cdot\Delta X^o-(\Delta X\gamma_X+\Delta Y\gamma_Y+\Delta Z\gamma_Z)\cdot\gamma_X}{\gamma^2\sqrt{\gamma^2\cdot(s_{12}^o)^2-(\Delta X\gamma_X+\Delta Y\gamma_Y+\Delta Z\gamma_Z)^2}}\\
e_{1Z} &= \frac{\gamma^2\cdot\Delta Y^o-(\Delta X\gamma_X+\Delta Y\gamma_Y+\Delta Z\gamma_Z)\cdot\gamma_Y}{\gamma^2\sqrt{\gamma^2\cdot(s_{12}^o)^2-(\Delta X\gamma_X+\Delta Y\gamma_Y+\Delta Z\gamma_Z)^2}}\\
f_{1Z} &= \frac{\gamma^2\cdot\Delta Z^o-(\Delta X\gamma_X+\Delta Y\gamma_Y+\Delta Z\gamma_Z)\cdot\gamma_Z}{\gamma^2\sqrt{\gamma^2\cdot(s_{12}^o)^2-(\Delta X\gamma_X+\Delta Y\gamma_Y+\Delta Z\gamma_Z)^2}}.
\end{aligned} \tag{4.61}
$$

4.3.4 Astronomical Azimuth

Let A_{12} denote the astronomical azimuth of the observation line between the geodetic network points P_1 and P_2. The expression for the astronomical azimuth A_{12} is

$$
A(t) = \arctan\frac{-\Delta X\sin\Lambda+\Delta Y\cos\Lambda}{-\Delta X\sin\Phi\cos\Lambda-\Delta Y\sin\Phi\sin\Lambda+\Delta Z\cos\Phi}
$$

$$= \quad F(\mathbf{x}(t), LW(\mathbf{x}(t), t)) \tag{4.62}$$

where a time argument t, has been introduced and Φ, Λ are taken at point P_1. The azimuth can also be expressed in terms of the gravity potential as

$$A(t) = \arctan \frac{(W_X^2 + W_Y^2 + W_Z^2)^{1/2}(W_Y \Delta X - W_X \Delta Y)}{-W_Z(W_X \Delta X + W_Y \Delta Y) + (W_X^2 + W_Y^2)\Delta Z} \tag{4.63}$$

where again a time argument has been introduced.

Equation (4.63) is linearized in two steps: first as a functional of W with respect to the position vector $\mathbf{x}$ as in equation (4.54)

$$\begin{aligned} W_i(\mathbf{x}(t), t) &= \frac{\partial U}{\partial x_i}(\mathbf{x}^o(t_o)) + \frac{\partial^2 U}{\partial x_i \partial x_j}(\mathbf{x}^o(t_o)) \cdot [\Delta x_j(t_o) + \delta x_j(t)] \\ &+ \frac{\partial T}{\partial x_i}(\mathbf{x}^o(t_o)) + \frac{\partial \delta T}{\partial x_i}(\mathbf{x}^o(t_o), t) \end{aligned} \tag{4.64}$$

and secondly as an explicit function of F with respect to the position vector $\mathbf{x}$. In equation (4.64) the Einstein summation convention has been used. All higher order terms including products of first order terms of T or δT with $(\Delta \mathbf{x}(t_o) + \delta \mathbf{x}(t))$ are ignored.

Thus the final linearised observation equation for astronomical azimuth in four-dimensional geodesy is

$$\begin{aligned} A(t) - \alpha(t_o) &= \frac{\partial A(\mathbf{x}^o(t_o))}{\partial U_i} \cdot \{\frac{\partial^2 U}{\partial x_i \partial x_j}(\mathbf{x}^o(t_o)) \cdot [\Delta x_j(t_o) + \delta x_j(t)]_1 \\ &+ \frac{\partial T}{\partial x_i}(\mathbf{x}^o(t_o)) + \frac{\partial \delta T}{\partial x_i}(\mathbf{x}^o(t_o), t)\} \\ &+ \frac{\partial A(\mathbf{x}^o(t_o))}{\partial x_i} \cdot [(\Delta x_i(t_o) + \delta x_i(t))_2 - (\Delta x_i(t_o) + \delta x_i(t))_1] \\ &+ v_A. \end{aligned} \tag{4.65}$$

Now letting

$$\begin{aligned} \Delta A_x &= (\frac{\partial A(\mathbf{x}^o(t_o)}{\partial U_i} \cdot M_{ij} + \frac{\partial A(\mathbf{x}^o(t_o)}{\partial x_i})\Delta \mathbf{x}(t_o) \\ \delta A_{\delta x} &= (\frac{\partial A(\mathbf{x}^o(t_o)}{\partial U_i} \cdot M_{ij} + \frac{\partial A(\mathbf{x}^o(t_o)}{\partial x_i})\delta \mathbf{x}(t) \\ \Delta A_{TX} &= \frac{\partial A(\mathbf{x}^o(t_o)}{\partial U_i} \cdot T_i \mathbf{x}^o(t_o)) \\ \delta A_{\delta TX} &= \frac{\partial A(\mathbf{x}^o(t_o)}{\partial U_i} \cdot \delta T_i(\mathbf{x}^o(t_o), t) \end{aligned} \tag{4.66}$$

and

$$\mathbf{M} = M_{ij} = \begin{bmatrix} \frac{\partial^2 U(\mathbf{X}^o(t_o))}{\partial X^2} & \frac{\partial^2 U(\mathbf{X}^o(t_o))}{\partial X \partial Y} & \frac{\partial^2 U(\mathbf{X}^o(t_o))}{\partial X \partial Z} \\ \frac{\partial^2 U(\mathbf{X}^o(t_o))}{\partial Y \partial X} & \frac{\partial^2 U(\mathbf{X}^o(t_o))}{\partial Y^2} & \frac{\partial^2 U(\mathbf{X}^o(t_o))}{\partial Y \partial Z} \\ \frac{\partial^2 U(\mathbf{X}^o(t_o))}{\partial Z \partial X} & \frac{\partial^2 U(\mathbf{X}^o(t_o))}{\partial Z \partial Y} & \frac{\partial^2 U(\mathbf{X}^o(t_o))}{\partial Z^2} \end{bmatrix}$$

is the normal gravity tensor matrix. The observation equation can be thus written as

$$A(t) - \alpha^o(t_o) = \Delta A_x + \delta A_{\delta x} + \Delta A_{TX} + \delta A_{\delta TX} + v_A \tag{4.67}$$

or explicitly in terms of the parameters as

$$\begin{aligned} A(t) - \alpha(t_o) \; = & \\ & a_{2A}\Delta X_2(t_o) + b_{2A}\Delta Y_2(t_o) + c_{2A}\Delta Z_2(t_o) \\ - & \; (a_{1A} + a_{2A})\Delta X_1(t_o) - (b_{1A} + b_{2A})\Delta Y_1(t_o) \\ - & \; (c_{1A} + c_{2A})\Delta Z_1(t_o) \\ + & \; a_{2A}\delta X_2 + b_{2A}\delta Y_2 + c_{2A}\delta Z_2 \\ - & \; (a_{1A} + a_{2A})\delta X_1 - (b_{1A} + b_{2A})\delta Y_1 \\ - & \; (c_{1A} + c_{2A})\delta Z_1 \\ + & \; d_{1A}T_X(t_o) + e_{1A}T_Y(t_o) + f_{1A}T_Z(t_o) \\ + & \; d_{1A}\delta T_X(t) + e_{1A}\delta T_Y(t) + f_{1A}\delta T_Z(t) \\ + & \; v_A \end{aligned} \tag{4.68}$$

where the coefficients are given by

$$\begin{aligned} a_{2A} \; = \; & \frac{1}{v^2 + u^2}\{ \\ & [v(\frac{(U_X U_Y \Delta X - U_X^2 \Delta Y)}{\gamma} - \gamma\Delta Y) - u(-U_Z\Delta X + 2U_X\Delta Z)]U_{XX} \\ + \; & [v(\frac{(U_Y^2 \Delta X - U_Y U_X \Delta Y)}{\gamma} + \gamma\Delta X) - u(-U_Z\Delta Y + 2U_Y\Delta Z)]U_{YX} \\ + \; & [v(\frac{U_Z(U_Y\Delta X - U_X\Delta Y)}{\gamma}) + u(U_X\Delta X + U_Y\Delta Y)]U_{ZX} \quad \} \end{aligned} \tag{4.69}$$

$$\begin{aligned} b_{2A} \; = \; & \frac{1}{v^2 + u^2}\{ \\ & [v(\frac{(U_X U_Y \Delta X - U_X^2 \Delta Y)}{\gamma} - \gamma\Delta Y) - u(-U_Z\Delta X + 2U_X\Delta Z)]U_{XY} \\ + \; & [v(\frac{(U_Y^2 \Delta X - U_X U_Y \Delta Y)}{\gamma} + \gamma\Delta X) - u(-U_Z\Delta Y + 2U_Y\Delta Z)]U_{YY} \end{aligned}$$

$$+ \quad [v(\frac{U_Z(U_Y\Delta X - U_X\Delta Y)}{\gamma}) + u(U_X\Delta X + U_Y\Delta Y)]U_{ZY} \quad \} \tag{4.70}$$

$$\begin{aligned} c_{2A} &= \frac{1}{v^2+u^2}\{ \\ & [v(\frac{(U_XU_Y\Delta X - U_X^2\Delta Y)}{\gamma} - \gamma\Delta Y) - u(-U_Z\Delta X + 2U_X\Delta Z)]U_{XZ} \\ &+ [v(\frac{(U_Y^2\Delta X - U_XU_Y\Delta Y)}{\gamma} + \gamma\Delta X) - u(-U_Z\Delta Y + 2U_Y\Delta Z)]U_{YZ} \\ &+ [v(\frac{U_Z(U_Y\Delta X - U_X\Delta Y)}{\gamma}) + u(U_X\Delta X + U_Y\Delta Y)]U_{ZZ} \quad \} \end{aligned} \tag{4.71}$$

$$\begin{aligned} d_{1A} &= \frac{1}{v^2+u^2}\{v[\frac{(U_XU_Y\Delta X - U_X^2\Delta Y)}{\gamma} - \gamma\Delta Y] - u(-U_Z\Delta X + 2U_X\Delta Z)\} \\ e_{1A} &= \frac{1}{v^2+u^2}\{v[\frac{(U_Y^2\Delta X - U_XU_Y\Delta Y)}{\gamma} + \gamma\Delta X] - u(-U_Z\Delta Y + 2U_Y\Delta Z)\} \\ f_{1A} &= \frac{1}{v^2+u^2}\{v[\frac{U_Z(U_Y\Delta X - U_X\Delta Y)}{\gamma}] + u(U_X\Delta X + U_Y\Delta Y) \quad \} \end{aligned} \tag{4.72}$$

where

$$\begin{aligned} u &= \sqrt{(U_X^2 + U_Y^2 + U_Z^2)} \cdot (U_Y\Delta X - U_X\Delta Y) \\ v &= -U_ZU_X\Delta X - U_ZU_Y\Delta Y + U_X^2\Delta Z + U_Y^2\Delta Z. \end{aligned} \tag{4.73}$$

The other values evaluated at the observation point P_1 are

$$\begin{aligned} a_{1A} &= \frac{1}{(u^2+v^2)} \cdot [v \cdot \gamma U_Y + u \cdot U_XU_Z] \\ b_{1A} &= \frac{1}{(u^2+v^2)} \cdot [-v \cdot \gamma U_X + u \cdot U_YU_Z] \\ c_{1A} &= \frac{1}{(u^2+v^2)} \cdot [-u \cdot ({U_X}^2 + {U_Y}^2)]. \end{aligned} \tag{4.74}$$

4.3.5 Horizontal Directions

The horizontal direction observation equation differs from an azimuth observation equation in that an orientation parameter O_1 at the observation station is required in the case of horizontal direction observation.

Let $\Psi_{12}(t)$ represent the observed horizontal direction between the network points P_1 and P_2 at observation epoch t. Then

$$\Psi_{12}(t) = A_{12}(t) + O_1(t) + v_\Psi \tag{4.75}$$

where A_{12} is the corresponding azimuth of the same line $P_1 - P_2$ at the same observation epoch. Thus the linearised observation equation of horizontal direction observation follows that of the astronomical azimuth equation (4.63) containing the orientation parameter O_1. It may be written thus

$$\Psi(t) - \psi(t_o) = \Delta\Psi_x + \delta\Psi_{\delta x} + \Delta\Psi_{TX} + \delta\Psi_{\delta TX} + O_1 + v_\Psi. \tag{4.76}$$

The functionals $\Delta\Psi_x$, $\delta\Psi_{\delta x}$, $\Delta\Psi_{TX}$, $\delta\Psi_{\delta TX}$ have the same expressions as those of azimuth, respectively ΔA_x, $\delta A_{\delta x}$, ΔA_{TX}, $\delta A_{\delta TX}$ (see equations (4.69) through (4.74)).

4.3.6 Gravity Potential Differences

The gravity potential difference is an observation arising from the combination of spirit levelling and gravity measurements along the same lines of the network. Let $W_1(t)$ and $W_2(t)$ denote the potentials at network points P_1 and P_2 respectively. The difference in potential ΔW_{12} between the two points becomes

$$\Delta W_{12}(t) = W_2(t) - W_1(t) \tag{4.77}$$

which according to equation (3.8) is written

$$\begin{aligned} \Delta W_{12}(t) &= F(\mathbf{x}(t), LW(\mathbf{x}(t), t)) \\ &= LW(\mathbf{x}(t), t)). \end{aligned} \tag{4.78}$$

The gravity potential depends on the position vector $\mathbf{x}$ only implicitly and therefore $grad_{\mathbf{x}} F(\mathbf{x}(t), LW(\mathbf{x}(t), t)) \equiv 0$.

The linearised equation for gravity potential difference is therefore developed according to equation (3.16) considering that it is a difference between two potentials, as:

$$\begin{aligned} &\Delta W_{12}(t) - [U_2(\mathbf{x}^o(t_o)) - U_1(\mathbf{x}^o(t_o))] = \\ &[U_i(\mathbf{x}^o(t_o))[\Delta x_i(t_o) + \delta x_i(t)]]_2 - [U_i(\mathbf{x}^o(t_o))[\Delta x_i(t_o) + \delta x_i(t)]]_1 \\ &+ LT_2(\mathbf{x}^o(t_o)) - LT_1(\mathbf{x}^o(t_o)) \\ &+ L\delta T_2(\mathbf{x}^o(t)) - L\delta T_1(\mathbf{x}^o(t)) + v_{\Delta W}. \end{aligned} \tag{4.79}$$

In terms of the geocentric coordinates the above equations can be expressed as

$$
\begin{aligned}
&\Delta W_{12}(t) - [U_2(\mathbf{x}^o(t_o)) - U_1(\mathbf{x}^o(t_o))] = \\
&a_{1p}\Delta X_1 + b_{1p}\Delta Y_1 + c_{1p}\Delta Z_1 + a_{2p}\Delta X_2 + b_{2p}\Delta Y_2 + c_{2p}\Delta Z_2 \\
&a_{1p}\delta X_1 + b_{1p}\delta Y_1 + c_{1p}\delta Z_1 + a_{2p}\delta X_2 + b_{2p}\delta Y_2 + c_{2p}\delta Z_2 \\
&+T_2(\mathbf{x}^o(t)) - T_1(\mathbf{x}^o(t)) + \delta T_2(\mathbf{x}^o(t)) - \delta T_1(\mathbf{x}^o(t)) + v_{\Delta W}
\end{aligned}
\tag{4.80}
$$

where

$$
\begin{aligned}
a_{1p} &= -U_X(X^o(t_o), P_1) \\
b_{1p} &= -U_Y(Y^o(t_o), P_1) \\
c_{1p} &= -U_Z(Z^o(t_o), P_1) \\
a_{2p} &= U_X(X^o(t_o), P_2) \\
b_{2p} &= U_Y(Y^o(t_o), P_2) \\
c_{2p} &= U_Z(Z^o(t_o), P_2)
\end{aligned}
\tag{4.81}
$$

and $T, T_2, \delta T_1, \delta T_2$ refer to the approximate coordinates $\mathbf{x}(t_o)$.

4.4 Three Point Observations

4.4.1 Horizontal Angles

A horizontal angle is a difference between two directions. If Ψ_{12} represents the direction of P_1 to P_2 and Ψ_{13} that of P_1 to P_3 then

$$\Psi_{123}(t) = \Psi_{13}(t) - \Psi_{12}(t) \tag{4.82}$$

is the horizontal angle between the rays to points P_2 and P_3 at point P_1. The orientation unknown is eliminated by subtraction so that the horizontal angle remains a difference between two azimuths. Thus

$$\Psi_{123}(t) = A_{13}(t) - A_{12}(t). \tag{4.83}$$

The derivation of the observation equation of horizontal angle follows that of a difference between two azimuths. Referring to equation (4.68),

$$
\begin{aligned}
&A_{13}(t) - A_{12}(t) - \alpha_{13}(t_o) + \alpha_{12}(t_o) = \\
&a_{3A}\Delta X_3(t_o) + b_{3A}\Delta Y_3(t_o) + c_{3A}\Delta Z_3(t_o) \\
-\ &a_{2A}\Delta X_2(t_o) - b_{2A}\Delta Y_2(t_o) - c_{2A}\Delta Z_2(t_o)
\end{aligned}
$$

$$
\begin{aligned}
&+ \quad (a_{2A} - a_{3A})\Delta X_1(t_o) + (b_{2A} - b_{3A})\Delta Y_1(t_o) + (c_{2A} - c_{3A})\Delta Z_1(t_o) \\
&+ \quad a_{3A}\delta X_3(t) + b_{3A}\delta Y_3(t) + c_{3A}\delta Z_3(t) \\
&- \quad a_{2A}\delta X_2(t) - b_{2A}\delta Y_2(t) - c_{2A}\delta Z_2(t) \\
&+ \quad (a_{2A} - a_{3A})\delta X_1(t) + (b_{2A} - b_{3A})\delta Y_1(t) + (c_{2A} - c_{3A})\delta Z_1(t) \\
&+ \quad d_{1A}T_X(t_o) + e_{1A}T_Y(t_o) + f_{1A}T_Z(t_o) \\
&+ \quad d_{1A}\delta T_X(t) + e_{1A}\delta T_Y(t) + f_{1A}\delta T_Z(t) \\
&+ \quad v_{\Psi_{123}} \qquad (4.84)
\end{aligned}
$$

is the form of the observation equation for horizontal angle. The coefficients of (4.84) are found in equations (4.69) through (4.74).

4.5 Space Observations

4.5.1 GPS Observations

The Global Positioning System (GPS) provides two basic observables:

- code pseudoranges and
- carrier phase pseudoranges.

The pseudorange is a measure of the distance between the satellite and the receiver at the epochs of transmission and reception of the signals. The pseudorange measurements are based on timing systems in both the satellite transmitter and the receiver. Timing and synchronization errors contribute to pseudorange measurements, too.

In carrier phase measurements, the difference between the phase of the carrier signal of the satellite, measured at the receiver, and the phase of the local oscillator within the receiver system at the time of measurements is observed. The code pseudorange measurement involves measuring the time taken by the satellite signal to arrive at the receiver. The measured time is multiplied by the speed of light to obtain the range which is biased by clock errors and other noise.

From either of these observations, network points which have been occupied by a satellite receiver can be coordinated. In usual geodetic applications the GPS raw measurements are first pre-processed by appropriate software e.g. Bernese GPS software [Rothacher et al., 1993]. This pre-processing may be done in two ways: either as uncorrelated baselines whereby observations at a pair of network points are processed together, or as a network whereby all network points are pre-processed simultaneuosly, usually as a free-network. This study does not go into the details of the pre-processing of the raw GPS data and details may be found in e.g. [Leick, 1990], [Hofmann-Wellenhof et al., 1992], [Kleusberg and Teunissen., 1996].

The pre-processing stage yields baselines or coordinates together with their full covariance matrices. The adjusted observations are used as quasi-observations in further adjustment with other geodetic data. Usually only station coordinates enter the second adjustment as parameters although other parameters e.g. orbital elements may be also included.

In the present work the observation equations for GPS quasi-observations are derived for both baselines or absolute coordinates. Further, and of particular importance is the use of GPS in the field of geodynamics as being carried out among others by the International GPS service for Geodynamics (IGS). Here the accuracy requirement is quite high - in the range of millimetre level. This high accuracy requirement can only be realised if all known systematic biases in the GPS are controlled. One such source of error is associated with the antenna phase center i.e. the location at the GPS antenna to which the GPS signal is referred. The next subsection is devoted to the GPS antenna calibrations and the observation equations follow shortly.

The GPS antenna calibration

The GPS antenna converts the energy in the electromagnetic waves that it receives from the GPS satellites into an electric current, which is processed to yield the required parameters for positioning. The electric point which the measurement of these electromagnetic waves is referred to is the antenna phase centre and generally does not coincide with the physical antenna centre which on the other hand is used as the reference for the actual ground point (see also [Langley, 1995]). Studies have shown (e. g. [Geiger, 1988]) that this difference is not just a constant offset but a variation depending on several factors e. g. the antenna type, frequency of the received signal, elevation and azimuth of the emitting satellite. For the GPS antennas only two frequencies need to be considered, the L1 and the L2 which the GPS satellites transmit. The usual way to find the phase centre variations is by first estimating the mean antenna phase centre offsets and finally estimating the elevation - and azimuth dependent phase centre variations.

Two distinct methods of GPS antenna calibration exist. These are:

- Anechoic chamber calibrations or laboratory methods
- Field calibration methods.

Anechoic chambers assumed free from electromagnetic signal reflections are used. The GPS antenna is mounted on an arm that can be rotated in both azimuth and elevation while a source transmitting at GPS frequencies (comparable with the satellite emissions) is kept at a fixed position. By varying both the azimuth and the elevation of the antenna, the antenna characteristics are determined (e. g. [Schupler et al., 1995]). While this method provides absolute results, inconsistencies still remain when the method is used alone ([Rothacher et al., 1995]). This method is also expensive and generally not accessible to the antennas that are already in the field since anechoic chamber facilities are limited.

In most geodetic applications, differential GPS procedures are applied, relying on two receivers and antennas of the same type. For short baselines, the satellite configuration at both end points are (nearly) the same. Assuming that the antennas of one and the same product show the same characteristics, the antenna offsets will cancel. This property will not hold for large baselines or when receiver/ antenna types are mixed. In the second method, a terrestrial network established by geodetic methods of high accuracy is used. The GPS antennas to be calibrated are then used to recontrol this network so that direct GPS data is used for calibration of the antennas. Basically the procedure involves comparison of the GPS antenna results with those of the ground control (e. g. [Geiger, 1988]; [Vogel and Jäger, 1994]; [Breuer and Wohlleben, 1995]). The antennas are exchanged between the test network points during the campaign and are oriented in the same direction during each session. The antenna directions are alternated by 180 degrees between the sessions. By so doing only the vertical offsets essentially remain in the differential GPS solution. Rotation of the antennas by 180 degrees after each session also helps to detect the multipath effect if azimuth curves are plotted.

In this study the field calibration method is considered and only mean offsets are estimated. In particular a new approach within the minimum norm solutions in the definition of height datum is used. Since resulting parameters are non-estimable the approach of [Koch, 1978] for testing of non-estimable parameters is used in the hypothesis testing. The results and more details are found in Appendix A.

The GPS observation equations

Like with distances, the derived GPS baselines or absolute coordinates (observations) are independent of the gravity potential function LW in the main linearised equation of four-dimensional geodesy.

Following the general equation of four-dimensional geodesy (3.19),

$$\begin{aligned} \mathbf{x}^s(t) &= \mathbf{x}^s(t_o) + \Delta\mathbf{x}^s(t_o) + \delta\mathbf{x}^s(t) \\ &\equiv F(\mathbf{x}(t), t) \end{aligned} \tag{4.85}$$

holds in a conventional coordinate system induced in the evaluation of GPS data. Referring these GPS observations to a global frame e.g. the geocentric coordinate frame (WGS84)

$$\begin{aligned} \mathbf{x}^s(t) &= \mu\mathbf{R}(\mathbf{x}^o(t_o) + \Delta\mathbf{x}(t_o) + \delta\mathbf{x}(t)) + \mathbf{t}_x \\ \mu &= \mu^o + \delta\mu, \quad \mu^o = 1 \\ \mathbf{R} &= \mathbf{I} + \delta\mathbf{R} \end{aligned} \tag{4.86}$$

results. $\mathbf{R}$ is a rotation matrix containing the values of the trigonometrical functions of the angular deviations between the corresponding axes of the two coordinate systems (see e.g. [Heck, 1987]). When the rotation angles are small (usually less than 10”), $\mathbf{R}$ is expressed as

$$\mathbf{R}(t_o) = \begin{bmatrix} 1 & \epsilon_z & -\epsilon_y \\ -\epsilon_z & 1 & \epsilon_x \\ \epsilon_y & -\epsilon_x & 1 \end{bmatrix}, \qquad \delta\mathbf{R}(t) = \begin{bmatrix} 0 & \delta\epsilon_z & -\delta\epsilon_y \\ -\delta\epsilon_z & 0 & \delta\epsilon_x \\ \delta\epsilon_y & -\delta\epsilon_x & 0 \end{bmatrix}$$

where $(\epsilon_x, \epsilon_y, \epsilon_z)$ are the rotation angles between the WGS84 system and the conventional coordinate system under consideration. The translation parameters are contained in the vector $\mathbf{t}_x$ and μ is a scale factor. $\delta\mathbf{R}$ is a differential rotation matrix.

Expanding the equations in (4.86) and substituting (4.85) above

$$\begin{aligned} \mathbf{x}^s(t) - \mathbf{x}^o(t_o) &= \mu\mathbf{R}\mathbf{x}(t) + \mathbf{t}_x - \mathbf{x}^o(t_o) \\ &= (1+\delta\mu)(\mathbf{I}+\delta\mathbf{R})[\mathbf{x}^o(t_o) + \Delta\mathbf{x}(t_o) + \delta\mathbf{x}(t)] - \mathbf{x}^o(t_o) + \mathbf{t}_x \end{aligned} \tag{4.87}$$

results. The products of small order quantities will be left out as being *small*, such that equation (4.87) can be now written as

$$\mathbf{x}^s(t) - \mathbf{x}^o(t_o) = \Delta\mathbf{x}(t_o) + \delta\mathbf{x}(t) + \delta\mathbf{R}\cdot\mathbf{x}^o(t_o) + \delta\mu\cdot\mathbf{x}^o(t_o) + \mathbf{t}_x. \tag{4.88}$$

Absolute GPS coordinates: The linearised observation equation for a GPS observation at a station P_1 is derived from (4.88) as

$$\begin{aligned} \mathbf{x}_1^s(t) - \mathbf{x}_1^o(t_o) &= \Delta\mathbf{x}_1(t_o) + \delta\mathbf{x}_1(t) + \delta\mathbf{R}\cdot\mathbf{x}_1^o(t_o) + \delta\mu\cdot\mathbf{x}_1^o(t_o) \\ &+ \mathbf{t}_x + \mathbf{v}_{AGPS} \end{aligned} \tag{4.89}$$

or expanded in a matrix form as

$$\begin{aligned} \begin{bmatrix} x_1^s(t) - x_1^o(t_o) \\ y_1^s(t) - y_1^o(t_o) \\ z_1^s(t) - z_1^o(t_o) \end{bmatrix} &= \begin{bmatrix} \Delta x_1(t_o) \\ \Delta y_1(t_o) \\ \Delta z_1(t_o) \end{bmatrix} + \begin{bmatrix} \delta x_1(t_o) \\ \delta y_1(t_o) \\ \delta z_1(t_o) \end{bmatrix} + \delta\mu\cdot \begin{bmatrix} x_1^o(t_o) \\ y_1^o(t_o) \\ z_1^o(t_o) \end{bmatrix} \\ &+ \begin{bmatrix} 0 & \delta\epsilon_z & -\delta\epsilon_y \\ -\delta\epsilon_z & 0 & \delta\epsilon_x \\ \delta\epsilon_y & -\delta\epsilon_x & 0 \end{bmatrix} \begin{bmatrix} x_1^o(t_o) \\ y_1^o(t_o) \\ z_1^o(t_o) \end{bmatrix} + \begin{bmatrix} t_x \\ t_y \\ t_z \end{bmatrix} + \begin{bmatrix} v_x \\ v_y \\ v_z \end{bmatrix}_{AGPS} \end{aligned} \tag{4.90}$$

with $\mathbf{v}_{AGPS}$ occuring as an observational error. The differential rotation angles $(\epsilon_x, \epsilon_y, \epsilon_z)$, the scale factor $\delta\mu$ and the translation parameters t_x, t_y, t_z enter the equation as additional unknown parameters.

GPS baselines: The linearised observation equation for a GPS baseline considered as an observation at a pair of points P_1 and P_2 is derived from (4.88) as

$$\begin{aligned}
\mathbf{x}_2^s(t) - \mathbf{x}_1^s(t) - \mathbf{x}_2^o(t_o) + \mathbf{x}_1^o(t_o) &= \Delta\mathbf{x}_2(t_o) - \Delta\mathbf{x}_1(t_o) + \delta\mathbf{x}_2(t) - \delta\mathbf{x}_1(t) \\
&+ \delta\mathbf{R}\cdot\mathbf{x}_2^o(t_o) - \delta\mathbf{R}\cdot\mathbf{x}_1^o(t_o) \\
&+ \delta\mu\cdot\mathbf{x}_2^o(t_o) - \delta\mu\cdot\mathbf{x}_1^o(t_o) + \mathbf{v}_{DGPS} \qquad (4.91)
\end{aligned}$$

where $\mathbf{v}_{DGPS}$ is an observational error in a GPS baseline observation. Equation (4.91) can be written as a matrix in the form

$$\begin{aligned}
\begin{bmatrix} \Delta x_{12}^s(t) - \Delta x_{12}^o(t_o) \\ \Delta y_{12}^s(t) - \Delta y_{12}^o(t_o) \\ \Delta z_{12}^s(t) - \Delta z_{12}^o(t_o) \end{bmatrix} &= \begin{bmatrix} \Delta x_2(t_o) - \Delta x_1(t_o) \\ \Delta y_2(t_o) - \Delta y_1(t_o) \\ \Delta z_2(t_o) - \Delta z_1(t_o) \end{bmatrix} + \begin{bmatrix} \delta x_2(t) - \delta x_1(t) \\ \delta y_2(t) - \delta y_1(t) \\ \delta z_2(t) - \delta z_1(t) \end{bmatrix} \\
&+ \begin{bmatrix} 0 & \delta\epsilon_z & -\delta\epsilon_y \\ -\delta\epsilon_z & 0 & \delta\epsilon_x \\ \delta\epsilon_y & -\delta\epsilon_x & 0 \end{bmatrix} \begin{bmatrix} \Delta x_{12}^o(t_o) \\ \Delta y_{12}^o(t_o) \\ \Delta z_{12}^o(t_o) \end{bmatrix} \\
&+ \delta\mu\cdot\begin{bmatrix} \Delta x_{12}^o(t_o) \\ \Delta y_{12}^o(t_o) \\ \Delta z_{12}^o(t_o) \end{bmatrix} + \begin{bmatrix} v_{\Delta x} \\ v_{\Delta y} \\ v_{\Delta z} \end{bmatrix} \qquad (4.92)
\end{aligned}$$

where

$$\begin{aligned}
\Delta x_{12}^s(t_o) &= x_2^s(t_o) - x_1^s(t_o) && (4.93) \\
\Delta y_{12}^s(t_o) &= y_2^s(t_o) - y_1^s(t_o) && (4.94) \\
\Delta z_{12}^s(t_o) &= z_2^s(t_o) - z_1^s(t_o) && (4.95) \\
\Delta x_{12}^o(t_o) &= x_2^o(t_o) - x_1^o(t_o) && (4.96) \\
\Delta y_{12}^o(t_o) &= y_2^o(t_o) - y_1^o(t_o) && (4.97) \\
\Delta z_{12}^o(t_o) &= z_2^o(t_o) - z_1^o(t_o). && (4.98)
\end{aligned}$$

The translation parameters $\mathbf{t}_x$ between the two coordinate systems are now eliminated.

4.5.2 Very Long Baseline Interferometry - VLBI

Extragalactic sources (quasars) are used as radio sources for VLBI observations. The radio signals originating from a quasar are assumed parallel by the time they reach ground (or even space) based antennas. The arrival time of the signal from the radio source is recorded and a crosscorrelation procedure is carried out which gives the difference in arrival time of the signal at a pair of VLBI antennas. A VLBI baseline is processed from the signal.

Since VLBI is an interferometric method, it is independent of the potential function LW appearing in the equation for four-dimensional geodesy, just like the GPS baselines. In this case, the observation equations (4.91) can be adopted for the VLBI system. Further modelling of the VLBI observations is found in e.g. [Dermanis, 1980],

5. The Integrated Four-dimensional Network Adjustment Models

5.1 Basic considerations

The usual geodetic observations of type angular and distances contain sufficient information to describe the size and shape of the geodetic network provided there is no configuration defect. On the other hand, coordinates are convenient means of describing a network but unfortunately these geodetic observations do not carry information about the position (coordinates) of a network. This results in a datum defect which becomes a part of the problem of adjustment of redundant observations in which coordinates are involved. If instead of placing the network on to a coordinate frame, the coordinate frame itself is to be placed on the network, then the datum problem arises. The datum problem was pioneered by [Meissl, 1969] and further developed by introduction of Baarda's S-transformation [Baarda, 1973], [van Mierlo, 1980]. The datum problem was so far treated in its linearized form and an extensive mathematical treatment of the nonlinear geodetic datum problem has been discussed in [Dermanis, 1998].

The adjustment problem involves mapping the observation space Y_n of n-dimension onto the model space (manifold) $\mathbf{M}_u$ of u-dimension by a mapping $\mathbf{f}$ with m parameters. The usual case is $n > u$ and due to unavoidable observation errors the mapping is done outside the actual model space. The adjustment problem is returning from this *apparent model space* to the actual model space. The datum problem results in the case $m > u$ (i.e the mapping function has more parameters than the rank of model space), when the model is without full rank. The datum problem is solved by introducing a set of minimal constraints $r(\mathbf{x}) = d, \quad d = m - u$. The final solution depends on the choice of these minimal constraints. In order to remove this dependency, the minimal solution is transformed by a *Baarda* S-transformation into an inner solution, or inner constraints are used instead.

In four-dimensional networks a further defect occurs due to lack of a reference motion. This problem has been discussed in [Dermanis, 1980] with connection to VLBI observations.

5.2 The Four-dimensional Adjustment Models

The general linearised observation equation of four-dimensional geodesy (3.20) may be written in simpler notation as

$$\mathbf{y} = \mathbf{A}\mathbf{x}_o + \mathbf{A}\mathbf{x}_p + \mathbf{B}\mathbf{s}_o + \mathbf{B}\mathbf{s}_t + \mathbf{v} \tag{5.1}$$

where

- $\mathbf{x}_o$ contains coordinate corrections at reference epoch and auxiliary parameters
- $\mathbf{x}_p$ represents displacements
- $\mathbf{s}_o$ represents disturbing gravity potential signals
- $\mathbf{s}_t$ represents disturbing gravity potential signal variations.

The coordinate corrections $\mathbf{x}_o$ are considered as deterministic quantities. The other parameters are signals which can treated in one of the following ways: (see e.g. [Dermanis, 1985]):

- as deterministic,
- as analytical expressions,
- as stochastic quantities and
- as of hybrid type.

The most general case of these approaches is the hybrid approach because it considers that the signal consists of a *trend* part (which can be modeled by analytical functions) and a stochastic part. The stochastic case simply assumes that the signal does not contain a *trend* part while the analytical case assumes that the signal does not contain a stochastic part. The deterministic approach is a particular case of the analytical approach where the assumed underlying function is now represented by a discrete element. If $\mathbf{s}$ represents the signal, $\mathbf{f}$ the trend function with $\mathbf{a}$ being a column vector of unknown coefficients and $\mathbf{S}$ the stochastic function, then the signal can be represented as

$$\mathbf{s} = \mathbf{f}\mathbf{a} + \mathbf{S}. \tag{5.2}$$

Table (5.2) below shows the various ways of how each of the signals can be modeled. Obviously the gravity signal variation will be neither suited to the deterministic nor to the analytical modeling since the coefficients required may be just too many. From Table (5.2), the most general equation of four-dimensional geodesy can be expanded as

$$\mathbf{y} = \mathbf{A}\mathbf{x}_o + \mathbf{A}(\mathbf{f}_x\mathbf{a}_x + \mathbf{S}_x) + \mathbf{B}(\mathbf{f}_s\mathbf{a}_s + \mathbf{S}_s) + \mathbf{B}(\mathbf{f}_{st}\mathbf{a}_s + \mathbf{S}_{st}) + \mathbf{v} \tag{5.3}$$

	Displacements $\mathbf{x}_p$	Disturbing potential $\mathbf{s}_o$	Potential variations $\mathbf{s}_t$
Deterministic	$\mathbf{x}_p = a_{xi}$	$\mathbf{s}_o = a_{si}$	$\mathbf{s}_t = a_{sti}$
Analytical	$\mathbf{x}_p = \mathbf{f}_x a_{xi}$	$\mathbf{s}_o = \mathbf{f}_s a_{si}$	$\mathbf{s}_t = \mathbf{f}_{st} a_{sti}$
Stochastic	$\mathbf{x}_p = \mathbf{S}_x$	$\mathbf{s}_o = \mathbf{S}_s$	$\mathbf{s}_t = \mathbf{S}_{st}$
Hybrid	$\mathbf{x}_p = \mathbf{f}_x a_{xi} + \mathbf{S}_x$	$\mathbf{s}_o = \mathbf{f}_s a_{si} + \mathbf{S}_s$	$\mathbf{s}_t = \mathbf{f}_s a_{sti} + \mathbf{S}_{st}$

Table 5.2: Signal modeling in four-dimensional geodesy

Only the two extreme cases - the purely deterministic and the purely stochastic cases will be given a further consideration here.

5.2.1 The Deterministic Approach

The signals are in this case regarded as additional parameters and are not assumed dependent on some common underlying function. Thus every observation introduces its own unknowns - a situation which is not possible to solve due to presence of more unknowns than there are observations. This approach is made practical by considering a group of observations to have been made at the same instant or in short enough campaigns for there not to have been changes either in position or gravity field. This leads to the discrete epoch approach with three types of unknowns:

(1.) the coordinate corrections

(2.) the signal parameters

(3.) other additional unknowns of type e. g. refraction coefficients, orientation unknowns etc.

The epoch adjustment
When individual observation epochs are considered, the parameters present are the coordinate corrections and disturbing gravity field unknowns. Thus from (5.3) all the stochastic parts $\mathbf{S}$ and all the variations are not present. If both type of unknowns are treated as deterministic then the formulation of this problem of adjustment follows the Gauss-Markov model of the form

$$\mathbf{y} = \mathbf{A}\mathbf{x} + \mathbf{v}, \quad \text{such that} \quad E\{\mathbf{y}\} = \mathbf{A}\mathbf{x}, \quad E\{\mathbf{v}\} = 0, \qquad D\{\mathbf{y}\} = D\{\mathbf{v}\} = \mathbf{C}(\mathbf{y},\mathbf{y}) \tag{5.4}$$

where all the deterministic parts have been put together and

- $\mathbf{y}$: $n \times 1$ random vector of observations
- $\mathbf{A}$: $n \times u$ design matrix, usually $n > u$
- $\mathbf{x}$: $u \times 1$ vector of unknown parameters

- $\mathbf{v}$: $n \times 1$ random vector of residuals

- $\mathbf{C}(\mathbf{y}, \mathbf{y})$: $n \times n$ covariance matrix of the observations.

In the least squares principle, the residual vector $\mathbf{v}$ is minimised; thus $\mathbf{v}^T\mathbf{W}\mathbf{v} \rightarrow min$. The estimation of the parameters $\mathbf{x}$ in (5.4) follows from

$$\mathbf{A}^T\mathbf{W}\mathbf{A}\mathbf{x} = \mathbf{A}^T\mathbf{W}\mathbf{y}, \quad \mathbf{W} = \mathbf{C}(\mathbf{y}, \mathbf{y})^{-1}, \quad \mathbf{N} = \mathbf{A}^T\mathbf{W}\mathbf{A}. \tag{5.5}$$

In the event that the normal equation matrix $\mathbf{N}$ is not singular, i.e. of full rank, then a Cayley inverse of $\mathbf{N}$ exists and the least squares estimate of $\mathbf{x}$, $\hat{\mathbf{x}}$ is given by

$$\hat{\mathbf{x}} = \mathbf{N}^{-1}\mathbf{A}^T\mathbf{W}\mathbf{y}. \tag{5.6}$$

When the normal equation matrix $\mathbf{N}$ is singular, some constraints have to be introduced. This involves elimination of the additional unknowns of type (3) from the system of normal equations. Using subscript $(_X)$ to denote the part of the normal equations containing unknowns of types (1) and (2) and U to denote additional unknowns of type (3) above, then the normal equations are represented as

$$\begin{bmatrix} \mathbf{N}_{XX} & \mathbf{N}_{XU} \\ \mathbf{N}_{XU}^T & \mathbf{N}_{UU} \end{bmatrix} \begin{bmatrix} \Delta\mathbf{X} \\ \Delta\mathbf{U} \end{bmatrix} = \begin{bmatrix} \mathbf{n}_X \\ \mathbf{n}_U \end{bmatrix}$$

and

$$\overline{\mathbf{N}}_{XX} = \mathbf{N}_{XX} - \mathbf{N}_{XU}\mathbf{N}_{UU}^{-1}\mathbf{N}_{XU}^T \tag{5.7}$$
$$\overline{\mathbf{n}}_X = \mathbf{n}_X - \mathbf{N}_{XU}\mathbf{N}_{UU}^{-1}\mathbf{n}_{UX} \tag{5.8}$$

(since $\mathbf{N}_{UU}$ is usually of full rank and therefore regular). The matrix $\overline{\mathbf{N}}_{XX}$ can be now split into two parts: the coordinate (x subscript) part and the signal (s subscript) part as follows:

$$\begin{bmatrix} \mathbf{N}_{xx} & \mathbf{N}_{xs} \\ \mathbf{N}_{xs}^T & \mathbf{N}_{ss} \end{bmatrix} \begin{bmatrix} \Delta\hat{\mathbf{x}} \\ \Delta\hat{\mathbf{s}} \end{bmatrix} = \begin{bmatrix} \mathbf{n}_x \\ \mathbf{n}_s \end{bmatrix}$$

from which

$$\overline{\mathbf{N}}_{xx} = \mathbf{N}_{xx} - \mathbf{N}_{xs}\mathbf{N}_{ss}^{+}\mathbf{N}_{xs}^T \tag{5.9}$$
$$\overline{\mathbf{n}}_x = \mathbf{n}_x - \mathbf{N}_{xs}\mathbf{N}_{ss}^{+}\mathbf{n}_s \tag{5.10}$$

where (+) denotes the pseudoinverse, is obtained. The part $\mathbf{N}_{ss}$ is generally not of full rank indicating some datum defect. This defect in rank concerns lack of information about the motion (displacement field) and can be removed by use of minimal constraints. [Dermanis, 1980] has used the inertia matrix of the network to derive constraints necessary to provide for the rank defect relating the displacements. The final solution when using the pseudoinverse is given by

$$
\begin{aligned}
\Delta\hat{\mathbf{x}} &= \overline{\mathbf{N}}_{xx}{}^{+}\overline{\mathbf{n}}_x = (\mathbf{N}_{xx} - \mathbf{N}_{xs}\mathbf{N}_{ss}^{+}\mathbf{N}_{xs}^{T})^{+}(\mathbf{n}_x - \mathbf{N}_{xs}\mathbf{N}_{ss}^{+}\mathbf{n}_s) \qquad (5.11)\\
\Delta\hat{\mathbf{s}} &= \mathbf{N}_{ss}^{+}(\mathbf{n}_s - \mathbf{N}_{xs}^{T}\Delta\hat{\mathbf{x}}). \qquad (5.12)
\end{aligned}
$$

Due to lack of datum information $\overline{\mathbf{N}}_{xx}$ has a datum defect - 3 translations, 3 rotations and 1 scale in the case of three-dimensional network where no distance, zenith, azimuth and GPS observations are made (see also [Illner, 1985] for other cases), a datum defect exists which again can be eliminated by use of minimal constraints or computing the network as a free one. The constraint required is

$$\Delta\mathbf{x}^T\Delta\mathbf{x} = minimum. \qquad (5.13)$$

For a three-dimensional network with all possible datum defects (7), the constraint is related to a matrix $\mathbf{G}$ of the form [Illner, 1985]

$$
\mathbf{G}_{\Delta x}^{T} = \begin{bmatrix}
 & 1 & 0 & 0 & \\
 & 0 & 1 & 0 & \\
 & 0 & 0 & 1 & \\
\ldots & 0 & z_i & -y_i & \ldots \\
 & -z_i & 0 & x_i & \\
 & y_i & -x_i & 0 & \\
 & x_i & y_i & z_i &
\end{bmatrix}
$$

with corresponding rows representing

- x - shift
- y - shift
- z - shift
- x - rotation
- y - rotation
- z - rotation
- scale.

The constraints that remove the defect as far as the gravity field parameters are concerned are [Klein, 1997] for disturbing gravity potential

$$\mathbf{G}_T^T = \begin{bmatrix} \dots & 1 & \dots \end{bmatrix}$$

and for first derivatives of potential

$$\mathbf{G}_{T_X} = \begin{bmatrix} \vdots \\ \cos\Phi_P \cos\Lambda_P \\ \cos\Phi_P \sin\Lambda_P \\ \sin\Phi_P \\ \vdots \\ \cos\Phi_Q \cos\Lambda_Q \\ \cos\Phi_Q \sin\Lambda_Q \\ \sin\Phi_Q \\ \vdots \end{bmatrix}$$

The deterministic approach as presented here corresponds to the adjustment of a three-dimensional integrated network e. g. [Klein, 1997] in the deterministic case. The adjustment of the reference epoch is carried out exactly in the same way as in a three-dimensional integrated network to obtain a solution $\mathbf{x}^0(t_o)$. The datum problem is solved and the problem becomes four-dimensional when the epoch solutions are interrelated by a similarity transformation as explained in section (3.2) (see also [Dermanis, 1995]).

The deterministic case is simple in application and makes no assumptions about the hypothesis of functions that govern the signals. This method can however not predict signals in points different from the network sites.

The model testing
In order to obtain an overall view about the model of four-dimensional geodesy, the *global test* (see e.g. [Koch, 1988] under *hypothesis testing for the variance of unit weight*) is applied. The form of the general equation of four-dimensional geodesy, equation (5.21), is referred to and σ_0^2 is the a priori variance of unit weight while $\hat{\sigma}_0^2$ is the a posteriori variance of unit weight. The null hypothesis H_0 is set out as: $H_0 : \hat{\sigma_0}^2 = \sigma_0^2$. The null hypothesis is tested against the alternative hypothesis H_a such that $H_a : \hat{\sigma_0}^2 \neq \sigma_0^2$. The computation of $\hat{\sigma}_0^2$ is done over all stochastic parameters of the model [Dermanis, 1991a]. Thus letting

$$\boldsymbol{\epsilon} = \mathbf{G}\mathbf{s} + \mathbf{v} \sim (\mathbf{0}, \sigma_0^2\mathbf{M}), \qquad \mathbf{M} = \mathbf{C}(\mathbf{v}, \mathbf{v}) \tag{5.14}$$

equation (5.21) can be now written as

$$\mathbf{y} = \mathbf{A}\mathbf{x} + \boldsymbol{\epsilon}. \tag{5.15}$$

The estimation of $\hat{\mathbf{x}}$ is already given in equation (5.28) so that $\hat{\boldsymbol{\epsilon}}$ can be estimated from

$$\hat{\boldsymbol{\epsilon}} = \mathbf{y} - \mathbf{A}\hat{\mathbf{x}}. \tag{5.16}$$

and $\hat{\sigma}_0^2$ is estimated from (f is the degree of freedom)

$$\begin{aligned}
\hat{\sigma}_0^2 &= \frac{\hat{\boldsymbol{\epsilon}}^T \mathbf{M}^{-1} \hat{\boldsymbol{\epsilon}}}{f}, \quad \text{and} \\
T_e &= \frac{f\hat{\sigma}_0^2}{\sigma_0^2} \sim \chi_f^2
\end{aligned} \tag{5.17}$$

where T_e is the test statistic and has a χ^2 distribution. The null hypothesis is accepted when the test statistic T_e lies within $\chi_f^{2(1-\frac{\alpha}{2})}$ and $\chi_f^{2(\frac{\alpha}{2})}$, where α is the level of significance. The failure of T_e is not an automatic rejection of the model and further tests may be carried out (see e.g. [Dermanis, 1991a]).

5.2.2 The Functional Signal Approach

Since the discrete deterministic method of treating the signals appearing in (5.1) has the disadvantage of having too many unknowns, a function assumed to model the signals and which has fewer unknowns can be used instead. This is possible where there is prior information about the signals. This approach has been considered in [Holdahl and Hardy, 1979], [Vanicek, 1975], [Hein and Kistermann, 1981], [Heck, 1989] among others.

It cannot be expected to model the parameters of the gravity field this way because of the irregular nature of this field which would result in too many unknowns. It may be expected that on a local scale and in regions which are not tectonically active, the use of analytical models may suffice for the case of representing displacements. The parameters of the chosen model are estimated in the adjustment together with the other unknowns.

5.2.3 The Stochastic Signal Approach

The signals appearing in equation (5.1)are now regarded as random variables with zero means such that

$$\begin{aligned}
E\{\delta\mathbf{x}(t)\} &= 0 \\
E\{T(\mathbf{x}^o(t_o))\} &= 0 \\
E\{\delta T(\mathbf{x}^o(t_o)\} &= 0
\end{aligned} \tag{5.18}$$

and known covariances

$$\begin{aligned}
C(\delta\mathbf{x}(t)_P, \delta\mathbf{x}(t)_Q) &= E\{\delta\mathbf{x}(t)_P . \delta\mathbf{x}(t)_Q^T\} \\
C(T(\mathbf{x}^o(t_o))_P, T(\mathbf{x}^o(t_o))_Q) &= E\{T(\mathbf{x}^o(t_o))_P . T(\mathbf{x}^o(t_o))_Q^T\} \\
C(\delta T(\mathbf{x}^o(t_o), t)_P, \delta T(\mathbf{x}^o(t_o), t)_Q) &= E\{\delta T(\mathbf{x}^o(t_o), t)_P . \delta T(\mathbf{x}^o(t_o), t)_Q^T\}.
\end{aligned} \tag{5.19}$$

Thus equation (5.1) now consists of

- deterministic parameters in form of coordinate corrections $\Delta\mathbf{x}(t_o)$,
- stochastic signals, $\mathbf{s} \in \{\delta\mathbf{x}(t), T(\mathbf{x}^o(t_o)), \delta T(\mathbf{x}^o(t_o), t)\}$,
- a vector of observational errors.

Considering equation (5.3) the purely stochastic approach is of the form

$$\mathbf{y} = \mathbf{A}\mathbf{x}_o + \mathbf{S}_x + \mathbf{S}_s + \mathbf{S}_{st} + \mathbf{v}. \tag{5.20}$$

By separating the deterministic and the stochastic parts and grouping each type, equation (5.20) can be simplified to the form

$$\mathbf{y} = \mathbf{A}\mathbf{x}_o + \mathbf{G}\mathbf{s} + \mathbf{v} \tag{5.21}$$

(and still regarding all the parameters as time dependent) where

- $\mathbf{y}$ is a $n \times 1$ vector of observations
- $\mathbf{x}_o$ is a $m \times 1$ vector of unknown deterministic parameters
- $\mathbf{A}$ is a $m \times n$ design matrix
- $\mathbf{G}$ is a $n \times m$ matrix resulting from the operator acting on $\mathbf{s}$
- $\mathbf{s}$ is a m-dimensional signal vector
- $\mathbf{v}$ is a n-dimensional vector of residuals.

Using the method of least squares collocation (see e.g. [Moritz, 1972]), new signals $\mathbf{s}_p$ at non- network points can be predicted. These predicted signals also depend on the respective linear functions that the network point signals $\mathbf{s}$ depend. Thus

$$\begin{aligned} \mathbf{s}_{p\delta x} &= A\delta\mathbf{x}(t) \\ \mathbf{s}_{pT} &= BT(\mathbf{x}^o(t_o)) \\ \mathbf{s}_{p\delta T} &= B\delta T(\mathbf{x}^o(t_o), t). \end{aligned} \tag{5.22}$$

Again using the new notation, the mean and the covariance functions of $\mathbf{s}_P$ are given by

$$\begin{aligned} E\{\mathbf{s}_P\} &= 0 \\ \mathbf{C}(\mathbf{s}_P, \mathbf{s}_Q) &= E\{\mathbf{s}_P.\mathbf{s}_Q^T\} \end{aligned} \tag{5.23}$$

respectively. The cross-covariance $C(\mathbf{s}_P, \mathbf{s}_Q)$ between the predicted signal and the network point signal is

$$\mathbf{C}(\mathbf{s}_P, \mathbf{s}_Q) = E\{\mathbf{s}_P.\mathbf{s}_Q^T\}. \tag{5.24}$$

The stochastic model $\mathbf{C}(\mathbf{y},\mathbf{y})$ of equation (5.21) is related to both the observational errors and the signals at the concerned points. Thus

$$\mathbf{C}(\mathbf{y},\mathbf{y}) = \mathbf{C}(\mathbf{v},\mathbf{v}) + \mathbf{C}(\mathbf{s},\mathbf{s}) \tag{5.25}$$

and the solution follows from the hybrid minimum condition

$$\mathbf{v}^T\mathbf{C}(\mathbf{v},\mathbf{v})^{-1}\mathbf{v} + \mathbf{s}_P^T\mathbf{C}(\mathbf{s}_P,\mathbf{s}_P)^{-1}\mathbf{s}_P \rightarrow minimum. \tag{5.26}$$

The solution of equation (5.21) for general linear predictors is given by [Dermanis, 1991b] as

$$\begin{aligned} \mathbf{M} &= \mathbf{G}\mathbf{C}(\mathbf{s},\mathbf{s})\mathbf{G}^T + \mathbf{C}(\mathbf{v},\mathbf{v}), \quad \mathbf{N} = \mathbf{A}^T\mathbf{M}^{-1}\mathbf{A}, \\ \boldsymbol{\mu}_s &= E\{\mathbf{s}\}, \quad \boldsymbol{\mu}_v = E\{\mathbf{v}\} \end{aligned} \tag{5.27}$$

$$\hat{\mathbf{x}} = \mathbf{N}^{-1}\mathbf{A}^T\mathbf{M}^{-1}(\mathbf{y} - \upsilon\boldsymbol{\mu}_v - \upsilon\mathbf{G}\boldsymbol{\mu}_s) \tag{5.28}$$

$$\hat{\mathbf{s}}_P = \upsilon\boldsymbol{\mu}_s + \mathbf{C}(s_P, s_Q)\mathbf{G}^T\mathbf{M}^{-1}(\mathbf{y} - \mathbf{A}\hat{\mathbf{x}} - \upsilon\boldsymbol{\mu}_v - \upsilon\boldsymbol{\mu}_s) \tag{5.29}$$

with

$$\upsilon = 1, \quad \text{or} \tag{5.30}$$

$$\upsilon = \frac{(\mathbf{G}\boldsymbol{\mu}_s + \boldsymbol{\mu}_v)^T\mathbf{M}^{-1}\mathbf{H}\mathbf{y}}{(\mathbf{G}\boldsymbol{\mu}_s + \boldsymbol{\mu}_v)^T\mathbf{H}^T\mathbf{M}^{-1}\mathbf{H}(\mathbf{G}\boldsymbol{\mu}_s + \boldsymbol{\mu}_v)} \tag{5.31}$$

$$\mathbf{H} = \mathbf{I} - \mathbf{A}\mathbf{N}^{-1}\mathbf{A}^T\mathbf{M}^{-1}. \tag{5.32}$$

The *Best inhomogeneously Linear weakly Unbiased Prediction - inhomBLUP* is here followed by setting the value of υ to one ($\upsilon = 1$). When the mean of the signals μ_s and that of the observation random errors μ_v is zero, then the estimation and prediction given in equations (5.28) and (5.29) respectively are the same as the least squares collocation solutions of [Moritz, 1972] i.e. estimation of $\hat{\mathbf{x}}$,

$$\hat{\mathbf{x}} = (\mathbf{A}^T\mathbf{C}(\mathbf{y},\mathbf{y})^{-1}\mathbf{A})^{-1}\mathbf{A}^T\mathbf{C}(\mathbf{y},\mathbf{y})^{-1}\mathbf{y} \tag{5.33}$$

and prediction of the signals $\hat{\mathbf{s}}_p$

$$\hat{\mathbf{s}}_P = \mathbf{C}(\mathbf{s}_P,\mathbf{s}_Q)\mathbf{G}^T\mathbf{C}(\mathbf{y},\mathbf{y})^{-1}(\mathbf{y} - \mathbf{A}\hat{\mathbf{x}}). \tag{5.34}$$

The displacement $\delta\mathbf{x}(t)$ is a vector function and each component $\delta X, \delta Y, \delta Z$ in some coordinate system is considered separately ([Blaha, 1977], [Dermanis and Rossikopoulos, 1988]). The derivation of suitable covariance functions is discussed in section(5.3).

		P_i			
		$\Delta\mathbf{x}_i$	$\delta\mathbf{x}_i$	T_i	δT_i
	$\Delta\mathbf{x}_j$	$(\Delta\mathbf{x}_i, \Delta\mathbf{x}_j)$	$(\Delta\mathbf{x}_i, \delta\Delta\mathbf{x}_j)$	$(\Delta\mathbf{x}_i, T_j)$	$(\Delta\mathbf{x}_i, \delta T_j)$
P_j	$\delta\mathbf{x}_j$	$(\delta\mathbf{x}_i, \Delta\mathbf{x}_j)$	$(\delta\mathbf{x}_i, \delta\mathbf{x}_j)$	$(\delta\mathbf{x}_i, T_j)$	$(\delta\mathbf{x}_i, \delta T_j)$
	T_j	$(T_i, \Delta\mathbf{x}_j)$	$(T_i, \delta\mathbf{x}_j)$	(T_i, T_j)	$(T_i, \delta T_j)$
	δT_j	$(\delta T_i, \Delta\mathbf{x}_j)$	$(\delta T_i, \delta\mathbf{x}_j)$	$(\delta T_i, T_j)$	$(\delta T_i, \delta T_j)$

Table 5.3: Signal pairing

5.3 The Covariance Functions

When the stochastic case is considered, covariance functions that express the propagation of the signals both in space and time have to be established. The set of the parameters is $p = \{\Delta\mathbf{x}, \delta\mathbf{x}, T, \delta T\}$. Except for the coordinate corrections $\Delta\mathbf{x}$ which are usually treated as deterministic, the other parameters appearing in p will be considered as stochastic.

5.3.1 Covariance Functions of Four-dimensional Geodesy

As it is usual in geodetic practice, the correlations between the signals and the observational random errors will be ignored as being small. Table (5.3) below shows all possible pairing where covariances can be established when only potential functionals are present.

From Table (5.3) and considering symmetry the following covariances are established

$$\begin{gathered} C(\delta T_i, \delta T_j), \quad C(T_i, T_j), \quad C(T_i, \delta T_j), \quad C(\delta\Delta\mathbf{x}_i, \delta\mathbf{x}_j), \quad C(\delta\Delta\mathbf{x}_i, T_j), \\ C(\delta\Delta\mathbf{x}_i, \delta T_j), \quad C(\Delta\mathbf{x}_i, \Delta\mathbf{x}_j), \quad C(\Delta\mathbf{x}_i, \delta\mathbf{x}_j), \quad C(\Delta\mathbf{x}_i, T_j), \quad C(\Delta\mathbf{x}_i, \delta T_j). \end{gathered} \tag{5.35}$$

The coordinate corrections $\Delta\mathbf{x}_i$ will be always treated as deterministic quantities and therefore the covariances relating to them will be neglected. The remaining parameters of the set p are treated as signals. The cross-covariances between the signals can be neglected under the assumption that the processes causing the signals are uncorrelated. Under these assumptions, only the auto-covariances remain. The signals whose covariance functions finally need to be established are

$$C(T_i, T_j), C(\delta T_i, \delta T_j), C(\delta\mathbf{x}_i, \delta\mathbf{x}_j) \tag{5.36}$$

The form of the covariance function that will be adopted will require the choice of a local coordinate system which is here denoted by (x, y, z). The direction of z is the same as that of the local plumbline but pointing upwards instead, while x points in the direction of north and y is on the same horizontal plane with x but pointing in the direction of east. The necessary covariance functions are then identified as follows:

$$\begin{aligned}
&C(T_i, T_j), C(\delta T_i, \delta T_j),\\
&C(\delta x_i, \delta x_j), C(\delta x_i, \delta y_j), C(\delta x_i, \delta z_j),\\
&C(\delta y_i, \delta x_j), C(\delta y_i, \delta y_j), C(\delta y_i, \delta z_j),\\
&C(\delta z_i, \delta x_j), C(\delta z_i, \delta y_j), C(\delta z_i, \delta z_j).
\end{aligned} \tag{5.37}$$

In this ordered pair of parameters, cross-correlations are inevitable. Their covariance functions thus need to be established.

5.3.2 The Covariance Functions

Below are considered some covariance functions in common use:

Hirvonen's covariance function.
This is of the form

$$C(\Delta g, \Delta g) = \frac{C_0}{1 + (\frac{r}{D})^2} \tag{5.38}$$

with variance C_0, characteristic distance D and r is the horizontal distance between any pair of points.

The Gaussian covariance function.
This is expressed as

$$C(\Delta g, \Delta g) = C_0 e^{-\frac{r}{D}} \tag{5.39}$$

where C_0, D again denote the variance and characteristic distance respectively. Both the Hirvonen and the Gaussian functions have been choosen as candidates for the gravity anomalies [Heiskanen and Moritz, 1967]. However, they are only suitable as one-dimensional functions. Figure (5.1) shows a plot of the two functions
$(C_0 = 337 \quad mgal^2, \qquad D = 40 \quad km)$.

The global covariance function.
On the sphere, the covariance functions concerning the gravity field parameters are usually expanded into a series of Legendre polynomials as [Moritz, 1972]:

$$C(\psi) = \sum_{n=0}^{\infty} c_n P_n(cos\psi) \tag{5.40}$$

where c_n are coefficients in a Legendre series expansion and ψ is the spherical distance between points P_i and P_j. The coefficients c_n are different for each gravity field quantity.

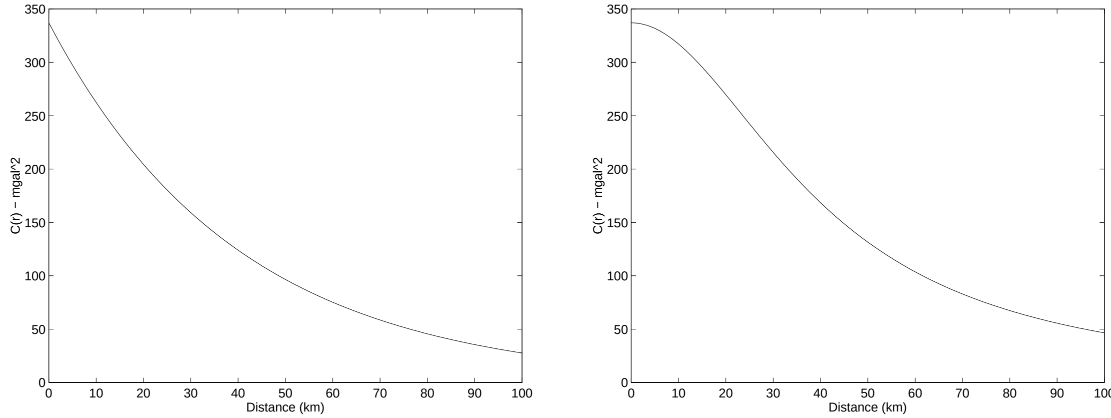

Figure 5.1: The Hirvonen and the Gaussian covariance functions

The covariance for the harmonic disturbing potential function in space the case of spherical approximation is given by

$$K(P_i, P_j) = \sum_{n=0}^{\infty} k_n (\frac{R}{r_P r_Q})^{n+1} P_n(\cos\psi) \tag{5.41}$$

and for the gravity anomaly is

$$K(P_i, P_j) = \sum_{n=0}^{\infty} c_n (\frac{R}{r_P r_Q})^{n+2} P_n(\cos\psi). \tag{5.42}$$

Regional covariance functions.
Most covariance functions in use are limited to planar approximation, for example the Gaussian function of the form

$$C(P_i, P_j) = \frac{1}{2} A d^2 e^{-\frac{1}{2}(\frac{r^2}{d^2})}, \tag{5.43}$$

with A and d as free parameters (also equivalent to the form given in (5.39). In order to extend the application of the Gaussian function in space applications, its Hankel transform (see e.g [Heck, 1984])

$$G(t) = \frac{A}{4\pi} d^4 e^{-\frac{1}{2}t^2 d^2} \tag{5.44}$$

is incorporated so that the spatial covariance function becomes

$$C(P_i, P_j) = \frac{1}{2} A d^4 \int_0^{\infty} J_0(tr) e^{-\frac{1}{2}t^2 d^2} e^{-t(z_i+z_j)} t dt \tag{5.45}$$

where J_o is the Bessel function of order zero. A generalization of this function is given by [Reilly, 1979] as

$$\Phi_T(q,n) = \frac{1}{2}Ad^4 \int_{t=0}^{\infty} t^q e^{-t(z_i+z_j)} e^{\frac{-t^2d^2}{2}} J_n(t.r)dt, \tag{5.46}$$

where q and n take integer values while A and d are free parameters and J_n are Bessel functions of order n. It is this form of the function that will be analysed further in order to deduce suitable forms of covariance functions for the signals present in four-dimensional geodesy.

The covariance function of the disturbing potential $C(T_i, T_j)$ is obtained from (5.46) when $q = 1$ and $n = 0$ (see [Reilly, 1979]) so that

$$C(T_i,T_j) = \Phi_T(1,0) = \frac{1}{2}A_T.d_T^4 \int_{t=0}^{\infty} te^{-t(z_i+z_j)} e^{\frac{-t^2d_T^2}{2}} J_0(t.r)dt \tag{5.47}$$

where A_T and d_T are again free parameters and J_0 is the Bessel function of order zero. Similarly the covariance function of the temporal change of potential ($C(\delta T_i, \delta T_j)$) is given by

$$C(\delta T_i,\delta T_j) = \Phi_{\delta T}(1,0) = \frac{1}{2}A_{\delta T}.d_{\delta T}^4 \int_{t=0}^{\infty} te^{-t(z_i+z_j)} e^{\frac{-t^2d_{\delta T}^2}{2}} J_0(t.r)dt \tag{5.48}$$

with $A_{\delta T}$ and $d_{\delta T}$ being treated as free parameters. The covariance function of the derivatives of the disturbing potential (T_x, T_y, T_z) are simply derived from the fundamental covariance function (5.47) by differentiating it accordingly. Thus, the covariance function of the vertical derivative of the disturbing potential $C(T_{zi}, T_{zj})$ is

$$\begin{aligned} C(T_{zi},T_{zj}) = \Phi(3,0) &= \frac{\partial}{\partial z_i}\frac{\partial}{\partial z_j}C(T_i,T_j) \\ &= \frac{1}{2}A_T.d_T^4 \int_{t=0}^{\infty} t^3 e^{-t(z_i+z_j)} e^{\frac{-t^2d_T^2}{2}} J_0(t.r)dt. \end{aligned} \tag{5.49}$$

A special case occurs when $z_i = z_j = 0$, i. e. on the reference plane when now the covariances defined by the functions $\Phi_T(1,0)$ and $\Phi_{\delta T}(1,0)$ take the following forms:

$$\overline{C}(T_i,T_j) = \overline{\Phi}_T(1,0) = \frac{1}{2}A_T d_T^2 e^{-\frac{1}{2}(\frac{r}{d_T})^2} \tag{5.50}$$

$$\overline{C}(\delta T_i,\delta T_j) = \overline{\Phi}_{\delta T}(1,0) = \frac{1}{2}A_{\delta T} d_{\delta T}^2 e^{-\frac{1}{2}(\frac{r}{d_{\delta T}})^2} \tag{5.51}$$

with the respective variances C_{oT}, $C_{o\delta T}$ and correlation length ξ_T and $\xi_{\delta T}$ as

$$C_{oT} = \frac{1}{2}A_T d_T^2; \qquad \xi_T = 1.177 d_T \tag{5.52}$$

$$C_{o\delta T} = \frac{1}{2}A_{\delta T}d_{\delta T}^2; \qquad \xi_{\delta T} = 1.177 d_{\delta T}. \tag{5.53}$$

The corresponding covariance functions on the reference plane of the first derivatives of the disturbing potential and its temporal variation in the vertical direction are respectively

$$\overline{C}(T_{zi}, T_{zj}) = \overline{\Phi}_T(3,0) = A_T(1 - \frac{1}{2}(\frac{r}{d_T})^2)e^{-\frac{1}{2}(\frac{r}{d_T})^2} \tag{5.54}$$

$$\overline{C}(\delta T_{zi}, \delta T_{zj}) = \overline{\Phi}_{\delta T}(3,0) = A_{\delta T}(1 - \frac{1}{2}(\frac{r}{d_{\delta T}})^2)e^{-\frac{1}{2}(\frac{r}{d_{\delta T}})^2}. \tag{5.55}$$

Their respective variances C_{oT_Z}, $C_{o\delta T_Z}$ and correlation lengths ξ_{T_Z}, $\xi_{\delta T_Z}$ are given by

$$\begin{aligned} C_{oT_Z} &= A_T; \qquad \xi_{T_Z} = 0.794 d_T \\ C_{o\delta T_Z} &= A_{\delta T}; \qquad \xi_{\delta T_Z} = 0.794 d_{\delta T}. \end{aligned} \tag{5.56}$$

Reilly used the values of $A_T = 5 \times 10^{-8} N^2/kg^2$ and $d_T = 10km$ for New Zealand.

Assuming symmetry and using the same notation as before, the covariance functions of the first derivatives of the signals are [Reilly, 1979]

$$\begin{aligned} C(T_{xi}, T_{xj}) &= \frac{1}{2}\Phi_{Tx}(3,0) - \frac{1}{2}\Phi_{Tx}(3,2)\cos 2\alpha \\ C(T_{yi}, T_{yj}) &= \frac{1}{2}\Phi_{Ty}(3,0) + \frac{1}{2}\Phi_{Ty}(3,2)\cos 2\alpha \\ C(T_{zi}, T_{zj}) &= \Phi_{Tz}(3,0) \\ C(T_{xi}, T_{yj}) &= -\frac{1}{2}\Phi_{Tx}(3,2)\sin 2\alpha \\ C(T_{xi}, T_{zj}) &= -\Phi_{Tx}(3,1)\cos\alpha \\ C(T_{yi}, T_{zj}) &= -\Phi_{Ty}(3,1)\sin\alpha \end{aligned} \tag{5.57}$$

where α is the azimuth of the observation line. These covariance functions of the first order derivatives of gravity potential depend on the azimuth of the observation line (α) and are therefore non-isotropic.

Displacement covariance functions.
The covariance functions relating the displacements are derived by adopting the Gaussian model as follows:

$$C(\delta z_i, \delta z_j) = \frac{1}{2}A_{zz}.d_{zz}^2 e^{\frac{-r^2}{2d_{zz}^2}} \tag{5.58}$$

$$C(\delta x_i, \delta x_j) = \frac{1}{2}A_{xx}.d_{xx}^2 e^{\frac{-r^2}{2d_{xx}^2}} \tag{5.59}$$

$$C(\delta y_i, \delta y_j) = \frac{1}{2}A_{yy}.d_{yy}^2 e^{\frac{-r^2}{2d_{yy}^2}} \tag{5.60}$$

$$C(\delta x_i, \delta y_j) = \frac{1}{2}A_{xy}.d_{xy}^2 e^{\frac{-r^2}{2d_{xy}^2}} \tag{5.61}$$

$$C(\delta x_i, \delta z_j) = \frac{1}{2}A_{xz}.d_{xz}^2 e^{\frac{-r^2}{2d_{xz}^2}} \tag{5.62}$$

$$C(\delta y_i, \delta z_j) = \frac{1}{2}A_{yz}.d_{yz}^2 e^{\frac{-r^2}{2d_{yz}^2}} \tag{5.63}$$

with respective variances and correlation lengths given by

$$C_{oIJ} = \frac{1}{2}A_{IJ}d_{IJ}^2; \qquad \xi_{IJ} = 1.177 d_{IJ} \tag{5.64}$$

where I, J can take symbols x, y, z.

Empirical covariance functions.
The coefficients of the covariance function are computed empirically by use of existing prior information, for example free air gravity anomalies, map of existing information on displacements. The region under investigation is divided into zones or classes with respect to distances of the discrete data points, for example at $10km$ intervals. Mean values for every class are obtained and plotted against the mean distances of their respectice classes. From this graphical plot, an empirical covariance function is established. A covariance function is completely characterised by its variance C_0, the correlation length ξ and the curvature parameter κ [Moritz, 1976]. The variance is the value of the covariance function evaluated at zero distance while the correlation length is the distance corresponding to a covariance which is half the variance. The curvature parameter gives the curvature of the covariance function at zero separation distance between the points. Reference to evaluation of empirical covariance functions can be made to [Kanngieser, 1982], [Kanngieser, 1983], [Stangl, 1979].

Propagation of covariance functions.
It is possible to have different quantities of the same field related to that field by different linear operators e. g. the gravity anomaly Δg, the geoidal height N and the elements of the deflection of the vertical ζ (north-south component), η (east-west component). In order to find the covariance between any two such signals the law of propagation of covariances [Moritz, 1972] is used. Let s_i and s_j be two signals at points P_i and P_j respectively. Let also L_a and L_b be the respective operators that produce s_i and s_j from a common function f that defines the field such that

$$\begin{aligned} s_i &= L_a f_i \\ s_j &= L_b f_j. \end{aligned} \tag{5.65}$$

The covariance between s_i and s_j is given by the law of covariance propagation as

$$cov(s_i, s_j) = L_a L_b K(P_i, P_j) \tag{5.66}$$

with $K(P_i, P_j)$ being the covariance function of the stochastic process f. This law is used in deriving covariances between the various signals that are present in four-dimensional geodesy.

5.3.3 Covariance Function for Absolute Potential on the Deformable Surface

Let the potential at point P_1 be denoted by W_1 and that at point P_j by W_2. The corresponding disturbing potentials are denoted by T_1 and T_2. The change in T due to time lapse is δT_1 and δT_2 respectively, for both points. U_i denotes the time independent normal potential at point i, $(i = 1(2))$. The potential W_1 at a point P_1 lying on this deformable surface is expressed as

$$W_1 = U_1 + T_1 + \delta T_1 - \gamma \delta r_1 \tag{5.67}$$

and similarly for the point P_2,

$$W_2 = U_2 + T_2 + \delta T_2 - \gamma \delta r_2 \tag{5.68}$$

on the same surface. Since U_i is known (fixed) and not stochastic it is dropped to obtain the covariance function between the signals at points P_1 and P_2 as

$$\begin{aligned} C(W_1, W_2) &= C(T_1 + \delta T_1 - \gamma \delta r_1, T_2 + \delta T_2 - \gamma \delta r_2) \\ &= C(T_1, T_2) + C(\delta T_1, \delta T_2) + \gamma^2 C(\delta r_1, \delta r_2) \\ &= \Phi_T(1, 0) + \Phi_{\delta T}(1, 0) + \gamma^2 C(\delta z_1, \delta z_2) \end{aligned} \tag{5.69}$$

where $\delta r \approx \delta z$. On the reference plane $z_1 = z_2 = 0$, the covariance function (5.69) becomes

$$\overline{C}(W_1, W_2) = \overline{\Phi}_T(1, 0) + \overline{\Phi}_{\delta T}(1, 0) + \gamma^2 C(\delta z_1, \delta z_2). \tag{5.70}$$

The covariance functions involved in equation (5.70) are expressed in equations (5.50), (5.51) and (5.58).

5.3.4 Covariance Function of the Potential Difference

The change in potential difference on the deformable surface between points P_1 and P_2 can be expressed as

$$\delta W_{12} = W_1 - W_2 \tag{5.71}$$

and similarly between points P_1' and P_2'

$$\delta W_{1'2'} = W_{1'} - W_{2'} \tag{5.72}$$

The covariance function of these signals is derived thus,

$$\begin{aligned} C(\delta W_{12}, \delta W_{1'2'}) &= C(W_1, W_{1'}) + C(W_2, W_{2'}) \\ &- C(W_1, W_{2'}) - C(W_2, W_{1'}) \end{aligned} \tag{5.73}$$

where

$$\begin{aligned} C(W_1, W_{1'}) &= C(T_1, T_{1'}) + C(\delta T_1, \delta T_{1'}) + \gamma^2 C(\delta z_1, \delta z_{1'}) \\ C(W_2, W_{2'}) &= C(T_2, T_{2'}) + C(\delta T_2, \delta T_{2'}) + \gamma^2 C(\delta z_2, \delta z_{2'}) \\ C(W_1, W_{2'}) &= C(T_1, T_{2'}) + C(\delta T_1, \delta T_{2'}) + \gamma^2 C(\delta z_1, \delta z_{2'}) \\ C(W_2, W_{1'}) &= C(T_2, T_{1'}) + C(\delta T_2, \delta T_{1'}) + \gamma^2 C(\delta z_2, \delta z_{1'}) \end{aligned} \tag{5.74}$$

All the covariance functions of equation (5.74) can be then written in the form

$$C(W, W) = \overline{\Phi}_T(1, 0) + \overline{\Phi}_{\delta T}(1, 0) + \gamma^2 C(\delta z, \delta z) \tag{5.75}$$

with covariance functions on the reference plane that can be inferred from equations (5.50), (5.51) and (5.58).

5.3.5 Covariance Function for Gravity Intensity

Referring to equation (5.67), and ignoring the fixed normal potential U, the corresponding change in gravity at P_1 can be expressed as

$$\begin{aligned} grad(W_1) &= grad(T_1 + \delta T_1 - \gamma \delta r_1) \\ &\approx -\frac{\partial T}{\partial Z_1} - \frac{\partial \delta T}{\partial Z_1} - \frac{2\gamma}{r} \delta Z_1. \end{aligned} \tag{5.76}$$

The covariance function between the gravity intensity signals at P_1 and P_2 is then derived as follows:

$$C(,_1,,_2) = C(-\frac{\partial T}{\partial Z_1} - \frac{\partial \delta T}{\partial Z_1} - \frac{2\gamma}{r}\delta Z_1, -\frac{\partial T}{\partial Z_2} - \frac{\partial \delta T}{\partial Z_2} - \frac{2\gamma}{r}\delta Z_2) \tag{5.77}$$

and simplification gives

$$C(,_1,,_2) = C(\frac{\partial T}{\partial Z_1}, \frac{\partial T}{\partial Z_2}) + C(\frac{\partial \delta T}{\partial Z_1}, \frac{\partial \delta T}{\partial Z_2}) + (\frac{2\gamma}{r})^2 C(\delta Z_1, \delta Z_2), \tag{5.78}$$

where cross-covariances have been omitted as being negligible. Further simplification of equation (5.78) gives

$$C(,_1,,_2) = \Phi_T(3,0) + \Phi_{\delta T}(3,0) + (\frac{2\gamma}{R})^2 C(\delta Z_1, \delta Z_2). \tag{5.79}$$

On the reference plane the covariance function for gravity intensity becomes

$$\overline{C}(,_1,,_2) = \overline{\Phi}_T(3,0) + \overline{\Phi}_{\delta T}(3,0) + (\frac{2\gamma}{R})^2 C(\delta Z_1, \delta Z_2) \tag{5.80}$$

with covariance expressions found in equations (5.54), (5.55) and (5.58).

5.3.6 Covariance Functions of Other Gravity Field Dependent Observations

These observations are astronomical latitude, longitude and azimuth, horizontal directions, (or alternatively) angles and zenith distances. The covariance functions of the first derivatives of potential are derived from the covariance function of the potential by the law of covariance propagation [Moritz, 1972]. These covariances are expressed in equation (5.57). The cross-covariances have been ignored.

Astronomical latitude:
It is referred to observation equation (4.17) of astronomical latitude. The gravity related signals T_x, T_y and T_z can be expressed using covariance functions by the law of propagation of covariances as:

$$\begin{aligned} C(T_{\Phi_1}, T_{\Phi_2}) &= C(d_{1\Phi}T_{xi} + e_{1\Phi}T_{yi} + f_{1\Phi}T_{zi}, d_{2\Phi}T_{xj} + e_{2\Phi}T_{yj} + f_{2\Phi}T_{zj}) \\ &= d_{1\Phi}d_{2\Phi}C(T_{xi}, T_{xj}) + e_{1\Phi}e_{2\Phi}C(T_{yi}, T_{yj}) + f_{1\Phi}f_{2\Phi}C(T_{zi}, T_{zj}) \end{aligned} \tag{5.81}$$

where cross-covariances have been neglected as before. The d, e, f coefficients are given in equations (4.18) and the covariance functions are expressed in equations (5.57). Similarly the covariance function of the gravity variation associated with the astronomical latitude is given by

$$\begin{aligned} C(\delta T_{\Phi_1}, \delta T_{\Phi_2}) &= C(d_{1\Phi}\delta T_{xi} + e_{1\Phi}\delta T_{yi} + f_{1\Phi}\delta T_{zi}, d_{2\Phi}\delta T_{xj} + e_{2\Phi}\delta T_{yj} + f_{2\Phi}\delta T_{zj}) \\ &= d_{1\Phi}d_{2\Phi}C(\delta T_{xi}, \delta T_{xj}) + e_{1\Phi}e_{2\Phi}C(\delta T_{yi}, \delta T_{yj}) \\ &+ f_{1\Phi}f_{2\Phi}C(\delta T_{zi}, \delta T_{zj}). \end{aligned} \tag{5.82}$$

The covariance function of astronomical latitude becomes

$$\begin{aligned} C(\Phi_1, \Phi_2) &= d_{1\Phi}d_{2\Phi}(C(T_{xi}, T_{xj}) + C(\delta T_{xi}, \delta T_{xj})) \\ &+ e_{1\Phi}e_{2\Phi}(C(T_{yi}, T_{yj}) + C(\delta T_{yi}, \delta T_{yj})) \\ &+ f_{1\Phi}f_{2\Phi}(C(T_{zi}, T_{zj}) + C(\delta T_{zi}, \delta T_{zj})) \\ &+ a_{1\Phi}a_{2\Phi}C(\delta x_i, \delta x_j) + a_{1\Phi}b_{2\Phi}C(\delta x_i, \delta y_j) \\ &+ a_{1\Phi}c_{2\Phi}C(\delta x_i, \delta z_j) + b_{1\Phi}b_{2\Phi}C(\delta y_i, \delta y_j) \\ &+ b_{1\Phi}c_{2\Phi}C(\delta y_i, \delta z_j) + c_{1\Phi}c_{2\Phi}C(\delta z_i, \delta z_j) \end{aligned} \tag{5.83}$$

with expressions for coefficients a, b and c being found in equation (4.18).

Astronomical longitude:
Equation (4.29) for astronomical longitude is considered. The covariance function of longitude becomes

$$\begin{aligned} C(\Lambda_1, \Lambda_2) &= d_{1\Lambda}d_{2\Lambda}(C(T_{xi}, T_{xj}) + C(\delta T_{xi}, \delta T_{xj})) \\ &+ e_{1\Lambda}e_{2\Lambda}(C(T_{yi}, T_{yj}) + C(\delta T_{yi}, \delta T_{yj})) \\ &+ f_{1\Lambda}f_{2\Lambda}(C(T_{zi}, T_{zj}) + C(\delta T_{zi}, \delta T_{zj})) \\ &+ a_{1\Lambda}a_{2\Lambda}C(\delta x_i, \delta x_j) + a_{1\Lambda}b_{2\Lambda}C(\delta x_i, \delta y_j) \\ &+ a_{1\Lambda}c_{2\Lambda}C(\delta x_i, \delta z_j) + b_{1\Lambda}b_{2\Lambda}C(\delta y_i, \delta y_j) \\ &+ b_{1\Lambda}c_{2\Lambda}C(\delta y_i, \delta z_j) + c_{1\Lambda}c_{2\Lambda}C(\delta z_i, \delta z_j) \end{aligned} \tag{5.84}$$

with the coefficients given by equation (4.30).

Astronomical azimuth:
From equation (4.68), the covariance function of astronomical azimuth is

$$\begin{aligned} C(A_1, A_2) &= d_{1A}d_{2A}(C(T_{xi}, T_{xj}) + C(\delta T_{xi}, \delta T_{xj})) \\ &+ e_{1A}e_{2A}(C(T_{yi}, T_{yj}) + C(\delta T_{yi}, \delta T_{yj})) \\ &+ f_{1A}f_{2A}(C(T_{zi}, T_{zj}) + C(\delta T_{zi}, \delta T_{zj})) \\ &+ a_{1A}a_{2A}C(\delta x_i, \delta x_j) + a_{1A}b_{2A}C(\delta x_i, \delta y_j) \\ &+ a_{1A}c_{2A}C(\delta x_i, \delta z_j) + b_{1A}b_{2A}C(\delta y_i, \delta y_j) \\ &+ b_{1A}c_{2A}C(\delta y_i, \delta z_j) + c_{1A}c_{2A}C(\delta z_i, \delta z_j) \end{aligned} \tag{5.85}$$

with the coefficients a, b, c, d, e, f given by equation (4.72).

These covariance functions are also used for horizontal direction observations.

Zenith distance observations:
From equation (4.56), the covariance function of zenith distance observations is

$$\begin{aligned}
C(Z_1, Z_2) &= d_{1Z}d_{2Z}(C(T_{xi}, T_{xj}) + C(\delta T_{xi}, \delta T_{xj})) \\
&+ e_{1Z}e_{2Z}(C(T_{yi}, T_{yj}) + C(\delta T_{yi}, \delta T_{yj})) \\
&+ f_{1Z}f_{2Z}(C(T_{zi}, T_{zj}) + C(\delta T_{zi}, \delta T_{zj})) \\
&+ a_{1Z}a_{2Z}C(\delta x_i, \delta x_j) + a_{1Z}b_{2Z}C(\delta x_i, \delta y_j) \\
&+ a_{1Z}c_{2Z}C(\delta x_i, \delta z_j) + b_{1Z}b_{2Z}C(\delta y_i, \delta y_j) \\
&+ b_{1Z}c_{2Z}C(\delta y_i, \delta z_j) + c_{1Z}c_{2Z}C(\delta z_i, \delta z_j) \qquad (5.86)
\end{aligned}$$

with the coefficients a, b, c, d, e, f given by equation (4.60).

Spatial distance observations:
The covariance function used for spatial distance observations is

$$\begin{aligned}
C(S_1, S_2) &= a_{1s}a_{2s}C(\delta x_i, \delta x_j) + a_{1s}b_{2s}C(\delta x_i, \delta y_j) \\
&+ a_{1s}c_{2s}C(\delta x_i, \delta z_j) + b_{1s}b_{2s}C(\delta y_i, \delta y_j) \\
&+ b_{1s}c_{2s}C(\delta y_i, \delta z_j) + c_{1s}c_{2s}C(\delta z_i, \delta z_j) \qquad (5.87)
\end{aligned}$$

with expression for coefficients being given in equations (4.49).

GPS baselines:
The covariance function for GPS baselines takes the form:

$$\begin{aligned}
C(x_{gps12}, x_{gps1'2'}) &= C(\delta x_1, \delta x_{1'}) + C(\delta x_2, \delta x_{2'}) \\
&- C(\delta x_1, \delta x_{2'}) - C(\delta x_2, \delta x_{1'}) \\
C(y_{gps12}, y_{gps1'2'}) &= C(\delta y_1, \delta y_{1'}) + C(\delta y_2, \delta y_{2'}) \\
&- C(\delta y_1, \delta y_{2'}) - C(\delta y_2, \delta y_{1'}) \\
C(z_{gps12}, z_{gps1'2'}) &= C(\delta z_1, \delta z_{1'}) + C(\delta z_2, \delta z_{2'}) \\
&- C(\delta z_1, \delta z_{2'}) - C(\delta z_2, \delta z_{1'}). \qquad (5.88)
\end{aligned}$$

These covariances are expressed in equations (5.58) through equation (5.63).

5.4 The Time Covariance Function

Both the gravity field related covariance functions and the spatial covariance functions for quantities referring to the same epoch have been presented in the previous section. However the continuation of the signals in time require a covariance function of time.

Letting $\Delta t = t_j - t_i$, where t_i and t_j denote different time epochs, then the time covariance function will be

$$\begin{aligned} C(\delta T_1(t_j), \delta T_2(t_i)) &= C(\delta T_1, \delta T_2) \cdot (e^{-\frac{1}{2}\frac{\Delta t^2}{\sigma^2}}) \\ &= \frac{1}{2} A_{\delta T}.d_{\delta T}^4 (e^{-\frac{1}{2}\frac{\Delta t^2}{\sigma^2}}) \int_{t=0}^{\infty} t e^{-t(z_1+z_2)} e^{\frac{-t^2 d_{\delta T}^2}{2}} J_0(t.r) dt \end{aligned} \tag{5.89}$$

in the case of variations of the disturbing potential. The exponential $(e^{-\frac{1}{2}\frac{\Delta t^2}{\sigma^2}})$ denotes the time dependence on the signal and σ is the time correlation length. For points on the reference plane equation (5.89) can be simplified as

$$C(\delta T_1(t_j), \delta T_2(t_i)) = \frac{1}{2} A_{\delta T}.d_{\delta T}^2 (e^{-\frac{1}{2}\frac{\Delta t^2}{\sigma^2}}) e^{-\frac{1}{2}(\frac{r}{d})^2}. \tag{5.90}$$

The variance $C_{0\delta T}$ of this function, evaluated at $\Delta t = 0$ and $r = 0$ is

$$C_{0\delta T} = \frac{1}{2} A_{\delta T}.d_{\delta T}^2$$

which is the same as the variance of the disturbing potential at the initial epoch given by equation (5.53) but the time correlation length is given by

$$\xi_{\delta T} = d_{\delta T} (1.3863 - \frac{\Delta t^2}{\sigma^2})^{\frac{1}{2}}. \tag{5.91}$$

The disturbing potential functional $T(t_o)$ does not require a time covariance function because the time variation of this potential has a covariance function (5.89) instead. The displacements, however require time covariance functions which are derived by introducing a time element in their respective spatial covariance functions. Thus

$$C(\delta z_1(t_i), \delta z_2(t_j)) = C(\delta z_1, \delta z_2) \cdot (e^{-\frac{1}{2}\frac{\Delta t^2}{\sigma^2}}) = \frac{1}{2} A_{zz}.d_{zz}^2 e^{\frac{-r^2}{2d_{zz}^2}} \cdot (e^{-\frac{1}{2}\frac{\Delta t^2}{\sigma^2}}) \tag{5.92}$$

$$C(\delta x_1(t_i), \delta x_2(t_j)) = C(\delta x_1, \delta x_2) \cdot (e^{-\frac{1}{2}\frac{\Delta t^2}{\sigma^2}}) = \frac{1}{2} A_{xx}.d_{xx}^2 e^{\frac{-r^2}{2d_{xx}^2}} \cdot (e^{-\frac{1}{2}\frac{\Delta t^2}{\sigma^2}}) \tag{5.93}$$

$$C(\delta y_1(t_i), \delta y_2(t_j)) = C(\delta y_1, \delta y_2) \cdot (e^{-\frac{1}{2}\frac{\Delta t^2}{\sigma^2}}) = \frac{1}{2} A_{yy}.d_{yy}^2 e^{\frac{-r^2}{2d_{yy}^2}} \cdot (e^{-\frac{1}{2}\frac{\Delta t^2}{\sigma^2}}) \tag{5.94}$$

$$C(\delta x_1(t_i), \delta y_2(t_j)) = C(\delta x_1, \delta y_2) \cdot (e^{-\frac{1}{2}\frac{\Delta t^2}{\sigma^2}}) = \frac{1}{2} A_{xy}.d_{xy}^2 e^{\frac{-r^2}{2d_{xy}^2}} \cdot (e^{-\frac{1}{2}\frac{\Delta t^2}{\sigma^2}}) \tag{5.95}$$

$$C(\delta x_1(t_i), \delta z_2(t_j)) = C(\delta x_1, \delta z_2) \cdot (e^{-\frac{1}{2}\frac{\Delta t^2}{\sigma^2}}) = \frac{1}{2} A_{xz}.d_{xz}^2 e^{\frac{-r^2}{2d_{xz}^2}} \cdot (e^{-\frac{1}{2}\frac{\Delta t^2}{\sigma^2}}) \tag{5.96}$$

$$C(\delta y_1(t_i), \delta z_2(t_j)) = C(\delta y_1, \delta z_2) \cdot (e^{-\frac{1}{2}\frac{\Delta t^2}{\sigma^2}}) = \frac{1}{2} A_{yz}.d_{yz}^2 e^{\frac{-r^2}{2d_{yz}^2}} \cdot (e^{-\frac{1}{2}\frac{\Delta t^2}{\sigma^2}}). \tag{5.97}$$

The time covariance functions

It is now possible to express covariance functions for the various geodetic observables that express the signals in time. Some of the classical and space observations are considered below.

Potential difference The time covariance function of the signals involved in potential is derived by taking into account equation (5.73)

$$\begin{aligned} C(\delta W_{12}(t_i), \delta W_{1'2'}(t_j)) &= C(W_1(t_i), W_{1'}(t_j)) + C(W_2(t_i), W_{2'}(t_j)) \\ &- C(W_1(t_i), W_{2'}(t_j)) - C(W_2(t_i), W_{1'}(t_j)) \end{aligned} \tag{5.98}$$

where

$$\begin{aligned} C(W_1(t_i), W_{1'}(t_j)) &= C(T_1(t_o), T_{1'}(t_o)) + C(\delta T_1(t_i), \delta T_{1'}(t_j)) \\ &+ \gamma^2 C(\delta z_1(t_i), \delta z_{1'}(t_j)) \\ C(W_2(t_i), W_{2'}(t_j)) &= C(T_2(t_o), T_{2'}(t_o)) + C(\delta T_2(t_i), \delta T_{2'}(t_j)) \\ &+ \gamma^2 C(\delta z_2(t_i), \delta z_{2'}(t_j)) \\ C(W_1(t_i), W_{2'}(t_j)) &= C(T_1(t_o), T_{2'}(t_o)) + C(\delta T_1(t_i), \delta T_{2'}(t_j)) \\ &+ \gamma^2 C(\delta z_1(t_i), \delta z_{2'}(t_j)) \\ C(W_2(t_i), W_{1'}(t_j)) &= C(T_2(t_o), T_{1'}(t_o)) + C(\delta T_2(t_i), \delta T_{1'}(t_j)) \\ &+ \gamma^2 C(\delta z_2(t_i), \delta z_{1'}(t_j)). \end{aligned} \tag{5.99}$$

Gravity intensity observations The time covariance function for gravity intensity is obtained by considering equation (5.78)

$$\begin{aligned} C(,{}_1(t_i),,{}_2(t_i)) &= C(\frac{\partial T}{\partial Z_1}(t_i), \frac{\partial T}{\partial Z_2}(t_j)) + C(\frac{\partial \delta T}{\partial Z}{}_1(t_i), \frac{\partial \delta T}{\partial Z_2}(t_j)) \\ &+ (\frac{2\gamma}{r})^2 C(\delta Z_1(t_i), \delta Z_2(t_j)), \end{aligned} \tag{5.100}$$

Astronomical latitude:
This covariance function is deduced by considering equation (5.83)

$$C(\Phi_1(t_i), \Phi_2(t_j)) = d_{1\Phi} d_{2\Phi} (C(T_{x_1}(t_o), T_{x_2}(t_o)) + C(\delta T_{x_1}(t_i), \delta T_{x_2}(t_j)))$$

$$
\begin{aligned}
&+ \quad e_{1\Phi}e_{2\Phi}(C(T_{y_1}(t_o), T_{y2}(t_o)) + C(\delta T_{y_1}(t_i), \delta T_{y2}(t_j))) \\
&+ \quad f_{1\Phi}f_{2\Phi}(C(T_{z1}(t_o), T_{z2}(t_o)) + C(\delta T_{z1}(t_i), \delta T_{z2}(t_j))) \\
&+ \quad a_{1\Phi}a_{2\Phi}C(\delta x_1(t_i), \delta x_2(t_j)) + a_{1\Phi}b_{2\Phi}C(\delta x_1(t_i), \delta y_2(t_j)) \\
&+ \quad a_{1\Phi}c_{2\Phi}C(\delta x_1(t_i), \delta z_2(t_j)) + b_{1\Phi}b_{2\Phi}C(\delta y_1(t_i), \delta y_2(t_j)) \\
&+ \quad b_{1\Phi}c_{2\Phi}C(\delta y_1(t_i), \delta z_2(t_j)) + c_{1\Phi}c_{2\Phi}C(\delta z_1(t_i), \delta z_2(t_j)). \qquad (5.101)
\end{aligned}
$$

The covariances in the above equation are expressed in equations (5.90) and (5.92) through (5.97).

Astronomical longitude:
Considering equation (5.84) the time covariance function for astronomical longitude becomes

$$
\begin{aligned}
C(\Lambda_1(t_i), \Lambda_2(t_j)) &= d_{1\Lambda}d_{2\Lambda}(C(T_{x1}(t_o), T_{x2}(t_o)) + C(\delta T_{x1}(t_i), \delta T_{x2}(t_j))) \\
&+ \quad e_{1\Lambda}e_{2\Lambda}(C(T_{y1}(t_o), T_{y2}(t_o)) + C(\delta T_{y1}(t_i), \delta T_{y2}(t_j))) \\
&+ \quad f_{1\Lambda}f_{2\Lambda}(C(T_{z1}(t_o), T_{z2}(t_o)) + C(\delta T_{z1}(t_i), \delta T_{z2}(t_j))) \\
&+ \quad a_{1\Lambda}a_{2\Lambda}C(\delta x_1(t_i), \delta x_2(t_j)) + a_{1\Lambda}b_{2\Lambda}C(\delta x_1(t_i), \delta y_2(t_j)) \\
&+ \quad a_{1\Lambda}c_{2\Lambda}C(\delta x_1(t_i), \delta z_2(t_j)) + b_{1\Lambda}b_{2\Lambda}C(\delta y_1(t_i), \delta y_2(t_j)) \\
&+ \quad b_{1\Lambda}c_{2\Lambda}C(\delta y_1(t_i), \delta z_2(t_j)) + c_{1\Lambda}c_{2\Lambda}C(\delta z_1(t_i), \delta z_2(t_j)). \qquad (5.102)
\end{aligned}
$$

The covariances in the above equation are expressed in equations (5.90) and (5.92) through (5.97).

Zenith distance observations:
The time covariance function involved in zenith distance obseravtions is derived by considering equation (5.86)

$$
\begin{aligned}
C(Z_1(t_i), Z_2(t_j)) &= d_{1Z}d_{2Z}(C(T_{x1}(t_o), T_{x2}(t_o) + C(\delta T_{x1}(t_i), \delta T_{x2}(t_j))) \\
&+ \quad e_{1Z}e_{2Z}(C(T_{y1}(t_o), T_{y2}(t_o)) + C(\delta T_{y1}(t_i), \delta T_{y2}(t_j))) \\
&+ \quad f_{1Z}f_{2Z}(C(T_{z1}(t_o), T_{z2}(t_o)) + C(\delta T_{z1}(t_i), \delta T_{z2}(t_j))) \\
&+ \quad a_{1Z}a_{2Z}C(\delta x_1(t_i), \delta x_2(t_j)) + a_{1Z}b_{2Z}C(\delta x_1(t_i), \delta y_2(t_j)) \\
&+ \quad a_{1Z}c_{2Z}C(\delta x_1(t_i), \delta z_2(t_j)) + b_{1Z}b_{2Z}C(\delta y_1(t_i), \delta y_2(t_j)) \\
&+ \quad b_{1Z}c_{2Z}C(\delta y_1(t_i), \delta z_2(t_j)) + c_{1Z}c_{2Z}C(\delta z_1(t_i), \delta z_2(t_j)) \qquad (5.103)
\end{aligned}
$$

Spatial distance observations:
The time covariance function for spatial distance observations is derived by considering equations (5.87), (5.92) through (5.97)

$$
\begin{aligned}
C(S_1(t_i), S_2(t_j)) &= a_{1s}a_{2s}C(\delta x_1(t_i), \delta x_2(t_j)) + a_{1s}b_{2s}C(\delta x_1(t_i), \delta y_2(t_j)) \\
&+ \quad a_{1s}c_{2s}C(\delta x_1(t_i), \delta z_2(t_j)) + b_{1s}b_{2s}C(\delta y_1(t_i), \delta y_2(t_j)) \\
&+ \quad b_{1s}c_{2s}C(\delta y_1(t_i), \delta z_2(t_j)) + c_{1s}c_{2s}C(\delta z_1(t_i), \delta z_2(t_j)). \qquad (5.104)
\end{aligned}
$$

GPS baselines:

The time covariance function for GPS baselines is derived from equation (5.88) and considering equations (5.92) through (5.97) as

$$\begin{aligned}
C(x_{gps12}(t_i), x_{gps1'2'}(t_j)) &= C(\delta x_1(t_i), \delta x_{1'}(t_j)) + C(\delta x_2(t_i), \delta x_{2'}(t_j)) \\
&- C(\delta x_1(t_i), \delta x_{2'}(t_j)) - C(\delta x_2(t_i), \delta x_{1'}(t_j)) \\
C(y_{gps12}(t_i), y_{gps1'2'}(t_j)) &= C(\delta y_1(t_i), \delta y_{1'}(t_j)) + C(\delta y_2(t_i), \delta y_{2'}(t_j)) \\
&- C(\delta y_1(t_i), \delta y_{2'}(t_j)) - C(\delta y_2(t_i), \delta y_{1'}(t_j)) \\
C(z_{gps12}(t_i), z_{gps1'2'}(t_j)) &= C(\delta z_1(t_i), \delta z_{1'}(t_j)) + C(\delta z_2(t_i), \delta z_{2'}(t_j)) \\
&- C(\delta z_1(t_i), \delta z_{2'}(t_j)) - C(\delta z_2(t_i), \delta z_{1'}(t_j)). \qquad (5.105)
\end{aligned}$$

6. The Test Examples

6.1 The Karlsruhe Network

6.1.1 General Information about the Network

The Karlsruhe test network is situated in Germany and lies between the latitudes $48°48'$N and $49°30'$N and longitudes $7°50'$E and $9°00'$E in the upper Rhine Graben area. It was established since 1967 and covers an area of about $50 \times 60km^2$. It consists of eleven network points. These have however, been reduced owing to optimisation studies. This study limits itself to seven points of this network. These are Letzenberg (3), Michaelsberg (2), Turmberg (1), Stäffelsberg (6), Madenburg (5), Kalmit (4) and Herxheim (7).

The network was setup originally for the purpose of carrying out investigations on electronic distance meters (EDM). Today it serves as a network for geodynamic investigations. Measurements made in this network include distances, directions, zenith angles, astronomical- latitudes and longitudes, gravity measurements and lately *GPS* measurements. More information about the network is found in [Kuntz, 1971], [Klein, 1997], [Heck et al., 1995].

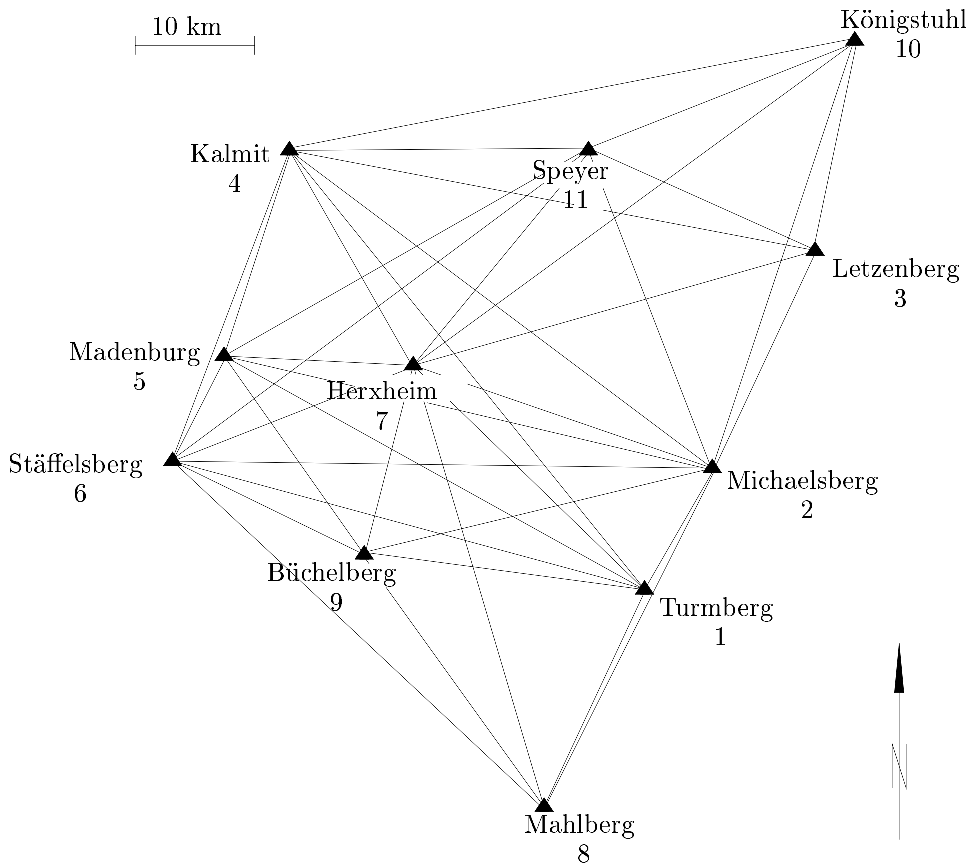

Figure. 6.1: The Karlsruhe test network.

By no means can the Karlsruhe test network be considered a regional network owing to its small size (see Fig. 6.1 above). However due to the availability of some data for this network, it was chosen as test example for demonstration purposes.

6.1.2 The Computation of the Test Network

Only classical type of observations of type spatial distances, zenith distances, horizontal directions, astronomical latitude and longitude and gravity intensity see Table (6.1) were considered. All the observations present were considered to have been made at the same instant (epoch).

This choice led to a single epoch type of adjustment that corresponds to the three-dimensional integrated case. Only the spatial covariance functions (see section 5.3.2) were required. The time covariance functions are required where the observations are made at different observation periods. In order to use the covariance functions, the free parameters are first determined separately from suitable data, for example free air gravity anomalies. In this example, after some preliminary investigations about the covariance functions, it turned out that the values of these free parameters did not vary greatly for the regions considered. Thus values given in [Reilly, 1979] were adopted. The value of the variance used was $C_{0\delta T} = 5 \times 10^{-8}(N/Kg)^2$ and the distance $d_T = 10km$. Variation of d_T even upto $d = 100km$ had very little influence on the results.

Table 6.1: Types of observations

No.	Observation type	No. of observations
1	Spatial distances	21
2	Horizontal directions	42
3	Zenith distances	42
4	Astro. latitude	7
5	Astro. longitude	7
6	Gravity intensity	7

Table 6.2: Approximate geocentric coordinates of the test network

STATION No.	X (m)	Y (m)	Z (m)
1	4147006.036	618709.483	4790583.678
2	4138576.887	623279.522	4797217.653
3	4123745.629	629406.577	4809061.013
4	4124664.462	585763.490	4814320.064
5	4137880.317	582130.796	4803209.231
6	4145159.421	578798.129	4797418.098
7	4135921.247	597614.197	4802590.615

The observations were then processed according to the model of four-dimensional geodesy given in equation (3.20) but with the time dependent signals missing. Thus the example did not include displacements and time disturbing potential variations. The resulting normal equation matrix showed a rank defect of four. This was due to three translations and a rotation about the z axis since no azimuth observations were present. The datum was then defined over all points of the network using the approximate coordinates thus resulting in a free network adjustment.

Tables (6.2) through (6.4) show some results about this network when computed using the proposed covariance functions.

Table 6.3: Adjusted coordinates

STATION No.	X (m)	Y (m)	Z (m)
1	4147006.107	618709.549	4790583.749
2	4138576.909	623279.555	4797217.806
3	4123745.683	629406.542	4809061.242
4	4124664.456	585763.413	4814319.956
5	4137880.100	582130.753	4803208.857
6	4145159.563	578798.180	4797418.120
7	4135921.277	597614.199	4802590.621

Table 6.4: Standard errors of adjusted coordinates

STATION No.	STD. ERR $\sigma_X(m)$	STD. ERR $\sigma_Y(m)$	STD. ERR $\sigma_Z(m)$
1	0.00864	0.00567	0.01339
2	0.00713	0.00293	0.01302
3	0.00930	0.00359	0.01845
4	0.01062	0.00594	0.01374
5	0.01085	0.00242	0.01743
6	0.00690	0.00299	0.01313
7	0.00690	0.00160	0.00872

6.2 The Kenyan Gravity Network

The gravity measurements that were available were observed along a section running in a northwest- southeast direction. For the computation of empirical covariance functions a section of this gravity network was used (see Figure (6.3)).

The covariance function An empirical covariance function for gravity anomalies was computed from free air gravity anomalies (see Figure (6.2)). The values of the parameters are:

$$\begin{aligned} C_{0\Delta g} &= 1205.0\text{mgal**2} \\ \xi_{\Delta g} &= 55.0\text{km} \end{aligned} \tag{6.1}$$

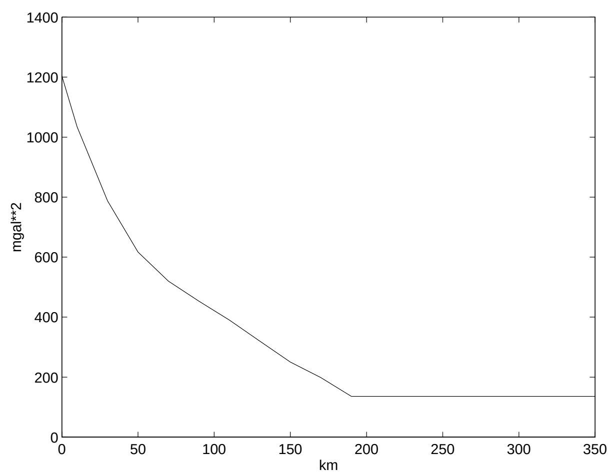

Figure 6.2: The empirical covariance function computed from free air gravity anomalies

The distribution of the points considered is shown in Figure (6.3). The model covariance

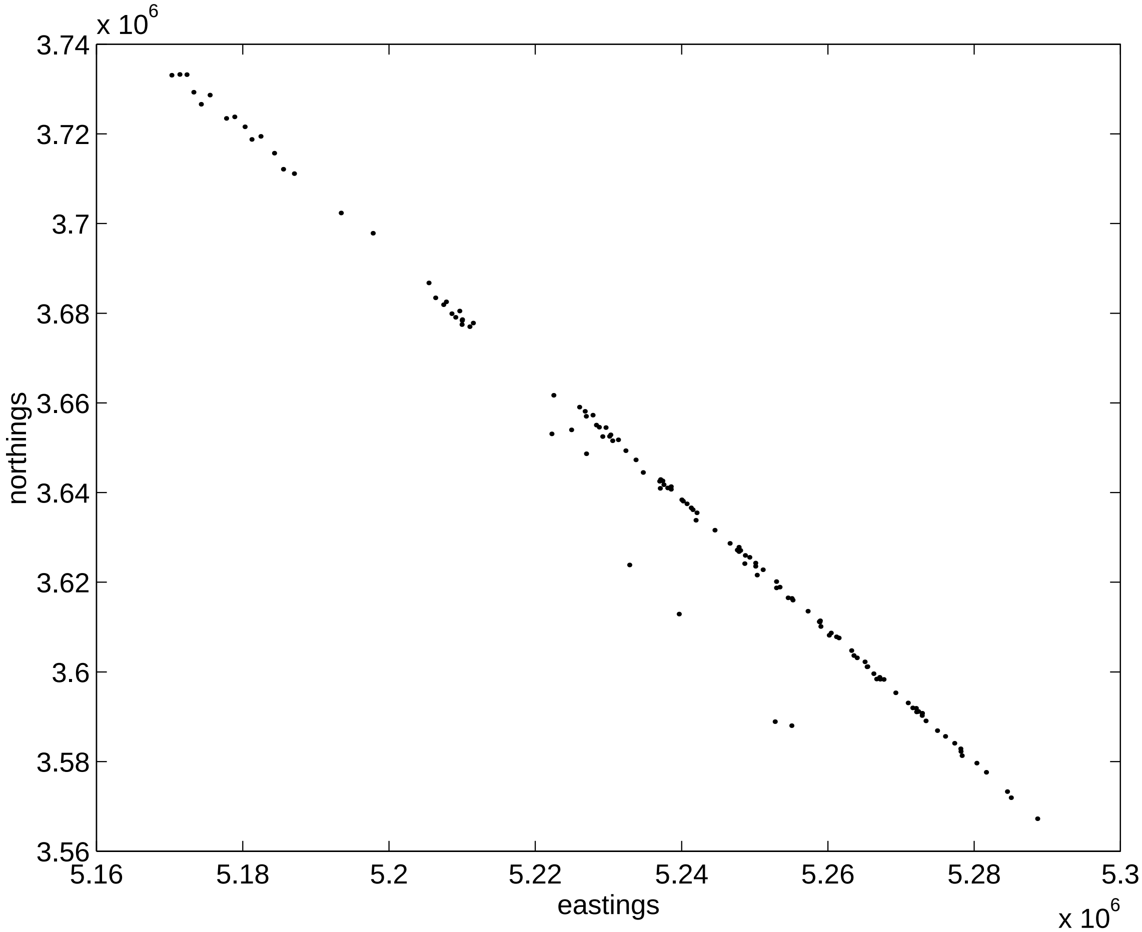

Figure 6.3: The distribution of the free air gravity anomaly points

functions of the potential and the vertical derivative resulting from the above empirical model are shown in Figures (6.4) and (6.5) respectively. The vertical component of gravity vector has a higher effect on the vertical displacements than the horizontal components.

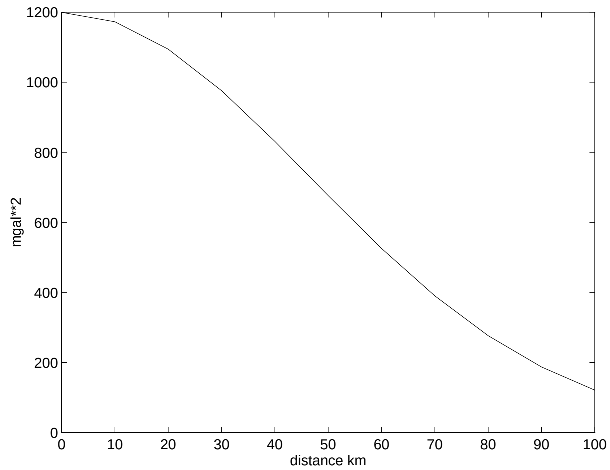

Figure 6.4: The model covariance function for potential

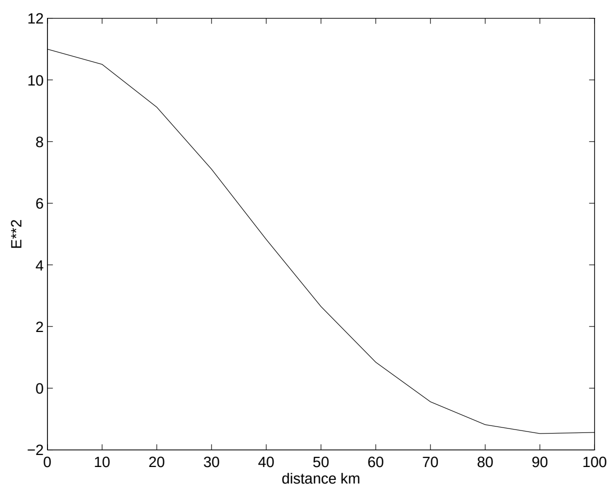

Figure 6.5: The model covariance function for the vertical derivative of potential -T_z

7. Summary and Conclusions

Four-dimensional geodesy deals with processing of integrated geodetic observations in order to analyse the network geometry and its variation with time, when these observations depend on the gravity field of the earth and its temporal variation. This consideration introduces the time dimension into the three-dimensional integrated model.

The usual way to establish a geodetic network is to choose a few discrete points and make observations from them. These measurements are influenced by the gravity field which is of continuous nature and also time variant. The earth's surface is also deformable with all its points being in a state of motion (see Figure (1.1)). The change in position of the points or the displacements are also dependent on time.

With this background in mind this study set out to establish a model whereby not only the continuous effect of the gravity field on the measurements is taken into account but also the time varying aspect of this field and the time variation of position (displacements) on the observations.

A general derivation of the observation equation considering the above mentioned aspects was made. The resulting equation of four-dimensional geodesy consists of essentially four different type of parameters - the coordinate corrections, the displacements, the disturbing potential function (or its derivatives) and their time variations. The coordinate corrections were considered as being of deterministic type while the other three were considered as stochastic signals. The signals were then considered as continuous both in time and space. Specific observation equations for some common geodetic observations were then derived.

Stochastic modelling was considered inducing covariance functions for both gravity potential field functionals and the displacements. The covariance model according to [Reilly, 1979] was adopted due to its spatial character and from it covariance functions for the disturbing potential and its common derivatives were derived. Further, displacement covariance functions were also derived. Based on some profile of the Kenyan gravity free air anomalies, covariance functions relating the potential field parameters were empirically computed. A test example based on the Karlsruhe test network was computed based on the stochastic signal model and the solution was obtained according to the least squares collocation.

In order to realise the high precisions available today from geodetic instruments and procedures, it can be concluded that it is necessary to model not only the gravity dependence on the observations but also the time dependent variations in both positioning and the gravity field in an integrated way. A four-dimensional integrated model for geodesy was developed in both time and space.

Further and in view of the increasing applications of the GPS in precise geodetic work, a GPS antenna calibration was carried out. By studying the spectrum of the normal equation matrix containing the information about the antenna offsets a method of testing for the significance of the non-estimable vertical component of the antenna offsets was presented.

As presented here the problem of modelling in four-dimensional geodesy is one of handling the continuous signals (see equation (3.20)) both in time and space. In the stochastic modelling the data used in the evaluation of covariance functions need to be well distributed both in space and time for these covariance functions to be more reliable. The significance of the cross-covariances between the gravity field related signals and the displacements may need to be investigated further so as to improve this modelling. In the event that the four-dimensional modelling is to be used for networks of vast extent, then the plane approximation of the covariance functions will require to be extended on to the sphere. For local area networks, for example in engineering surveys, simpler analytical expressions may be preferred against the stochastic approach because in small areas the displacements usually exhibit regular behaviour which can be modelled using only few parameters. In such cases the gravity field parameters may only have a negligible effect in relation to the achievable quality of the observations.

Bibliography

[Adam, 1990] Adam, J. (1990). *Estimability of Geodetic Parameters from space VLBI Observables.* The Ohio State University, Department of Geodetic Science, Columbus. Report No. 406.

[Aduol, 1989] Aduol, F. (1989). *Integrierte geodätische Netzanalyse mit stochastischer Vorinformation über Schwerefeld und Referenzellipsoid.* Deutsche Geodätische Kommission, Reihe C, Heft Nr. 351. München.

[Asteriadis and Schwan, 1998] Asteriadis, G. and Schwan, H. (1998). GPS and Terrestrial Measurements for Detecting Crustal Movements in Seismic Area. *Survey Review*, 34, No. 269 (July 1998):447–454.

[Baarda, 1973] Baarda, W. (1973). *S-Transformation and Criterion Matrices.* Netherlands Geodetic Commission, Publications on Geodesy, vol. 5, no. 1, Delft.

[Becker, 1984] Becker, M. (1984). *Analyse von hochpräzisen Schweremessungen.* Deutsche Geodätische Kommission, Reihe C, Heft Nr. 294. München.

[Bevis et al., 1997] Bevis, M., Bock, Y., Fang, P., Reilinger, R., Herring, T., Stowell, J., and Jr., R. S. (1997). Blending Old and New Approaches to Regional GPS Geodesy. *EOS*, 78:277–285.

[Blaha, 1977] Blaha, G. (1977). Least Squares Prediction and Filtering in any Dimensions using the Principles of Array Algebra, Ed. I. Mueller. *Bull. Geod.*, 51:265–286.

[Breuer and Wohlleben, 1995] Breuer, B. and Wohlleben, R. (1995). Kalibrierung von GPS-Antennen für hochgenaue geodätische Anwendungen. *SPN*, 2:49–59.

[Bruns, 1878] Bruns, H. (1878). *Die Figur der Erde.* Publ. Königl. Preuss. Geod. Inst., Berlin.

[Bullen, 1975] Bullen, K. E. (1975). *The Earth's Density.* Chapman and Hall, London.

[Collier et al., 1988] Collier, P. A., Eissfeller, B., Hein, G., and Landau, H. (1988). On a Four-dimensional Integrated Geodesy. *Bull. Geod.*, 62:71–91.

[Dermanis, 1980] Dermanis, A. (1980). VLBI: Principles and Geodynamic Prospectives. *Quaterniones Geodaesiae*, 3:213–230.

[Dermanis, 1985] Dermanis, A. (1985). Optimization Problems in Geodetic Networks with Signals. In *Optimization and Design of Geodetic Networks.*, pages 220–256, Springer-Verlag.

[Dermanis, 1991a] Dermanis, A. (1991a). *Statistical Inference in Integrated Geodesy.* XXth Congress of the IUGG, IAG., Vienna, August 11-24, 1991.

[Dermanis, 1991b] Dermanis, A. (1991b). *A Unified Approach to Linear Estimation and Prediction.* XXth Congress of the IUGG, IAG., Vienna, August 11-24, 1991.

[Dermanis, 1995] Dermanis, A. (1995). *The Nonlinear and Space-time Geodetic Datum Problem.* Mathematische Methoden der Geodäsie. Mathematische Forschungsinstitut Oberwolfach 01.10.1995.

[Dermanis, 1998] Dermanis, A. (1998). Generalized inverses of nonlinear mappings and the nonlinear geodetic datum problem. *Journal of Geodesy*, 72:71–100.

[Dermanis and Rossikopoulos, 1988] Dermanis, A. and Rossikopoulos, D. (1988). Modelling Alternatives in Four-dimensional Geodesy. In *International Symposium, Instrumentation, Theory and Analysis for Integrated Geodesy, May 16 - 20.*, pages 115–145, Sopron, Hungary.

[Dong et al., 1998] Dong, D., Herring, T. A., and King, R. W. (1998). Estimating Regional Deformation from a Combination of Space and Terrestrial Geodetic Data. *Journal of Geodesy.*, 72:200–214.

[Draheim, 1971] Draheim, H. (1971). Die Geodäsie ist die Wissenschaft von der Ausmessung und Abbildung der Erdoberfläche - eine Umfrage zur heutigen Situation in der Geodäsie. *Allgemeine Vermessungs-Nachrichten*, 78:237–251.

[Drewes, 1995] Drewes, H. (1995). *Stationäre und Kinematische Referenzsysteme.* Deutsches Geodätisches Forschungsinstitut - DGK Arbeitskreis - Rezente Krustenbewengung- Leipzig, 16. /17.2.1995.

[Eeg and Krarup, 1975] Eeg, J. and Krarup, T. (1975). Integrated geodesy. In *Mathematical Geodesy, Methoden und Verfahren der mathematischen Physik, Band 12, B I*, Wissenschafts- Verlag, Zurich.

[Geiger, 1988] Geiger, A. (1988). *Einfluss und Bestimmung der Variabilität des Phasenzentrums von GPS-Antennen.* Institut für Geodäsie und Photogrammetrie an der ETH Zürich Mitteilungen Nr. 43.

[Gendt et al., 1995] Gendt, G., Dick, G., and Reigber, C. (1995). Das IGS- Analysezentrum am GFZ Potsdam: Verarbeitungssystem und Ergebnisse. *Zeitschrift für Vermessungswesen.*, 9:438–448.

[Gendt et al., 1998] Gendt, G., Dick, G., and Soehne, W. (1998). *GFZ Analysis Center of IGS.* IGS Annual Report 1997., Analysezentrum am GFZ Potsdam.

[Grafarend, 1978a] Grafarend, E. W. (1978a). Dreidimensionale geodätische Abbildungsgleichungen und die Näherungsfigur der Erde. *Zeitschrift für Vermessungswesen.*, 3:132–140.

[Grafarend, 1978b] Grafarend, E. W. (1978b). Operational Geodesy. In *Approximation Methods in Geodesy. Eds. Moritz and Sünkel.*, pages 235–284, Herbert Wichmann Verlag Karlsruhe.

[Grafarend, 1979] Grafarend, E. W. (1979). Space-time Geodesy. *Boll. Di Geodesia e Scienze Affini. ANNO XXXVIII N. 2*, 2:305–343.

[Grafarend, 1981] Grafarend, E. W. (1981). Die Beobachtungsgleichungen der dreidimensionalen Geodäsie im Geometrie- und Schwereraum. *Zeitschrift für Vermessungswesen.*, 8:411–429.

[Grafarend, 1982] Grafarend, E. W. (1982). Space-time Geodesy Eds. H. Moritz and H. Sunkel. In *Geodesy and Global Geodynamics.*, pages 577–612, Mitteilungen der Geodätischen Institute der Technischen Universität Graz, Folge 41.

[Grafarend and Richter, 1978] Grafarend, E. W. and Richter, B. (1978). Threedimensional Geodesy II - the Datum Problem. *Zeitschrift für Vermessungswesen*, 103:44–59.

[Heck, 1984] Heck, B. (1984). *Zur Bestimmung vertikaler rezenter Erdkrustenbewegungen und zeitlicher Änderungen des Schwerefeldes aus wiederholten Schweremessungen und Nivellements.* Deutsche Geodätische Kommission, Reihe C, Heft Nr. 302. München.

[Heck, 1987] Heck, B. (1987). *Rechenverfahren und Auswertemodelle der Landesvermessung - klassische und moderne Methoden.* Herbert Wichmann Verlag Karlsruhe.

[Heck, 1989] Heck, B. (1989). Geodätische Methoden zur Bestimmung rezenter Krustenbewengungen im lokalen und regionalen Bereich. In *Rezente Krustenbewegungen, Eds. Kersting, N. und Welsch W.; Schriftenreihe Universität der Bundeswehr München. Heft 39, June 8 - 9.*, pages 143–170, Neubiberg, Germany.

[Heck, 1991] Heck, B. (1991). Referenzsysteme. In *GPS und Integration von GPS in bestehende geodätische Netze*, Geodätisches Institut, Universität Karlsruhe. p. 90-124.

[Heck et al., 1995] Heck, B., Illner, M., and Jäger, R. (1995). Deformationsanalyse zum Testnetz Karlsruhe auf der Basis der terrestrichen Nullmessung und aktueller GPS-Kampagnen. In *Festschrift für Heinz Draheim, Eugen Kuntz, Herman Mälzer.*, pages 75–91, Geodätisches Institut der Universität Karlsruhe (TH), Germany.

[Hein, 1986] Hein, G. (1986). Integrated Geodesy. In *Lecture Notes in Earth Sciences. Mathematical Techniques in Physical Geodesy. Lectures delivered at the International Summer School in the Mountains on Mathematical and Numerical Techniques in Physical Geodesy, Admont, Austria August 25 to September 5, 1986. Eds. H. Sünkel.*, pages 505–548, Springer-Verlag Berlin, Heidelberg, New York, London.

[Hein and Kistermann, 1981] Hein, G. and Kistermann, R. (1981). Mathematical Foundations of Non-tectonic Effects in Geodetic Recent Crustal Movement Models. *Tectonophysics*, 71:315–334.

[Hein and Landau, 1989] Hein, G. and Landau, H. (1989). *A Contribution to 3D-Operational Geodesy. Part 3: OPERA - A Multipurpose Program for Operational Adjustment of Observations of Terrestrial Type.* Deutsche Geodätische Kommission, Reihe B, Heft Nr. 264. München.

[Hein et al., 1987] Hein, G., Landau, H., Kakkuri, J., and Vermeer, M. (1987). Integrated 3D-Adjustment of the SW Finland Test Net with the FAF Munich OPERA 2.3 Software. *Reports of the Finnish Geodetic Institute, No. 87.3.*

[Heiskanen and Moritz, 1967] Heiskanen, W. A. and Moritz, H. (1967). *Physical Geodesy.* W. H. Freeman and Company, San Franscisco and London.

[Helmert, 1880] Helmert, F. R. (1880). *Die mathematischen und physikalischen Theorien der höheren Geodäsie - Einleitung und 1. Teil;.* B G Teubner, Leipzig.

[Hofmann-Wellenhof et al., 1992] Hofmann-Wellenhof, B., Lichtenegger, H., and Collins, J. (1992). *Global Positioning System - Theory and Practice.* Springer-Verlag - Wien - New York.

[Holdahl and Hardy, 1979] Holdahl, S. and Hardy, R. (1979). Solvability and Multiquadric Analysis as applied to Investigations of Crustal Movements. *Tectonophysics*, 52:139–155.

[Hotine, 1957] Hotine, M. (1957). *Metrical Properties of the Earth's Gravitational Field.* AIG Toronto.

[Illner, 1985] Illner, I. (1985). *Datumsfestlegung in freien Netzen.* Deutsche Geodätische Kommission, Reihe C, Heft Nr. 309. München.

[Jinsheng et al., 1992] Jinsheng, N., Dajie, L., and Dingbo, C. (1992). Theory of integrated geodesy and its practical applications. *Acta Geodetica et Cartographica Sinica*, pages 7–21.

[Kaniuth et al., 1996] Kaniuth, K., Drewes, H., Stuber, K., Tremel, H., and Moirano, J. (1996). *Report on the Processing of the SIRGAS 95 GPS Network - interner Bericht.* Deutsches Geodätisches Forschungsinstitut.

[Kanngieser, 1982] Kanngieser, E. (1982). *Untersuchung zur Bestimmung tektonisch bedingter zeitlicher Schwere- und Höhenänderungen in Nordisland.* Wiss. Arb. Fachr. Vermessungswesen der Universität Hannover, Nr. 114.

[Kanngieser, 1983] Kanngieser, E. (1983). Modellierung vertikaler Krustenbewegungen durch Kollokation. *Zeitschrift für Vermessungswesen*, 108:373–381.

[Klein, 1997] Klein, U. (1997). *Analyse und Vergleich unterschiedlicher Modelle der dreidimensionalen Geodäsie.* Deutsche Geodätische Kommission, Reihe C, Heft Nr. 479. München.

[Kleusberg and Teunissen., 1996] Kleusberg, A. and Teunissen., P. (1996). *GPS for Geodesy.* Springer Verlag.

[Koch, 1978] Koch, K. (1978). Hypothesentests bei singulären Ausgleichungsproblem. *Zeitschrift für Vermessungswesen.*, 103:1–9.

[Koch, 1988] Koch, K. (1988). *Parameter Estimation and Hypothesis Testing in Linear Models.* Springer-Verlag.

[Krarup, 1971] Krarup, T. (1971). *Introducing Integrated Geodesy.* Lectures read at the Technical University of Berlin.

[Kulkarni, 1992] Kulkarni, M. N. (1992). *A Feasibility Study of Space VLBI For Geodesy and Geodynamics.* The Ohio State University, Department of Geodetic Science, Columbus. Report No. 420.

[Kuntz, 1971] Kuntz, E. (1971). *Elektronische Entfernungsmessungen auf Teststrecken und im Testnetz Karlsruhe.* Deutsche Geodätische Kommission, Reihe B, Heft Nr. 182. München.

[Lambeck, 1988] Lambeck, K. (1988). *Geophysical Geodesy. The Slow Deformation of the Earth.* Oxford Science Publications.

[Lambeck, 1989a] Lambeck, K. (1989a). The Fourth Dimension in Geodesy: Observing the Deformation of the Earth Eds. F.K. Brunner and C. Rizos. In *Lecture Notes in Earth Sciences: Developments in Four-Dimensional Geodesy*, pages 1–14, Springer-Verlag.

[Lambeck, 1989b] Lambeck, K. (1989b). Glacial Rebound and Sea Level Change: An Example of Deformation of the Earth by Surface Loading. Eds. F.K. Brunner and C. Rizos. In *Lecture Notes in Earth Sciences: Developments in Four-Dimensional Geodesy*, pages 112–137, Springer-Verlag.

[Langley, 1995] Langley, R. (1995). GPS Receivers and the Observables. Eds. A. Kleusberg and P.J.G. Teunissen. In *GPS for Geodesy*, pages 141–173, Springer- Verlag.

[Le Pichon et al., 1973] Le Pichon, X., Francheteau, J., and Bonnin, J. (1973). *Plate Tectonics: Developments in Geotectonics 6.* Elsevier Scientific Publishing Company, Amsterdam - London - New York.

[Leick, 1990] Leick, A. (1990). *GPS Satellite Surveying.* John Wiley & Sons., New York/ Chichester/ Brisbane/ Toronto/ Singapore.

[Marussi, 1949] Marussi, A. (1949). *Fondements de geometrie differentielle absolue du champ potentiel terrestre.* Bull. Geod., No. 14, pp. 411 - 439.

[Marussi, 1950] Marussi, A. (1950). *Principles of Intrinsic Geodesy Applied to the Field of Somigliana. In Marussi A.; Intrinsic Geodesy (translated by W. I. Reilly).* Springer Verlag Berlin, 1985. pp. 101 - 108.

[Marussi, 1951] Marussi, A. (1951). *Foundations of Intrinsic Geodesy. In Marussi A.; Intrinsic Geodesy (translated by W. I. Reilly).* Springer- Verlag, Berlin,Heidelberg, New York, Tokyo 1985. pp. 13 - 58.

[Meissl, 1969] Meissl, P. (1969). Zusammenfassung und Ausbau der inneren Fehlertheorie eines Punkthaufens. *Deutsche Geodätische Kommission, Reihe A, München*, 61:8–21.

[Menard, 1975] Menard, H. W. (1975). *Epeirogeny and Plate Tectonics.* The Ohio State University, Department of Geodetic Science, Columbus. Report No. 231, pp 61-52.

[Morelli et al., 1974] Morelli, C., Gantar, C., Honkasalo, T., McConnell, R., Tanner, J., Szabo, B., Uotila, U., and Whalen, C. (1974). The International Gravity Standardization Net 1971 (IGSN 71). *International Association of Geodesy, Special Publication No. 4, Paris.*

[Moritz, 1972] Moritz, H. (1972). *Advanced Least- Squares Methods.* The Ohio State University, Department of Geodetic Science, Columbus. Report No. 175.

[Moritz, 1973] Moritz, H. (1973). *Least-Squares Collocation.* Deutsche Geodätische Kommission, Reihe A, Heft Nr. 75. München.

[Moritz, 1976] Moritz, H. (1976). *Covariance Functions in Least-squares Collocation.* The Ohio State University, Department of Geodetic Science, Columbus. Report No. 240.

[Moritz, 1978] Moritz, H. (1978). *The Operational Approach to Physical Geodesy.* The Ohio State University, Department of Geodetic Science, Columbus. Report No. 277.

[Moritz, 1979] Moritz, H. (1979). *Concepts in Geodetic Reference Frames.* The Ohio State University, Department of Geodetic Science, Columbus. Report No. 294.

[Mueller, 1982] Mueller, I. (1982). Reference coordinate systems for earth dynamics: a review. Eds. H. Moritz and H. Sünkel. In *Geodesy and Global Geodynamics.*, pages 71–92, Mitteilungen der Geodätisches Institute der Technischen Universität Graz, Folge 41.

[Mueller, 1988] Mueller, I. (1988). *Concepts in Geodetic Reference Frames.* The Ohio State University, Department of Geodetic Science, Columbus. Report No. 394.

[Reilly, 1979] Reilly, W. I. (1979). *Mapping the Local Geometry of the Earth's Gravity Field.* Geophysics Division, Department of Scientific and Industrial Research New Zealand. Report No. 143.

[Rothacher et al., 1993] Rothacher, M., Beutler, G., Werner, G., Brockman, E., and Mervert, L. (1993). *Bernese GPS Software Version 3.5.* Astronomical Institute, University of Bern.

[Rothacher et al., 1995] Rothacher, M., Schaer, S., Mervart, L., and Beutler, G. (1995). Determination of Antenna Phase Center Variations Using GPS Data. In *Paper presented at the IGS Workshop. May. 15th - 17th, 1995.*, Potsdam, Germany.

[Schaffrin, 1985] Schaffrin, B. (1985). *Das Geodätische Datum mit Stochastischer Vorinformation.* Deutsche Geodätische Kommission, Reihe C, Heft Nr. 313. München.

[Schaffrin, 1986] Schaffrin, B. (1986). New estimation/ prediction techniques for the determination of crustal deformations in the presence of prior geophysical information. *Tectonophysics*, 29:361–367.

[Schmitt et al., 1994] Schmitt, G., Jäger, R., Oppen, S., Leinen, S., and Nkuite, G. (1994). *NETZ2D Version 3.1. Programm zur Ausgleichung und Analyse (Plannung) zweidimensionaler terrestrischer Netze relativer und absoluter GPS-Netze und zur GPS-Integration.* Geodätisches Institut, Universität Karlsruhe, Germany.

[Schupler et al., 1995] Schupler, B. R., Clark, T. A., and Allshouse, R. L. (1995). Characterization of GPS User Antennas: Reanalysis and new results. In *Paper presented at IUGG General Assembly, July 1995*, Boulder, USA.

[SIRGAS, 1997] SIRGAS (1997). *Final Report - Working Groups I and II.* IBGE, Brazil 1997.

[Smith et al., 1989] Smith, D., Kolenkiewicz, R., Dunn, P., Torrance, M., Klosko, S., Robbins, J., Williamson, R., Pavlis, E., Douglas, N., and Fricke, S. (1989). The Determination of Present day Tectonic Motions from Laser Ranging to LAGEOS. Eds. F.K. Brunner and C. Rizos. In *Lecture Notes in Earth Sciences: Developments in Four-Dimensional Geodesy*, pages 221–240, Springer-Verlag.

[Stangl, 1979] Stangl, G. (1979). Lokale Kovarianzfunktionen von Freiluftanomalien in der Bundesrepublik Deutschland. *Allgemeine Vermessungs-Nachrichten.*, 86:81–88.

[Torge, 1980] Torge, W. (1980). *Geodesy - An Introduction.* Walter de Gruyter Berlin - New York.

[Tsuji et al., 1995] Tsuji, H., Hatanaka, Y., Sagiya, T., and Hashimoto, M. (1995). Coseismic crustal deformation from the 1994 Hokkaido-Toho-Oki earthquake monitored by a nationwide continous GPS array in Japan. *Geophysical Research Letters*, 22:1669.

[Uotila, 1978] Uotila, U. A. (1978). World Gravity Standards. In *Applications of Geodesy to Geodynamics; Ed. I.I Mueller. The Ohio State University, Department of Geodetic Science, Report No. 280.*, pages 237–238, 1958 Neil Avenue Columbus, Ohio 43210.

[van Mierlo, 1980] van Mierlo, J. (1980). Free network adjustment and S-transformations. *Deutsche Geodätische Kommission, Reihe B, München*, 252:41–54.

[Vanicek, 1975] Vanicek, P. (1975). Vertical Crustal Movements in Nova Scotia as Determined from Scattered Geodetic Releveling. *Tectonophysics*, 29:183–189.

[Vanicek et al., 1987] Vanicek, P., Cross, P., Hannale, J., Hradilek, L., Kelm, R., Mäkinen, J., Merry, C., Sjöberg, L., Steeves, R., and Zilkoski, D. (1987). Four-dimensional Geodetic Positioning. Report of the IAG. *Manuscripta Geodaetica*, 12:147–222.

[Vanicek and Krakiwsky, 1978] Vanicek, P. and Krakiwsky, E. (1978). Geodesy Reborn! *Surveying and Mapping XXXVIII*, 37:23–26.

[Vanicek and Krakiwsky, 1982] Vanicek, P. and Krakiwsky, E. (1982). *Geodesy: The concepts.* North-Holland Publishing Company Amsterdam - New York Oxford.

[Vogel, 1995] Vogel, M. (1995). *Analyse der GPS-Alpentraverse - Ein Beitrag zur geodätischen Erfassung rezenter Erdkrustenbewegungen in den Ostalpen.* Deutsche Geodätische Kommission, Reihe C, Heft Nr. 436. München.

[Vogel and Jäger, 1994] Vogel, M. and Jäger, R. (1994). Optimum design, parameter estimation, and testing procedures for the calibration of GPS antennas. In *Paper submitted to the Proceedings of the Fourth International Symposium on Recent Crustal Movements in Africa. Nov. 28th - Dec 2nd, 1994 Nairobi, Kenya.*, Nairobi, Kenya.

[Wolf, 1963a] Wolf, H. (1963a). Die Grundgleichungen der dreidimensionalen Geodäsie in elementarer Darstellung. *Zeitschrift für Vermessungswesen*, 88:225–233.

[Wolf, 1963b] Wolf, H. (1963b). Dreidimensionale Geodäsie, Herkunft, Methodik und Zielsetzung. *Zeitschrift für Vermessungswesen*, 88:109–116.

[Zippelt, 1988] Zippelt, K. (1988). *Modellbildung, Berechnungsstrategie und Beurteilung von Vertikalbewegungen unter Verwendung von Präsionsnivellements.* Deutsche Geodätische Kommission, Reihe C, Heft Nr. 343. München.

Appendix A

GPS Antenna Calibration

A.1 The Mathematical Approach

The total deviation of the phace center consists of a constant part representing the mean deviation of the phase centre and another part which depends on the direction α, and elevation z, of the incoming signal (see e.g. [Geiger, 1988], [Rothacher et al., 1995]). It is this constant part that is here further studied.

A.1.1 The Coordinate Systems.

Four types of coordinate systems are of interest (see e.g. [Vogel and Jäger, 1994]). First is the antenna coordinate system ACS, with the origin O_a situated at the antenna physical phase centre. In this coordinate system the vector of phase center offset is represented by the column vector $\mathbf{e}_a$ such that

$$\mathbf{e}_a = \begin{bmatrix} e_{ax} \\ e_{ay} \\ e_{az} \end{bmatrix}$$

The direction of e_{az} axis is chosen to be that of the local zenith, e_{ax} axis points in the direction of a definite mark on the antenna and e_{ay} axis completes the right-handed system.

The second coordinate system is the WGS-84 coordinate system which the GPS orbits are referred to (see e. g. [Hofmann-Wellenhof et al., 1992]). The column vector $\mathbf{g}$ describing the offsets in this system is,

$$\mathbf{g} = \begin{bmatrix} g_x \\ g_y \\ g_z \end{bmatrix}$$

Thirdly, the GPS topocentric coordinate (GTS) system is obtained by transforming the WGS-84 system into an equivalent topocentric system. The offset vector is expressed by the column vector $\mathbf{e}^\star$

$$\mathbf{e}^\star = \begin{bmatrix} e_x^\star \\ e_y^\star \\ e_z^\star \end{bmatrix}$$

The $\mathbf{e}^\star$ system is derived from the $\mathbf{g}$ system by the following relationship;

$$\begin{bmatrix} e_x^\star \\ e_y^\star \\ e_z^\star \end{bmatrix} = \begin{bmatrix} -\sin\phi\cos\lambda & -\sin\phi\sin\lambda & \cos\phi \\ -\sin\phi & \cos\lambda & 0 \\ \cos\phi\cos\lambda & \cos\phi\sin\lambda & \sin\phi \end{bmatrix} \cdot \begin{bmatrix} g_x \\ g_y \\ g_z \end{bmatrix} \tag{A.1}$$

where ϕ and λ are the geographic coordinates of the station of origin.

Finally, the ground control of the test network is based on a local coordinate system, LTS, possibly with one of the network points, P_o as the origin of this system. The offset vector in this system is represented by the column vector $\mathbf{t}$

$$\mathbf{t} = \begin{bmatrix} t_x \\ t_y \\ t_z \end{bmatrix}.$$

To be able to compute the offsets, various coordinate transformations are necessary. The LTS must be rotated by the angular amount θ, that $\mathbf{t}$ and $\mathbf{e}_a$ deviate from one another given by:

$$\cos\theta = \frac{<\mathbf{e}_a, \mathbf{t}>}{|\mathbf{e}_a| \cdot |\mathbf{t}|}. \tag{A.2}$$

The rotation matrix $\mathbf{R}$ between these two systems is represented by

$$\mathbf{R} = \begin{bmatrix} \cos\theta & \sin\theta & 0 \\ -\sin\theta & \cos\theta & 0 \\ 0 & 0 & 1 \end{bmatrix}.$$

Only coordinate differences shall be considered thus eliminating the need of knowing the translation parameters. The scale factor is also neglected owing to the small size of the network (longest length $< 20m$). The transformation of the GTS into the LTS is necessary. Since the angular deviations between all the three axes of these two systems are not known, they have to be estimated during the process of adjustment. If the angles of rotation about the coordinate axes are α, β, λ respectively, then the total rotation between the WGS-84 and the conventional topocentric system LTS (for small angles) is obtained from

$$\mathbf{R}_z(\delta\gamma)\mathbf{R}_y(\delta\beta)\mathbf{R}_x(\delta\alpha) = \begin{bmatrix} 1 & \delta\gamma & -\delta\beta \\ -\delta\gamma & 1 & \delta\alpha \\ \delta\beta & -\delta\alpha & 1 \end{bmatrix}.$$

A.1.2 The Method of Adjustment

The final linearised observation equation will be of the form

$$\mathbf{y} = \mathbf{A}\mathbf{x} + \mathbf{v} \quad \text{with} \quad E\{\mathbf{y}\} = \mathbf{A}\mathbf{x}, \quad D(\mathbf{y}) = \sigma^2\mathbf{Q}_{yy} \tag{A.3}$$

where

- $\mathbf{y}$ is $n \times 1$ vector of GPS coordinate differences and $\mathbf{Q}_{yy}$ is the corresponding cofactor matrix.
- $\mathbf{A}$ is $n \times m$ design matrix
- $\mathbf{x}$ is $m \times 1$ vector of parameters
- $\mathbf{v}$ is $n \times 1$ vector of residuals
- $\mathbf{C}_{yy}$ is the variance-covariance matrix of the GPS observations.

The solution of equation (A.3) is obtained through $\mathbf{N}\mathbf{x} = \mathbf{A}^T\mathbf{P}\mathbf{y}$ where $\mathbf{N} = \mathbf{A}^T\mathbf{P}\mathbf{A}$ is the normal equation matrix. Generally the ground control of the test network is observed at much higher accuracy than the GPS observations so that the ground control is considered errorless. The parameters of adjustment include the three offset components of each antenna and the rotation angles between the antenna system and the local GPS topocentric system. The spectral analysis of the normal equation matrix $\mathbf{N}$, shows one of the eigenvalues as zero. To facilitate the inversion of $\mathbf{N}$, and therefore a solution of $\mathbf{x}$, two approaches have so far been considered. These are the classical approach and the use of the pseudoinverse as discussed below.

A.1.3 The Classical Approach

In this approach one antenna is chosen as reference and its offsets assigned fixed values e.g. (0,0,0). The solution is then given by $\mathbf{x} = \mathbf{N}^{-1}\mathbf{A}^T\mathbf{P}\mathbf{y}$ where $\mathbf{N}^{-1}$ is the Cayley inverse of $\mathbf{N}$. The choice of the reference antenna may be one whose phase centre variations are known. The resulting offsets are thus depended on the the choice of the chosen antenna.

A.1.4 The Pseudoinverse Approach

The arbitrary choice of the reference antenna is avoided by computing the pseudoinverse of $\mathbf{N}$ ([Vogel and Jäger, 1994]). For $\mathbf{N}$ not of full rank, a defect $d = m - r$ exists. A null space of $\mathbf{N}$, denoted by $\mathbf{G}$ of dimension $m \times d$ and with properties $\mathbf{NG} = 0$ and $\mathbf{AG} = 0$ can be computed. $\mathbf{G}$ consists of eigenvectors that correspond with those eigenvalues that are equal to zero. In the case that the pseudoinverse is used, the datum is defined over all the parameters that are in the adjustment. In this case, the antenna offsets and the rotational parameters so that $\mathbf{G}$ is of the form

$$\mathbf{G} = \left[\begin{array}{cccccccccc} \zeta_{ex1} & \zeta_{ey1} & \zeta_{ez1} & \ldots & \zeta_{exn} & \zeta_{eyn} & \zeta_{ezn} & \zeta_{\alpha} & \zeta_{\beta} & \zeta_{\gamma} \end{array} \right]^T$$

where $\zeta_{exi}, \quad \zeta_{eyi}, \quad \zeta_{ezi}$ are the eigenvectors corresponding to the eigenvalues on the side of offsets and $\delta\alpha, \delta\beta, \delta\gamma$ are those eigenvectors on the side of the rotational elements. The pseudoinverse solution is given by $\mathbf{x} = \mathbf{N}^{+}\mathbf{A}^{T}\mathbf{Py}$ where $\mathbf{N}^{+}$ is the pseudoinverse of $\mathbf{N}$.

Since the spectral analysis of $\mathbf{N}$ indicates only one zero eigenvalue (see Figure (A.1)) which vanishes as soon as one of e_{az} value is fixed, then the rotational elements clearly need not be included in the datum definition. Two other approaches have been therefore proposed.

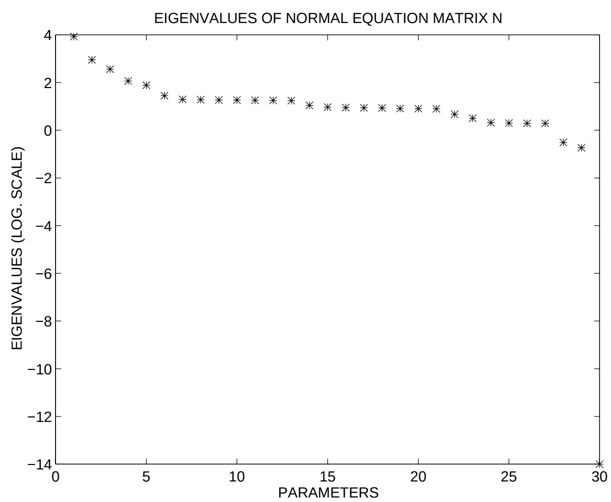

Figure A.1: The eigenvalues of $\mathbf{N}$ plotted against the parameters.

A.1.5 The Partial Norm Minimization Approach

The singular normal equation matrix $\mathbf{N}$ is regularised by introducing the matrix $\mathbf{G}$ of the null space just as in the case of pseudoinverse but this time $\mathbf{G}$ is defined in a different way. In this approach, the datum defect in $\mathbf{N}$ is overcome by defining the datum with respect to the offsets but not the rotational elements. The null space $\mathbf{G}$ is now a vector of m rows of the form

$$\mathbf{G} = \begin{bmatrix} \zeta_{ex1} & \zeta_{ey1} & \zeta_{ez1} & \dots & \zeta_{exn} & \zeta_{eyn} & \zeta_{ezn} & 0 & 0 & 0 \end{bmatrix}^T$$

where n is the total number of the antennae to be calibrated.

A.1.6 The Special Partial Norm Minimization

In the second aproach, since it is known that the datum defect arises from the inability to determine the height component of the offset in an absolute way, the datum can be instead defined over all the height components of the antenna offsets only. Thus $\mathbf{G}$ is of the form

$$\mathbf{G} = \begin{bmatrix} 0 & 0 & \zeta_{ez1} & \dots & 0 & 0 & \zeta_{ezn} & 0 & 0 & 0 \end{bmatrix}^T.$$

One therefore not only avoids the arbitrary choice of datum but also overcomes the only datum defect available. For both partial norm minimum solutions the final solution is given by

$$\mathbf{x} = \mathbf{N}^{++}\mathbf{A}^T\mathbf{P}\mathbf{y} \tag{A.4}$$

where $\mathbf{N}^{++}$ is a special generalized inverse of $\mathbf{N}$, corresponding to partial norm minimization.

A.2 Parameter Testing

Only estimates from models of full rank may be statistically tested. In this case the estimates obtained through the classical approach are fully estimable and can be therefore statistically tested. In all the other approaches described above the parameters of type vertical offsets (z-components) are non-estimable (estimates obtained from singular systems) and cannot be directly subjected to statistical testing.

However non-estimable parameters can be transformed into another set of parameters that can be subjected to statistical tests ([Koch, 1978]). The estimated parameters (antenna offset) are converted into estimable parameters or equivalently testable hypothesis by refering them to a particular antenna in which case the test shows whether or not significant differences exist between the offsets of the reference antenna and any other antenna i. The test statistic for the vertical antenna offset e_{ez} is given by

$$T = \frac{\Delta ez}{\hat{\sigma}_0\sqrt{q_{\Delta ez}}} = \frac{\Delta ez}{\hat{\sigma}_0\sqrt{q_{ii} + q_{rr} - 2q_{ir}}}. \tag{A.5}$$

where $\Delta ez = e_{ezi} - e_{ezr}$, $\hat{\sigma}_0^2$ is the a posteriori variance of unit weight and q_{ezi} is the element of the cofactor matrix corresponding to the e_{ez} value of the ith antenna and e_{ezr} refers to chosen reference antenna.

The quantity T has a Student-t distribution with r degrees of freedom symbolically written as $T \sim t(r)$. The null hypothesis, $Ho : \Delta\hat{e}_{ez} = 0$, is tested against the alternative hypothesis $Ha : \Delta\hat{e}_{ez} \neq 0$. The null hypothesis is accepted when the test statistic T is less than or equal to the tabulated value of t for r degrees of freedom at the chosen level of significance α, usually 5% or 1%. This is written as $t_{r,1-\alpha}$ for a two-sided test.

A.3 The Test Network and Results

A.3.1 The Ground Truth

The test network is situated on the roof of the building housing the Geodetic Institute at the University of Karlsruhe. The network was first established by means of terrestrial methods in July 1996. A *Kern E2* Theodolite of precision 1^{cc} in angular measurements was used while the Mekometer ME 5000 of precision $0.0002m + 0.01ppm^{\star}S$ (S is the distance measured) was used in distance measurents. The heights of the network stations were measured by means of spirit levelling. Both the angular and distance measurements were processed using the program *NETZ2D* ([Schmitt et al., 1994] for computation of the planimetric coordinates. The network was computed on the basis of a free network. The network mean error was 0.12mm. Table (A.3.2) shows the terrestrial network coordinates together with their standard deviations at some arbitrary coordinate system while Figure (A.2) shows the layout of the network.

A.3.2 The GPS Network

A GPS campaign was carried out on 5th July 1996 corresponding to the 865 GPS day and involving 9 GPS antennae from two different manufacturers. Seven of them were of type *LEICA SR299* and the other two were *TRIMBLE 4000SSI* with ground plane. The campaign covered four sessions of about ninety minutes each. The whole campaign lasted between 0600 hours and 1700 GPS time.

In session one all the antennae pointed approximately in the northern direction while in session two all the antennae pointed in the southern direction except the two reference antennae, one LEICA and one TRIMBLE antenna, which remained switched on and pointed to the northern direction throughout the campaign period.

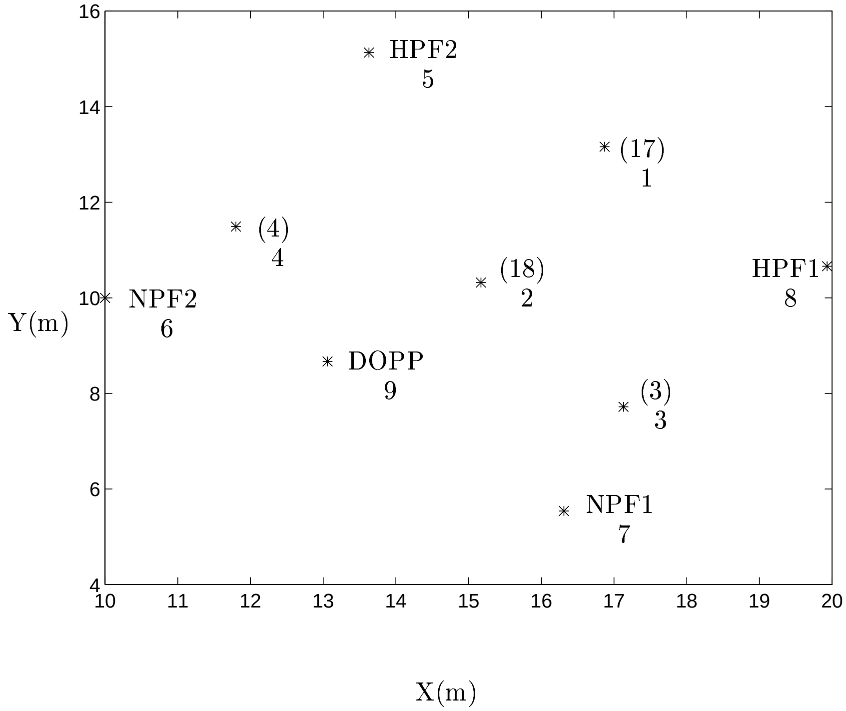

Figure. A.2: The layout of the GPS antenna calibration terrestrial network (scale: 1cm $\cong$ 1m).

In the third session all except the reference antennae were exchanged on their ground positions. Table (A.2) shows the antenna types and their assigned numbers while Tables (A.3) and (A.4) show the type of antennae, their ground positions and their directions during the entire campaign. Antenna heights were measured by means of spirit levelling.

A.3.3 Computation of the Antenna Offsets

The GPS phase observations were processed using the *Bernese GPS Software* (see [Rothacher et al., 1993]). The final solution was the relative position of the network coordinates with respect to reference station 5. The resulting variance- covariance matrix of the differential GPS solution was also calculated.

The program *PHACE* [Vogel, 1995] was modified so that offsets could be computed using various ways.

A.3.4 Adjustment of Offsets and only one Set of Rotation Transformation Parameters as Unknowns

The first computation involved the determination of the antenna offsets using data obtained from the first two sessions of the GPS campaign. Between the first two sessions the antennae were rotated in direction (see Table (A.3) above). The normal equation matrix **N** showed a rank defect of one. A plot of the eigenvalues versus the parameters is

Table A.1: The Terrestrial network coordinates

STATION NAME		X (m)	Y (m)	HEIGHT (m)
1	(17)	16.8679 0.0004	13.1561 0.0056	0.4060
2	(18)	15.1691 0.0004	10.3244 0.0004	0.4090
3	(3)	17.1339 0.0004	7.7241 0.0004	0.3862
4	(4)	11.7989 0.0004	11.4871 0.0004	0.3840
5	(HPF2)	13.6264 0.0004	15.1288 0.0004	1.4929
6	(NPF2)	9.9982 0.0004	9.9999 0.0004	1.5291
7	(NPF1)	16.3124 0.0004	5.5423 0.0004	1.5316
8	(HPF1)	19.9282 0.0004	10.6602 0.0004	1.4899
9	(DOPP)	13.0595 0.0004	8.6707 0.0004	0.4170

Table A.2: Types of antenna used and numbering adopted

ANTENNA NO.	TYPE	SERIAL NO.	INSTITUTION
1	LEICA SR299	100 308	UNI. STUTTGART
2	LEICA SR299	100 318	UNI. STUTTGART
3	LEICA SR299	100 066	LANDESVERM. KARLSRUHE
4	LEICA SR299	100 039	LANDESVERM. KARLSRUHE
5	TRIM. 4000SSI	220 039 556	UNI. KARLSRUHE
6	LEICA SR299	100 327	UNI. KARLSRUHE
7	TRIM. 4000SSI	220 039 555	UNI. KARLSRUHE
8	LEICA SR299	100 323	UNI. KARLSRUHE
9	LEICA SR299	100 303	UNI. STUTTGART

Note: All LEICA antennae were of internal type.

Table A.3: Antenna positions and directions in sessions 1 and 2

ANTENNA NO.	STATION	SESSION 1 (gon)	SESSION 2 (gon)
1	1	0	200
2	2	0	200
3	3	0	200
4	4	0	200
5	5	0	0
6	6	0	0
7	7	0	200
8	8	0	200
9	9	0	200

Table A.4: Antenna positions and directions in sessions 3 and 4

ANTENNA NO.	STATION	SESSION 3 (gon)	SESSION 4 (gon)
1	3	0	200
2	1	0	200
3	4	0	200
4	7	0	200
5	5	0	0
6	6	0	0
7	8	0	200
8	9	0	200
9	2	0	200

Table A.5: The null space of **N** for each of the three components of the offset when only one set of rotation parameters is used

ANTENNA NO.	e_{ax}	e_{ay}	e_{az}
1	0.0000	0.0000	-0.3333
2	0.0000	0.0000	-0.3333
3	0.0000	0.0000	-0.3333
4	0.0000	0.0000	-0.3333
5	0.0000	0.0000	-0.3333
6	0.0000	0.0000	-0.3333
7	0.0000	0.0000	-0.3333
8	0.0000	0.0000	-0.3333
9	0.0000	0.0000	-0.3333
ROTATIONS	0.0000	0.0000	0.0000

Table A.6: Results obtained by fixing one station $e_{az} = 0$ - classical approach

ANT.OFFSET	e_{ax}	T_x	e_{ay}	T_y	e_{az}	T_z
1	0.0004	0.129	-0.0031	-1.489	0.0190	1.911
2	0.0011	0.359	-0.0024	-1.110	0.0185	1.347
3	-0.0026	-0.888	-0.0013	0.637	0.0138	0.680
4	0.0041	1.427	-0.0005	-0.252	0.0196	1.756
5	-0.0023	-0.973	-0.0036	-1.323	0	-
6	-0.0008	-0.225	0.0000	0.006	0.0201	1.432
7	-0.0003	-0.101	-0.0007	-0.330	0.0035	0.146
8	0.0016	0.521	-0.0016	-0.731	0.0109	0.656
9	-0.0012	-0.414	-0.0012	-0.576	0.0187	1.099

Critical value at level of significance $\alpha = 99\%$: $t_{25,0.995} = 2.06$. The fixed antenna is antenna 5.

shown in Figure (A.1). Only one eigenvalue is seen to be zero and the difference between the rest of the eigenvalues does not depict an ill condition of **N**. The elements of the null space **G** of the normal equation matrix are shown in Table (A.5).

Four different ways to overcome the rank defect were applied as described in sections (A.1.3) to (A.1.6). Tables (A.6) and (A.7) show the results obtained using the classical approach. With respect to coordinates obtained using the partial norm minimization, the special partial norm minimization and the pseudoinverse were the same. These results however showed no significant variations from those of the previous approach.

All the four sessions were finally computed together and the results are shown in Tables (A.8) and (A.9).

Table A.7: The rotational angles in radians

$\delta\lambda$ / std. error	$\delta\beta$ / std. error	$\delta\gamma$ / std. error
0.000 622	0.000 192	-0.000 468
0.000 347	0.000 660	-0.000 011

Table A.8: Results of all four sessions

OFF.	e_{ax}	T_x	e_{ay}	T_y	e_{az}	T_z
1	0.0015	1.092	-0.0029	-2.829	0.0186	0.453
2	0.0015	1.082	-0.0021	-2.079	0.0183	0.448
3	-0.0011	-0.782	-0.0011	-1.079	0.0146	0.312
4	0.0035	2.621	-0.0007	-0.712	0.0172	0.427
5	-0.0024	-3.382	-0.0041	-4.080	0	-
6	-0.0009	-0.745	-0.0004	-0.566	0.0151	0.370
7	-0.0003	-0.231	-0.0006	-0.657	0.0001	0.004
8	0.0024	1.664	-0.0019	-1.803	0.0139	0.339
9	0.0003	0.185	-0.0014	-1.327	0.0142	0.377

Critical value at level of significance $\alpha = 99\%$: $t_{78,0.995} = 2.00$. The fixed antenna is antenna 5.

Table A.9: The rotational angles in radians

$\delta\lambda$ / std. error	$\delta\beta$ / std. error	$\delta\gamma$ / std. error
0.001 216	0.000 276	-0.000 489
0.000 035	0.000 036	0.000 003

Table A.10: Results according to classical approach (sessions 1 & 2)

OFF.	e_{ax}	T_x	e_{ay}	T_y	e_{az}	T_z
1	0.0002	0.064	-0.0029	-1.388	0.0166	2.678
2	0.0011	0.362	-0.0024	-1.114	0.0166	2.674
3	-0.0025	-0.888	-0.0015	-0.737	0.0109	1.805
4	0.0043	1.526	-0.0005	-0.238	0.0195	3.252
5	-0.0016	-1.424	-0.0005	-0.615	0	-
6	0.0017	0.939	0.0008	0.633	0.0216	7.920
7	-0.0002	-0.064	-0.0007	-0.357	0.0004	0.072
8	0.0014	0.459	-0.0014	-0.649	0.0068	1.080
9	-0.0011	-0.376	-0.0012	-0.643	0.0176	2.841

Critical value at level of significance $\alpha = 99\%$: $t_{28,0.995} = 2.05$. The fixed antenna is antenna 5.

A.3.5 Adjustment when Rotational Transformation Elements are excluded

The same experiments were carried out without including the transformation parameters i. e. the rotational angles. Table (A.10) shows the results obtained using the classical approach. The results obtained using the the other approaches i. e. partial, special partial and pseudoinverse solutions were the same and in addition showed no significant variation to those of the classical approach. The results obtained when all the four sessions were computed together showed no significant variations from the results obtained when all the four sessions where computed together but taking into account the presence of the rotation angles (see Table (A.8)).

A.3.6 Adjustment of Offsets and Transformation Parameters for each Session

Again the above experiments were repeated but this time taking into account one set of transformation parameters for each session. The results are shown in Tables (A.11) through (A.21).

Table A.11: Results according to the classical approach

OFF.	e_{ax}	T_x	e_{ay}	T_y	e_{az}	T_z
1	0.0021	1.125	-0.0043	-3.153	0.0193	3.172
2	0.0029	1.511	-0.0036	-2.443	0.0182	2.163
3	-0.0003	-0.181	-0.0023	-1.494	0.0134	1.076
4	0.0055	3.053	-0.0018	-1.299	0.0184	2.689
5	-0.0023	-1.582	-0.0040	-2.378	0	-
6	-0.0008	-0.362	-0.0005	-0.396	0.0184	2.141
7	0.0006	0.320	-0.0006	-0.385	0.0039	0.266
8	0.0025	1.243	-0.0015	-1.072	0.0119	1.180
9	0.0005	0.266	-0.0024	-1.598	0.0173	1.669

Critical value at level of significance $\alpha = 99\%$: $t_{22,0.995} = 2.06$. The fixed antenna is antenna 5.

Table A.12: The rotational angles in radians for session 1

$\delta\lambda$ / std. error	$\delta\beta$ / std. error	$\delta\gamma$ / std. error
-0.000 233	-0.001 131	-0.000 448
0.000 212	0.000 386	0.000 009

Table A.13: The rotational angles in radians for session 2

$\delta\lambda$ / std. error	$\delta\beta$ / std. error	$\delta\gamma$ / std. error
0.001 970	-0.001 201	-0.000 468
0.000 223	0.000 382	0.000 008

Table A.14: Results from partial, special partial and pseudoinverse solution - $e_{z5} = -0.0134$

OFF.	e_{ax}	T_x	e_{ay}	T_y	e_{az}	T_z
1	0.0021	1.152	-0.0043	-3.227	0.0193	3.247
2	0.0029	1.546	-0.0036	-2.500	0.0182	2.214
3	-0.0003	-0.185	-0.0023	-1.530	0.0134	1.101
4	0.0055	3.125	-0.0018	-1.329	0.0184	2.752
5	-0.0023	-1.620	-0.0040	-2.434	0	-
6	-0.0008	-0.371	-0.0005	-0.406	0.0184	2.191
7	0.0006	0.328	-0.0006	-0.395	0.0039	0.272
8	0.0025	1.272	-0.0015	-1.097	0.0119	1.208
9	0.0005	0.272	-0.0024	-1.636	0.0173	1.709

Critical value at level of significance $\alpha = 99\%$: $t_{22,0.995} = 2.06$. The fixed antenna is antenna 5.

Table A.15: The rotational angles in radians for session 1

$\delta\lambda$ / std. error	$\delta\beta$ / std. error	$\delta\gamma$ / std. error
-0.000 234	-0.001 131	-0.000 449
0.000 221	0.000 403	0.000 009

Table A.16: The rotational angles in radians for session 2

$\delta\lambda$ / std. error	$\delta\beta$ / std. error	$\delta\gamma$ / std. error
0.001 971	-0.001 201	-0.000 468
0.000 232	0.000 399	0.000 009

Table A.17: Results of all four sessions

OFF.	e_{ax}	T_x	e_{ay}	T_y	e_{az}	T_z
1	0.0022	2.403	-0.0036	-4.798	0.0182	0.614
2	0.0020	2.166	-0.0024	-3.424	0.0187	0.627
3	0.0001	0.064	-0.0013	-1.739	0.0126	0.424
4	0.0043	4.853	-0.0016	-2.202	0.0169	0.568
5	-0.0024	-5.191	-0.0044	-6.503	0	-
6	-0.0010	-1.216	-0.0006	-1.372	0.0148	0.497
7	0.0002	0.216	-0.0006	-0.814	0.0008	0.028
8	0.0029	2.953	-0.0018	-2.367	0.0137	0.460
9	0.0009	0.925	-0.0018	-2.425	0.0153	0.515

Critical value at level of significance $\alpha = 99\%$: $t_{79,0.995} = 2.00$. The fixed antenna is antenna 5.

Table A.18: The rotational angles in radians for session 1

$\delta\lambda$ / std. error	$\delta\beta$ / std. error	$\delta\gamma$ / std. error
0.000 282	-0.001 417	-0.000 512
0.000 041	0.000 032	0.000 003

Table A.19: The rotational angles in radians for session 2

$\delta\lambda$ / std. error	$\delta\beta$ / std. error	$\delta\gamma$ / std. error
0.002 279	0.000 864	-0.000 458
0.000 044	0.000 030	0.000 003

Table A.20: The rotational angles in radians for session 3

$\delta\lambda$ / std. error	$\delta\beta$ / std. error	$\delta\gamma$ / std. error
0.001 664	0.000 215	-0.000 437
0.000 043	0.000 034	0.000 003

Table A.21: The rotational angles in radians for session 3

$\delta\lambda$ / std. error	$\delta\beta$ / std. error	$\delta\gamma$ / std. error
0.001 029	-0.000 790	-0.000 583
0.000 039	0.000 030	0.000 004

Acknowledgement

This dissertation was written at the Geodetic Institute, University of Karlsruhe in the Federal Republic of Germany with the financial support of the German Academic Exchange Service (DAAD). I sincerely appreciate this financial assistance.

I sincerely thank Prof. Dr.-Ing. habil. B. Heck of the Geodetic Institute, University of Karlsruhe for accepting to be my main supervisor for my study at the University leading to the writing of this dissertation. I am grateful for his counsel, critisism and general guidance during my study period.

I also wish to thank Prof. Dr.-Ing. habil G. Schmitt of the University of Karlsruhe for his role as the second supervisor.

I am also very grateful to Prof. Dr.-Ing. F.W.O Aduol of the University of Nairobi, for his support and encouragement throughout my study period.

My deep appreciation also goes to my employers at the University of Nairobi for offering me the study leave to enable my studies in the Federal Republic of Germany. I also thank my colleagues at the Department of Surveying for the extra work that they took during my absence.

And to all staff of the Geodetic Institute, thank you very much for the cooperation and help that you offered me in different ways thereby making my stay at the Geodetic Institute conducive for completion of this dissertation.

The use of LaTeX in preparing this dissertation is highly appreciated.

And finally let me thank my parents, relatives and friends who have in one way or another given me courage throughout the study period.

Curriculum Vitae

28.07.1966:	Born in Makutano, Mwala Location, Machakos District, Kenya
1973 - 1979:	Primary School Education at Makutano Primary school
1980 - 1983:	Secondary School Education at Kangundo High School
1984 - 1985:	High School Education at Alliance High School, Kikuyu
1986:	Taught at Mwala Girls' Secondary School
1987:	Attended National Youth Service Training in Gilgil
1987 - 1990:	Bachelor of Science Degree in Surveying & Photogrammetry, University of Nairobi, Kenya.
1990 - 1993:	Master of Science in Surveying & Photogrammetry, University of Nairobi.
1994:	Assistant Lecturer, Department of Surveying, University of Nairobi.
1994 - 1995:	German language course at the Goethe Institute, Mannheim, Germany, under DAAD scholarship.
1995 - 1999:	Doctoral studies in Geodesy at the University of Karlsruhe, Germany, under DAAD scholarship.